


**A genetic approach to reveal determinants of mitochondrial tail-anchored
protein targeting**

by

Abdurrahman Keskin



**A Thesis Submitted to the
Graduate School of Sciences and Engineering
in Partial Fulfillment of the Requirements for
the Degree of**

**Master of Science
in
Molecular Biology and Genetics**

**Koç University
July 2016**

Koç University
Graduate School of Sciences and Engineering
This is to certify that I have examined this copy of a master's thesis by

Abdurrahman Keskin

and have found that it is complete and satisfactory in all respects,
and that any and all revisions required by the final
examining committee have been made.

Committee Members:

Cory D. Dunn, Ph. D. (Advisor)

I. Halil Kavaklı, Ph. D.

N. C. Tolga Emre, Ph. D.

Date:

ABSTRACT

Tail-anchored (TA) proteins are a group of integral membrane proteins anchored to the phospholipid bilayer by a carboxyl-terminal single transmembrane domain. TA proteins carry out a wide range of crucial functions, such as taking a role in protein translocation, mitochondrial dynamics, storage of transcription factors and regulation of apoptosis. Although how the ER and peroxisomal tail-anchored proteins are targeted to their corresponding membranes were elucidated, targeting of mitochondrial TA proteins to the outer membrane of mitochondria remains its mystery. In this study, we aimed to reveal the determinants of the mitochondrial TA protein targeting, using the organism *Saccharomyces cerevisiae*. We developed a genetic approach which is based on viability, following mislocalization of a chimeric protein whose function is necessary for survival under selective conditions. By coupling our genetic selection approach to next-generation sequencing, we revealed the structural and sequence characteristics essential for targeting of *Saccharomyces cerevisiae* Fis1p, a protein inserted into the outer membrane of mitochondria by a TA. We generated a library of Fis1p TA variants linked to the Gal4 transcription factor, then selected for mutations allowing Gal4 activity in the nucleus. We quantified TA variants in our mutant library both before and after selection for diminished TA targeting. Large-scale analysis results were recapitulated by further analysis of individual Fis1 TA constructs. We demonstrated that positively charged amino acids are more tolerated within the TA of Fis1p than negatively charged residues and they do not interfere with insertion and functionality of Fis1p. These findings present solid, *in vivo* evidence that arginine and lysine can “snorkel” by stably associating with a lipid bilayer and placing their terminal positively charged head group to water-lipid bilayer interface region. Moreover, our results exhibited that length of the TA of Fis1p does not influence targeting to mitochondria and proline is not tolerated at many positions within the TA of Fis1p due to its helix-disrupting feature. Finally, we revealed that positively charged amino acids found at the carboxyl terminus of the TA are crucial for specific targeting to mitochondria; however, not necessary for membrane localization. This

dissertation serves the first high-resolution analysis of a eukaryotic organelle targeting sequence by deep mutational scanning.



ÖZET

Tail-anchored (TA) proteinleri fosfo-lipit zara karboksil ucundaki tek transmembran bölge (TMD) aracılığı ile bağlanan, hücre membranına entegre olan proteinlerin familyasına ait proteinlerdendir. TA proteinleri, proteinlerin organellerin içine alınmasını sağlamaları, mitokondriyal dinamik fonksiyonlarında faaliyet göstermeleri ve hücrelerin kendilerini öldürmelerinde rol almaları gibi birçok önemli görevi yerine getirirler. TA proteinlerinin endoplazmik retikulum ve perokslzom zarlarına nasıl entegre oldukları bilinmesine rağmen, bu proteinlerin mitokondriye nasıl ulaştıkları ve ne şekilde mitokondrinin dış zarına entegre oldukları hala gizemini korumaktadır. Bu çalışmada, tek hücreli ökaryot *Saccharomyces cerevisiae* model organizmasını kullanarak ve seçici koşullar altında fonksiyonu yaşam için gerekli olan kimerik bir proteinin kullanıldığı genetik bir teknikten yararlanarak, TA proteinlerinin mitokondriye ulaşmalarını ve entegre olmalarını sağlayan özellikleri bulmayı amaçladık. Yeni nesil sekanslama adı verilen DNA sekanslama yöntemini bizim genetik tekniğimizle birleştirerek, *Saccharomyces cerevisiae* Fis1 proteininin mitokondriye entegre olmasını sağlayan TMD adı verilen bölgenin, yapısal ve dizisel özelliklerini gösterdik. Gal4 transkripsiyon faktörüne bağlı Fis1p TA varyantlarını içeren kütüphaneyi elde ettikten sonra, çekirdekte Gal4 aktivitesine izin veren mutasyonları seçtik. Yeni nesil sekanslama yardımı ile seçimden önce ve sonra TA lokalizasyonu etkilenen varyantların miktarını belirledik. Bu geniş çaplı analizin sonuçları önemli olan her bir Fis1 TA varyantında tekrarlandı. Sonuçlarımız, ilginç bir şekilde, pozitif yüklü aminoasitlerin TMD bölgesi içerisinde negatif yüklü aminoasitlere göre daha toleranslı bir şekilde bulunabildiklerini gösterdi. Bunlara ek olarak, TMD bölgesinin uzunluğunun TA proteinlerinin mitokondriye yönlendirilmelerinde bir etkisi olmadığını ve TMD bölgesinin heliks yapısını bozan prolinin TMD içinde kabul edilmediğini gösterdik. Son olarak da, TMD bölgesinin uç kısımlarında bulunan pozitif yüklü aminoasitlerin, TA proteinlerinin özellikle mitokondriye yönlendirilmeleri için önemli olduklarını; fakat herhangi bir organel zarına entegre olmalarına katkıda bulunmadıklarını ortaya çıkardık. Bildiğimiz kadarıyla bu çalışma

derin mutasyon incelemesi yapan bir tekniđi, ökaryotlara ait organel sinyal sekansını analiz etmek amaçlı kullanan ilk çalışmadır.





This thesis is dedicated to my family

ACKNOWLEDGEMENTS

I would like to express my deepest gratitude to my advisor Dr. Cory Dunn for his professional guidance that he had given throughout the past two years. I learned how to conduct a research in a logical, critical, passionate and controlled manner from him. His enthusiasm for science always inspired me to be a professional scientist. I am greatly thankful to him for giving me the opportunity to be one of his students.

I am indebted to my committee members, Dr. Halil Kavakli and Dr. Tolga Emre for their valuable contributions and comments.

I would like to thank my lab mates Emel Akdogan, Funda Mujgan Kar, Ayse Bengisu Seferoglu, Sara Nafisi and Guleycan Lutfullahoglu Bal for their friendship and critical readings and comments on my thesis.

My sincere thanks also go to my dear friends Nesligul Coskun, Gizem Zeren, Merve Mutlu, Bahriye Erkaya, Ekin Guney, Gulkiz Baytek, Deniz Conkar, Gizem Guzelsoy, Cansu Akkaya, Dingenis van der Linde and others whom I could not name here one by one for making this journey possible by sharing my life, listening to my complaints and problems and sometimes by just simply being next to me.

Special thanks to Gokhan Guner, Erdem Senal and Fatih Demirhan for helping me in the analysis of the next-generation sequencing data. I really enjoyed our DOTA discussions with Gokhan.

I am deeply thankful to my family, firstly for their unconditional love and support; and raising me and making me who I am today.

Finally, I want to thank *Saccharomyces cerevisiae* for making this study possible. I am really sorry for killing billions of you!

TABLE OF CONTENTS

Contents

ABSTRACT	iii
ÖZET	v
ACKNOWLEDGEMENTS	viii
TABLE OF CONTENTS	ix
LIST OF TABLES	xii
LIST OF FIGURES	xiii
NOMENCLATURE	xv
Chapter 1	1
INTRODUCTION	1
Chapter 2	5
LITERATURE REVIEW	5
2.1 Overview of mitochondria and mitochondrial protein import	5
2.1.1 Precursor protein translocation across to outer membrane of mitochondria	7
2.1.2 Insertion of the outer membrane proteins	10
2.1.3 Precursor protein translocation across to inner membrane of mitochondria	11
2.1.4 Insertion of the inner membrane proteins	12
2.2 The overview of tail-anchored (TA) proteins : synthesized in the cytosol and searching for a membrane	13
2.2.1 Tail-anchored proteins are targeted to particular intracellular membranes	15
2.2.2 How are tail-anchored proteins inserted into the membrane of various organelles?..	18
2.2.2.1 Insertion of TA proteins into the membrane of the ER	18
2.2.2.2 Insertion of TA proteins into the membrane of peroxisome	20
2.2.2.3 Insertion of TA proteins into the outer membrane of mitochondria	20
Chapter 3	23
MATERIAL AND METHODS	23
3.1 Yeast strains and plasmids	23
3.2 Culture conditions	23

3.3 Microscopy.....	24
3.4 Fis1p TA mutant library construction.....	24
3.5 Deep mutational scanning of the Fis1p TA library.....	25
Chapter 4.....	27
RESULTS.....	27
4.1 Targeting of the fusion protein to the outer membrane of mitochondria via the Fis1 tail anchor hampers Gal4-mediated transcription activation.....	27
4.2 Searching for the trans factors related to targeting of Fis1p to the outer membrane of mitochondria.....	32
4.3 <i>Cis</i> mutations allowed us to gain insight into the structural and sequence characteristics of the TA of Fis1p.....	34
4.4 Deep mutational scanning reveals determinants of Fis1p tail-anchor targeting.....	38
4.5 Proline is not tolerated at many regions within the TA of Fis1p.....	45
4.6 Lengthening or shortening of the TA of Fis1p does not influence targeting to mitochondria.....	50
4.7 The positively charged amino acids found at extreme carboxyl terminus of the Fis1p are involved in mitochondrial targeting.....	54
4.8 Positively charged amino acids are more tolerated than negatively charged amino acids within the TMD of Fis1p.....	57
4.9 Bacterial tail anchors insert into the various organelles in <i>S.cerevisiae</i> including mitochondria.....	64
Chapter 5.....	68
DISCUSSION.....	68
5.1 Positively charged amino acids within a mitochondrial transmembrane domain may ‘snorkel’ to the lipid bilayer.....	71
5.2 The TMD of the Fis1p may consist of two separable segments.....	71
5.3 Positively charged amino acids found at the carboxyl terminus of Fis1p are required for specific targeting to mitochondria.....	74
5.4 Bacteria may have separate IM domains that might approximate the different ER and mitochondrial lipid composition.....	74
Chapter 6.....	77
CONCLUSION AND OUTLOOK.....	77

BIBLIOGRAPHY	79
VITA	102
APPENDIX A: Details of strains used in this study.....	103
APPENDIX B: Plasmids used for experiments during this study.....	107
APPENDIX C: List of primers used in this study.....	119



LIST OF TABLES

Table 4.1 Potential candidate proteins playing a role in Fis1p insertion

Table 4.2 Amino acid sequence of the TA of wild type Fis1p and the four clones

Table 4.3 List of the bacterial TA proteins that may potentially be targeted to various organelles in *S. cerevisiae*

Table 4.4 Predicted amino acid sequence of the TA of bacterial TA proteins.

LIST OF FIGURES

Figure 1.1 A general model for insertion of integral membrane proteins.

Figure 2.1 Protein transport pathways into mitochondria.

Figure 2.2 $N_{\text{cytosol}}-C_{\text{lumen}}$ topology of a Tail-anchored protein.

Figure 2.3 Features that regulate targeting of TA proteins to the ER or the MOM.

Figure 4.1 A genetic selection method based on mislocalization of the Gal4-Fis1p fusion, which allows identification of *cis* or *trans* mutants by blocking mitochondrial localization of the chimeric protein.

Figure 4.2 A Gal4-Fis1 chimeric protein localizes to mitochondria.

Figure 4.3 Missense mutations within the TA of Fis1p result in cytosolic accumulation of a linked mCherry protein.

Figure 4.4 An illustration of amino acid replacement representation within the Fis1p TA library.

Figure 4.5 Mutations at specific locations within the TA of the Gal4-Fis1 chimeric protein enable Gal4-driven transcription.

Figure 4.6 Amino acid replacement frequencies within the Fis1p TA indicate that assessing histidine auxotrophy in the presence of 3-AT may provide the most informative results regarding Gal4-Fis1p location.

Figure 4.7 Codon usage has no role in Gal4-Fis1p targeting.

Figure 4.8 Representation of the most abundant Gal4-Fis1p clones that are significantly enriched upon selection for nuclear translocation of the fusion protein.

Figure 4.9 Proline is not tolerated at many regions within the TA of Fis1p.

Figure 4.10 Length of the TA of Fis1p has no influence on mitochondrial targeting.

Figure 4.11 mCherry fused to varying length of a Fis1 TA remains localized to the ER in the cells lacking Spf1p.

Figure 4.12 Positively charged amino acids located at the carboxyl-terminus of the TA of Fis1p are essential for mitochondrial targeting.

Figure 4.13 mCherry fused to the R151X TA is targeted to the ER in Get3p independent manner.

Figure 4.14 The TAs of human proteins are not universally targeted to mitochondria in yeast.

Figure 4.15 Positively charged amino acids are more tolerated within the TMD of Fis1p for targeting to mitochondria rather than negatively charged amino acids.

Figure 4.16 Fis1p variants containing positively or negatively charged amino acid substitutions within the TMD can promote fission activity.

Figure 4.17 Fis1p variants containing positively or negatively charged amino acid substitutions within the TMD can promote fission activity.

Figure 4.18 Bacterial tail anchors are targeted to various organelles in *S. cerevisiae*.

Figure 5.1 Longer aminoacids cluster at one side of the α -helix



NOMENCLATURE

- TA** Tail-anchor
- ER** Endoplasmic reticulum
- SRP** Signal recognition particle
- PTS1** Peroxisomal targeting signal type I
- PTS2** Peroxisomal targeting signal type II
- TMD** Transmembrane domain
- MAD** Membrane-anchoring domain
- IMS** Intermembrane space
- OXPHOS** Oxidative phosphorylation
- $\Delta\psi$ Membrane potential
- TOM** Translocase of outer membrane
- TIM** Translocase of inner membrane
- PAM** Presequence translocase associated motor
- SAM** Sorting and assembly complex
- MPP** Mitochondrial processing peptidase
- MOM** Mitochondrial outer membrane
- OM** Outer membrane
- UBC6** Ubiquitin conjugating enzyme 6
- TRC40** TMD recognition complex 40
- GET** Guided entry of tail-anchored proteins
- WRB** Tryptophan-rich basic protein
- CAML** Calcium-modulating cyclophilin ligand

3-AT 3-aminotriazole

CHX Cycloheximide

hFIS1 Human Fis1

mtDNA Mitochondrial DNA

S. cerevisiae *Saccharomyces cerevisiae*

E.coli *Escherichia coli*

CL Cardiolipin

SH3 SRC homology 3

SC Synthetic complete

SMM Supplemental minimal medium

Ura Uracil

His Histidine

Leu Leucine

Trp Tryptophan

Pro Proline

CHAPTER 1

INTRODUCTION

It was estimated that 30% - 40% of eukaryotic proteins are integral membrane proteins according to data obtained from growing genomic databases¹. Since these proteins have a role in various cellular processes, proper targeting of them is crucial for function and viability of the cells. Indeed, mislocalization of membrane proteins has been demonstrated in diseases such as Parkinson's, Prion, and Alzheimer's diseases²⁻³, and thus a further understanding of targeting mechanisms of integral membrane proteins has become one of the major interests of the researchers during the last 30 years. Protein targeting research have elucidated that proteins are targeted to different organelles by similar mechanisms which show diversity mainly in the specific components⁴.

Basically, a cytosolic chaperone binds to a targeting sequence of a nascent or fully synthesized protein for initial targeting. Later, the chaperone delivers its cargo to the target membrane. By the help of the specific receptor found on the membrane of the target organelle; the cargo is either taken into the organelle, or integrated into the lipid bilayer via a translocon complex⁴(Figure 1.1). Even though it is an oversimplification, this basic scenario is valid for proteins destined to go to the endoplasmic reticulum (ER), peroxisomes and mitochondria. The targeting sequence of the ER and mitochondrial proteins usually resides at the N-terminus of the proteins while some have internal targeting information. The ER targeting sequence is called a signal sequence or signal peptide, and is recognized by the chaperone Signal Recognition Particle (SRP), a ribonucleoprotein complex. The receptor found on the membrane of the ER, the SRP receptor, interacts with the SRP-ribosome-nascent peptide complex and transfers this complex to a translocon consisting of Sec61 α , Sec61 β , and Sec61 γ proteins⁵. After a protein is transported to the ER, it is sorted to its final destination, which can be the ER, plasma membrane, Golgi apparatus, nuclear envelope, or lysosome,

through the secretory pathway. Despite the presence of evidence showing that there is protein transport between the ER and both peroxisomes and mitochondria^{6,7,8}, almost all of the proteins targeted to either mitochondria or peroxisome are directly transported to these organelles^{9,10}.

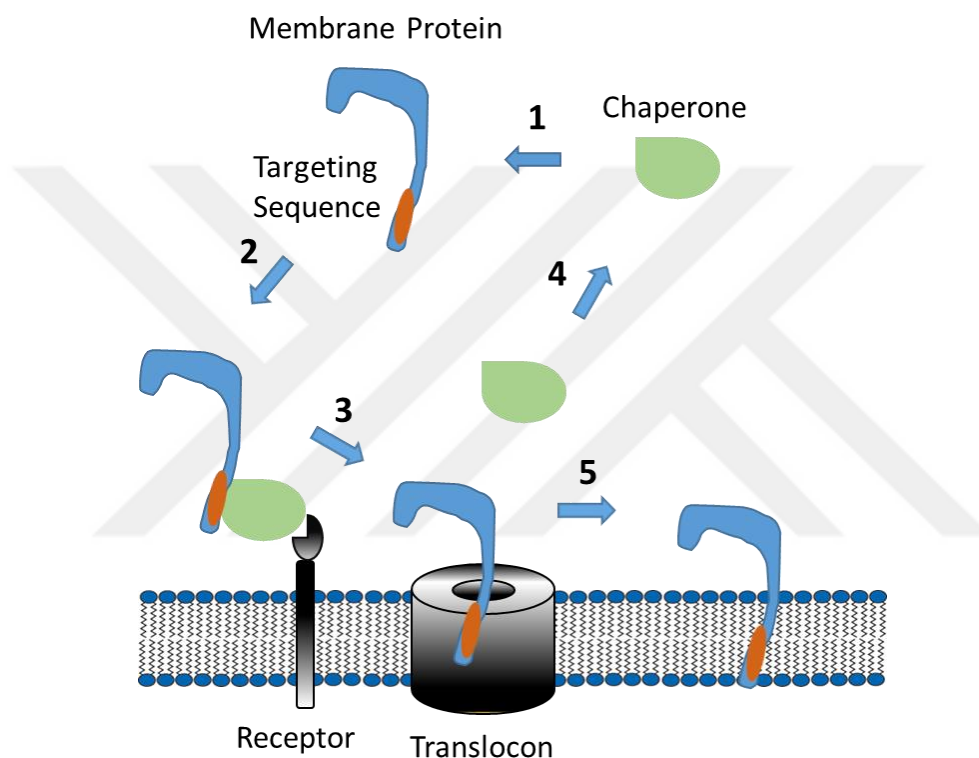


Figure 1.1. **A general model for insertion of integral membrane proteins.** 1) A cytosolic chaperone binds to targeting sequences of a nascent or fully synthesized integral protein. 2) The chaperone delivers the cargo to a target membrane by binding its receptor located on the target membrane. 3) After being released from the chaperone, the integral membrane protein is transferred to a translocon. 4) The chaperone is recycled for the next round and 5) the integral protein is released to the membrane. Adapted from¹¹

Peroxisomal protein targeting occurs post-translationally^{4,12}. One noteworthy feature of peroxisomes is that they are able to import fully folded proteins¹³. Proteins targeted to peroxisomes possess one of the two conserved peroxisomal targeting signals. Most of the peroxisomal matrix proteins contain peroxisomal targeting signal type 1 (PTS1) located at the

C-terminus of the proteins. PTS1 consists of either tripeptide sequence SKL (Ser-Lys-Leu) or its variants¹⁴. Peroxisomal targeting signal type 2 (PTS2) is found at the N-terminus of the peroxisomal proteins. While PTS1 is recognized by the cytosolic receptor Pex5, PTS2 interacts with Pex7 to be delivered to the peroxisomal membrane¹⁵. The multi-protein complex, importomer, found on the membrane of peroxisome consists of docking and RING complex¹⁶. Docking complex is involved in docking of cargo-loaded Pex7 and Pex5 and RING complex takes a role in translocation of these cargos into the matrix of peroxisomes^{17,18,19}. Pex19 is another cytosolic chaperone involved in insertion of the integral peroxisomal membrane proteins²⁰.

Mitochondrial protein translocation occurs both post-translationally and co-translationally which is discussed in detail in the literature review part.

Even though most of the integral membrane proteins have the targeting sequence at the N-terminus, another class of integral membrane proteins, termed tail-anchored (TA) proteins, possess targeting information within the hydrophobic region located at the C-terminus. TA proteins are integrated into the lipid bilayer via this hydrophobic transmembrane domain (TMD). The presence of the TMD and sequences flanking it are necessary and sufficient for proper targeting of TA proteins to the target membrane^{21,22,23}. This carboxy-terminal signal was initially termed 'insertion sequence' to manifest that insertion of these proteins into the lipid bilayer was believed to occur by a spontaneous mechanism.

Mitochondrial TA proteins carry out a wide range of crucial functions, such as taking a role in protein translocation, control of mitochondrial shape and number, and regulation of apoptosis²⁴. Although targeting mechanisms of the ER and peroxisomal TA proteins are known, how mitochondrial TA proteins are targeted to mitochondria is still a mystery^{25,26}. Mitochondrial TA proteins do not have sequence conservation in the TMD region; however, targeting information for mitochondria is harbored within the incompletely defined structural features of the TMD^{27,28}. Researchers have not been able to identify any component of a mitochondrial TA protein insertion machinery so far. Indeed, biochemical and genetics studies suggest that mitochondrial TA proteins might be inserted into the outer membrane of

mitochondria spontaneously, in an unassisted manner, unlike the ER TA proteins whose insertion requires a set of conserved soluble proteins and membrane receptors^{29,30}.

Our knowledge about the general principle of protein targeting to organelles in eukaryotic cells partially originates by the help of genetic selection methods using the organism *Saccharomyces cerevisiae*. In these kind of studies, targeting sequence recognized by the machinery being studied is fused to a protein, whose function is necessary for survival under selective conditions, to mislocalize the protein, and thereby making it inactive. Next, mutations that enable rerouting of the mistargeted protein to its native location where it can function are recovered in selective conditions. While *trans* factors taking a role in protein sorting can be identified by standard genetic methods, *cis* mutations within the targeting sequence can be easily revealed by Sanger sequencing of individual fusion construct clones. This genetic approach has been commonly utilized by different groups to elucidate protein transport through the endomembrane system^{31,32,33} and protein import and export at the mitochondrial inner membrane as well^{34,35}.

Despite the presence of powerful genetic approaches, no eukaryotic protein signal sequence has been analyzed rigorously. However, by taking advantage of next-generation sequencing, it is possible to investigate a protein targeting sequence in a more comprehensive way. In this study, one of our goals was to unravel the molecular mechanism of TA protein insertion into the outer membrane of mitochondria in *Saccharomyces cerevisiae*. However, our major aim was to reveal the structural and sequence features of the TMD of Fis1p - mitochondrial TA protein- required for proper localization of itself to the outer membrane of mitochondria.

Chapter two provides a literature review about an overview of mitochondria and mitochondrial import; a general information about tail-anchored proteins, their insertion mechanisms and physicochemical features of the transmembrane domain of tail-anchored proteins that influence specific membrane targeting preference of tail-anchored proteins. Chapter three contains materials and methods that were utilized in this study. Chapter four describes our findings. Implications and critiques of results were discussed in chapter five. Chapter six presents a summary of the accomplished work and provides an outlook for the future directions.

CHAPTER 2

LITERATURE REVIEW

2.1 Overview of mitochondria and mitochondrial protein import

The cytoplasm of the eukaryotic cells contains different membrane-bound organelles. The mitochondrion is found in the cytoplasm of almost all eukaryotic cells and it has a variety of crucial functions in the cell. It consists of two membranes, the inner and the outer membrane. The inner mitochondrial membrane confines two aqueous compartments which are the matrix and the intermembrane space (IMS). Tubular invaginations that are found in the inner mitochondrial membrane form the cristae that possess various sets of enzyme complexes taking a role in the oxidative phosphorylation (OXPHOS) ³⁶. Besides energy provision role, mitochondria bear other major metabolic pathways which include the Krebs cycle and the β -oxidation of fatty acids ³⁷. Mitochondria are also involved in calcium homeostasis ³⁸, synthesis of Fe-S clusters ³⁹, heme ⁴⁰, and certain phospholipids ⁴¹. Proteome analysis demonstrated that mitochondria have nearly 1000 to 1500 different proteins in yeast and mammals respectively ^{42,43,44}. Due to its endosymbiotic origin, mitochondria lost or transferred a big fraction of its genome to the nuclear chromosome ⁴⁵. Therefore, the mitochondrial genome can encode only about 1% of all mitochondrial proteins that are subunits of the F₁F₀-ATPase synthase and respiratory chain complexes. All other mitochondrial proteins are encoded by the nuclear genome. They are first synthesized in the cytosol as precursor proteins and subsequently imported into mitochondria ^{46,47,48}.

Targeting and sorting of mitochondrial precursor proteins to various mitochondrial subcompartments involve the existence of a signal sequence within the precursor protein. Mitochondrial import signal sequence is usually located at the N-terminus of the proteins,

termed presequence. It consists of positively charged amino acids that form an amphipathic α -helical segment. The length of the presequence may vary from 15 to 122 amino acids⁴⁹. After completion of the import, the presequence is usually proteolytically cleaved by peptidase and other proteases^{50,51}.

The precursor proteins that are destined to go to mitochondria can be divided into two main categories. Mitochondrial matrix proteins and a number of the inner membrane and the intermembrane space proteins with N-terminal cleavable presequence are in the first class. Presequence of these proteins interacts with the mitochondrial import receptors that are found both on the inner and the outer membranes^{46,48}. On the other hand, the second group of mitochondrial precursor proteins possesses internal targeting signals. Almost all of the outer membrane proteins, most of the intermembrane space, and the inner membrane proteins are included in this group. Because of the presence of non-cleavable internal signal sequence, the primary structure of these precursor proteins is same with the primary structure of the mature proteins^{52,48}.

The translocase of the outer mitochondrial membrane (TOM complex) is involved in entry of all nuclear-encoded mitochondrial proteins into mitochondria. The TOM complex is composed of an import pore and numerous preprotein receptors. The precursor proteins can pursue one of three main pathways after they successfully pass through the TOM complex^{52,47,53,54} (Figure 2.1). (1) The precursor proteins containing presequence are delivered to the translocase of the inner membrane (TIM23 complex) which comprises a channel through the inner membrane and collaborate with the matrix heat shock protein 70 (mtHsp70). The chaperone mtHsp70 is the major subunit of the presequence translocase-associated motor (PAM) that is required for ATP-driven transport of preproteins into the matrix. (2) The outer membrane proteins, such as the abundant protein porin, are incorporated into the outer membrane of mitochondria by the sorting and assembly machinery (SAM complex), TOM complex and preprotein import machinery of the inner membrane (MIM complex). (3) The inner membrane proteins, like the metabolite carriers, require chaperone-like proteins of the inner membrane space and the inner membrane translocases (TIM22 and TIM23 complex) for integration into the inner membrane⁵⁵.

Our knowledge related to the general principles of protein transport into mitochondria mainly come from biochemical and genetic studies conducted with the model organism baker's yeast, *Saccharomyces cerevisiae*. Most of the proteins taking a role in mitochondrial

protein import were initially identified in *S. cerevisiae*; however, they were later shown to be highly conserved in higher organisms.

2.1.1 Precursor protein translocation across to outer membrane of mitochondria

Tom70 complex is composed of seven various subunits which can be classified into three groups: Tom20, Tom22 and Tom70 are the receptors; Tom40 is the import pore; Tom5, Tom6, and Tom7 are small Tom proteins that are involved in assembly and stability of the TOM complex^{56,57,58}. A mitochondrial presequence usually consists of 15-122 amino acids that form an amphipathic α -helical segment. One part of the helix, which is recognized by Tom20 receptor⁵⁹, is composed of hydrophobic amino acids. On the other hand, other part of the helix consists of positively charged amino acids and is recognized by the Tom 22 receptor⁶⁰. After recognition of the presequence by Tom20 and Tom22, precursor protein is transferred to the import pore that is made of β -barrel protein Tom40 with the help of Tom5⁶¹. Basically, cytosolic receptors Tom20 and Tom22, small protein Tom5, and channel forming protein Tom40 guide preproteins containing cleavable presequence across to outer membrane. Tom6 and Tom7 are other small Tom proteins which are not involved in preprotein translocation. However, the presence of them in the TOM complex is essential for the stability and assembly of the complex⁶².

The inner membrane proteins, such as the ADP/ATP carrier, are recognized by the Tom70 receptor on the surface of mitochondria instead of Tom20 and Tom22. While these proteins possess several internal targeting signals, they usually lack presequence^{63,64,65}. Because of their hydrophobic nature, the inner membrane proteins are bound by the heat shock proteins, Hsp70 and Hsp90, in the cytosol to prevent their aggregation. Interaction of the heat shock proteins with Tom70 enables delivery of the precursor protein to this receptor⁶⁶. Another mechanism that impedes aggregation of these precursor proteins is binding of numerous Tom70 receptors simultaneously to one precursor protein⁶⁵. After delivery of the inner membrane precursor to Tom70, the precursor is transported to the import pore Tom40, which requires Tom20 and Tom22 receptors and small protein Tom5.

Most of the proteins that are destined to go to mitochondria, are first fully synthesized in the cytosol and subsequently imported into mitochondria (post-translational import), thereby requiring the guidance of cytosolic chaperones as mentioned for the hydrophobic

inner membrane precursors. Besides the heat shock proteins⁶⁶, other cytosolic factors, such as the aryl hydrocarbon receptor-interacting protein and the mitochondrial import stimulation factor⁶⁷, have been demonstrated to interact with preproteins and Tom20⁶⁸. It has been also reported that some mitochondrial precursor proteins can also be transported into mitochondria co-translationally⁶⁹. In this scenario, presequence of the precursor protein interacts with the TOM complex while the C-terminus of the protein is still being synthesized on the ribosome, reminiscent of proteins targeted to the endoplasmic reticulum (ER)⁷⁰. Another group measured translation effectively at the mitochondrial surface in yeast by utilizing proximity-specific ribosome profiling. They found out that mostly the inner membrane proteins are transported into mitochondria in co-translational manner⁷¹.

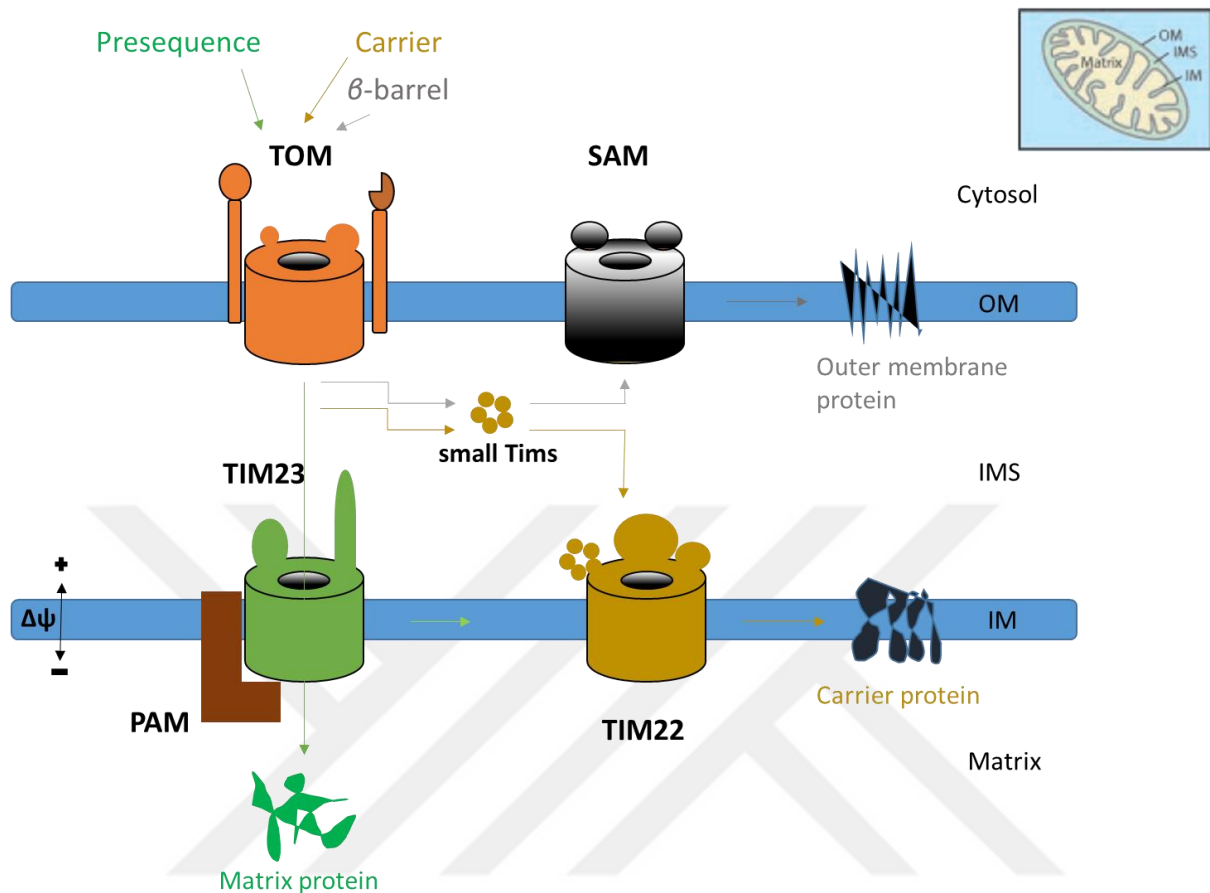


Figure 2.1. **Protein transport pathways into mitochondria.** Most of the mitochondrial precursor proteins with different targeting signals which target proteins to their final destinations within mitochondria are synthesized in the cytosol. After passing through the general entry gate, the TOM complex, precursor proteins are sorted into various mitochondrial sub-compartments. Integration of β -barrel proteins to the outer membrane of mitochondria involves the small Tim chaperones and the sorting and assembly machinery (SAM) complex. Carrier proteins are transported to the inner membrane of mitochondria with the help of small Tim chaperones and the insertion requires carrier translocase, TIM22 complex. Preproteins with presequence are either integrated into the inner membrane or transported into the matrix by the presequence translocase, TIM23 complex. Import into the matrix also requires the function of the presequence translocase-associated motor (PAM). OM, outer membrane; IM, inner membrane; IMS, intermembrane space; $\Delta\psi$, the membrane potential across the inner membrane. Adapted from ^{55,72}

2.1.2 Insertion of the outer membrane proteins

The outer membrane proteins having simple topology (the proteins containing only one transmembrane segment) involve only the TOM complex for integration into the outer membrane. On the other hand, other outer membrane proteins, like porin and Tom40, with a relatively complex topology (β -barrel proteins containing several β -strands) are first transported into the intermembrane space by the TOM complex⁶². In the next step, these precursor proteins are transferred to the SAM complex that is located in the outer membrane by the help of the Tim proteins found in the intermembrane space⁷³(Figure 2.1). The first identified subunit of the SAM complex is Mas37. In the absence of Mas37, mitochondria are able to import the inner membrane and the presequence containing preproteins while integration of the outer membrane proteins is vigorously hampered. The second subunit of the SAM complex, Sam50, which is highly conserved among species was identified later. The C-terminal domain of Sam50 exhibits noteworthy similarity to Omp85, which is the bacterial outer membrane protein and required for protein integration into the outer membrane of bacteria⁷⁴. Basically, the outer membrane proteins containing several β -strands are first imported into the intermembrane space⁶² where they subsequently pursue the bacteria-like pathway of export and insertion into the outer membrane of mitochondria.

Different insertion pathways have been identified for another classes of outer membrane proteins containing α -helical membrane-spanning domain. Tom20 and Tom70 are anchored to the outer membrane of mitochondria via single, N-terminal transmembrane domains. Insertion of these proteins into the lipid bilayer is provided by the outer membrane protein Mim1^{73,75}. Mim1 also supports the integration of multi-spanning outer membrane proteins, such as Ugo1^{76,77}. This process involves the Tom70 receptor while the rest of the TOM complex is dispensable. No insertion machinery has been identified for mitochondrial outer membrane proteins containing a single C-terminal transmembrane domain (tail-anchored), such as the fission protein Fis1^{78,79}.

2.1.3 Precursor protein translocation across to inner membrane of mitochondria

The translocase of the inner membrane is composed of three integral membrane proteins which are Tim17, Tim23, and Tim50⁵³. Presequence carrying preprotein interacts with Tim50 after being released from the TOM complex^{80,81}. With the help of Tim50, the preprotein is then transferred into the channel formed by Tim23⁶⁸. Tim23 consists of 2 domains: The C-terminal domain forms the import channel. On the other hand, N-terminus domain facing to the intermembrane space recognizes the presequence of the preprotein^{67,82,83}. Tim17 is found firmly associated with Tim23 and involved in regulation and stabilization of the channel activity^{84,85,86}. Insertion of the presequence of preproteins into the Tim23 pore is membrane potential dependent. The membrane potential $\Delta\psi$ across the inner membrane has a dual role in the import of the precursor proteins. $\Delta\psi$ is involved in activation of the channel protein. Furthermore, it helps pushing of the presequence towards to the matrix side by exerting an electrophoretic force on the presequence bearing positively charged amino acids^{62,83,87,88}.

Some mitochondrial preproteins contain both a hydrophobic stop transfer signal and a positively charged presequence. Because of the presence of the stop transfer signal, translocation of these proteins across the inner membrane is arrested, thereby resulting in the release of the precursor protein to the lipid bilayer of the inner membrane⁸⁹. Insertion of these kinds of proteins into the inner membrane can be achieved just by the $\Delta\psi$ -driven inner membrane translocase without the involvement of the ATP-dependent presequence translocase-associated motor (PAM)⁹⁰(Figure 2.1).

Most of the presequence containing preproteins are transported into the matrix with the collaboration of the import motor PAM and the presequence translocase. The import motor PAM consists of five subunits which are mtHsp70, Tim44, Mge1, Tim14, and Tim16. Interaction between the chaperone mtHsp70 and the TIM23 complex is provided by the peripheral inner membrane protein Tim44^{91,92,93}. Tim14 is a member of the J-protein family of co-chaperones and is involved in the stimulation of the ATPase activity of mtHsp70^{94,95,96}. Tim16 is required for the recruitment of Tim14 to the import motor PAM^{97,98}. mtHsp70 cooperates with other membrane-bound chaperones; Tim44, Tim14 and Tim16, to hold preproteins while they are leaving the import channel. There are two crucial functions of the

import motor which are passive capturing and active pulling of the precursor proteins^{91,92}. In the ATP-bound state, mtHsp70 can't interact with the preprotein and Tim44 with high affinity. Hydrolysis of ATP to ADP, which is stimulated by Tim14, stabilizes the interaction of mtHsp70 with the preprotein and Tim44. Later, Mge1 mediates releasing of ADP from mtHsp70⁹⁹.

Presequence is removed from the preprotein upon import by the mitochondrial processing peptidase (MPP) which is a metallopeptidase¹⁰⁰. In the matrix of the mitochondria, mitochondrial chaperones, such as Hsp60 and Hsp10, facilitate the folding of the transported proteins to their native conformation^{101,102}.

2.1.4 Insertion of the inner membrane proteins

Most of the multispanning inner membrane proteins lack a presequence. After passing through the outer membrane via the TOM complex, the inner membrane proteins bind to Tim9-Tim10 complex in the intermembrane space^{52,47,80}. The Tim9-Tim10 complex possesses chaperone-like activity which prevents aggregation of the hydrophobic inner membrane proteins in the intermembrane space^{103,104}. In addition to Tim9-Tim10 complex, the homologous but non-essential Tim8-Tim13 complex takes a role in insertion of the inner membrane proteins^{105,106}. The precursor protein is docked to insertion machinery of the inner membrane, TIM22 complex, by the Tim9-Tim10 complex. Tim12 subunit of the TIM22 complex which is a peripheral membrane protein interacts with the Tim9-Tim10 complex for docking of the precursor protein. In the next step, the cargo is transferred to the body of the insertion machinery which is the import channel formed by Tim22^{107,108}(Figure 2.1). Intriguingly, Tim22 exhibits homology with Tim23. Like the Tim23 channel (presequence translocase), the Tim22 channel is also activated by the $\Delta\psi$ ¹⁰⁸. In the insertion of the inner membrane proteins, the membrane potential is the only energy source that is involved, no ATP-driven machinery is required. The membrane potential has a role in insertion of the presequence into the translocase. It is also required for lateral release of the inner membrane proteins into the lipid bilayer¹⁰⁹.

The inner membrane of mitochondria contains another insertion machinery for the inner membrane proteins which are synthesized in the matrix^{110,111}. Oxa1 which is evolutionarily conserved translocase is the major component of this insertion machinery¹¹².

Some nuclear- encoded proteins with presequence are first imported into the matrix, subsequently integrated into the inner membrane by Oxa1¹¹³.

2.2 The overview of tail-anchored (TA) proteins : synthesized in the cytosol and searching for a membrane

Proposal of the signal hypothesis enabled scientists to identify various molecular machineries which target classes of proteins to common, specific destinations within the cell. However, recent studies have shown the existence of a certain group of proteins that are delivered to their target organelle by an unknown mechanism. Tail-anchored (TA) proteins are among these groups of proteins. Due to their diverse functions and localizations in the cell, a great scholarly interest arose in the identification of the targeting and insertion machinery of TA proteins.

TA proteins are a group of integral membrane proteins anchored to the phospholipid bilayer by a single transmembrane domain (TMD) which is located at the C-terminus of the proteins and consists of hydrophobic amino acids ~30 residues¹¹⁴ (Figure 2.2). The N-terminal portion of the proteins faces to the cytosol^{24,28}. TA proteins are found on almost all membranes abutting the cytosol. On those membranes, TA proteins carry out a range of crucial functions, such as playing a role in protein translocation, membrane fission, storage of transcription factors and regulation of apoptosis.

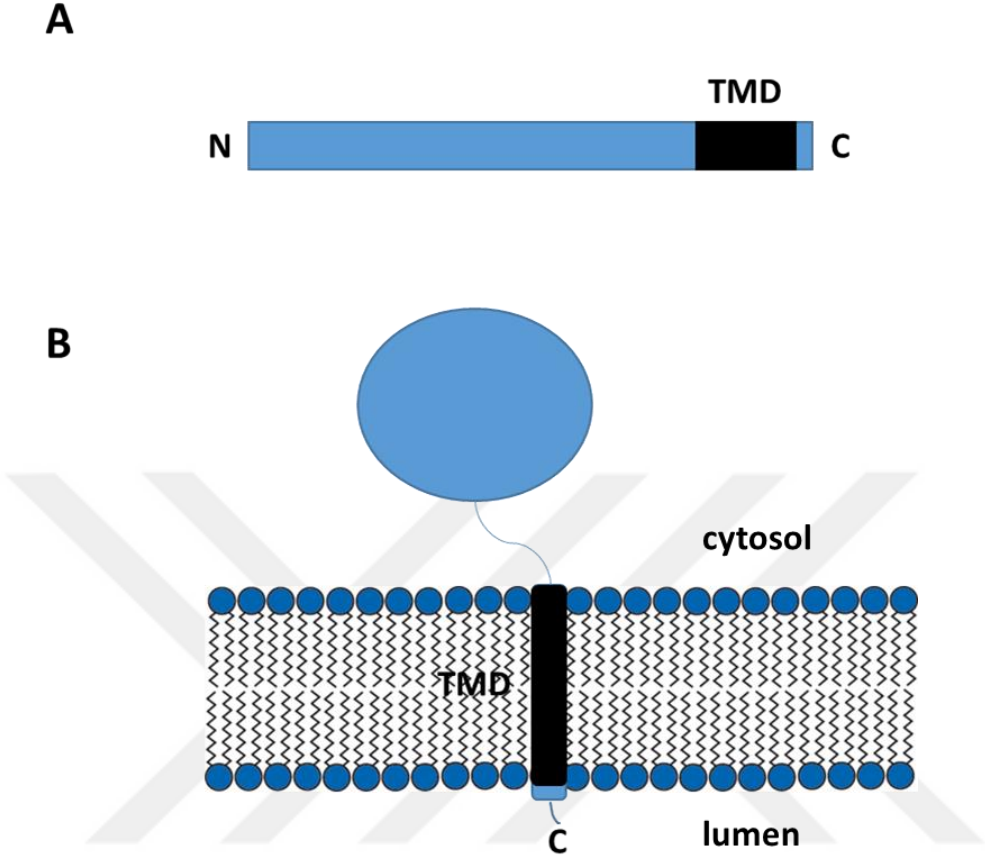


Figure 2.2 **N_{cytosol}-C_{lumen} topology of a Tail-anchored protein.** (A) Tail-anchored proteins contain a single hydrophobic TMD located at the C-terminus of the protein. (B) TA proteins are anchored to phospholipid bilayer via the carboxyl-terminal TMD. The N-terminal bulk of the protein faces to the cytosol.

TA proteins do not have N-terminal signal sequence. Their membrane-interacting domain is too close to the C-terminus and comes forth out of the ribosome only after the protein synthesis has been terminated. Recognition of the hydrophobic TMD by the signal recognition particle (SRP), which interacts with signal sequences only if they are part of a growing polypeptide chain, is highly unlikely¹¹⁴. Furthermore, the last ~ 40 amino acids of the nascent polypeptide chain are sequestered within the large subunit of ribosome¹¹⁵, which also makes the interaction of SRP with the TMD not possible. Therefore, TA proteins have to get to their target membranes post-translationally unlike classical type II membrane proteins. This type of membrane proteins contains a single TMD found at the N-terminus while the C-terminus is exoplasmic¹¹⁶ and are imported to the ER co-translationally in SRP-dependent manner.

Due to the presence of the small number of polar amino acids downstream to the hydrophobic TMD, it was challenging for years to determine whether TA proteins can span the bilayer²¹. The exact topology of the ER TA proteins was verified by taking advantage of recombinant DNA technology. TA proteins were engineered by fusing N-glycosylation sites into the C-terminal polar region^{117,118,119,120}. Glycosylation of these recombinant proteins in the ER lumen *in vivo* and in the cell-free translation system in which microsomes were added after completion of synthesis of the TA proteins demonstrated unequivocally that TA proteins can span the lipid bilayer and translocation of the polar residues across the membrane occurs post-translationally^{117,120}.

Each TA protein possesses its own distinctive tail which has complex and various roles, such as playing a role in the initial targeting and subsequently in the secretory pathway trafficking. The tail may also influence the function of some TA proteins. These properties of the tail of TA proteins distinguish it from other simple lipid anchors of isoprenylated and fatty acylated proteins.

2.2.1 Tail-anchored proteins are targeted to particular intracellular membranes

Even though previous studies have demonstrated that some TA proteins can be inserted into any membrane nonspecifically *in vitro*, like cytochrome b(5), it is now known that TA proteins associate only with particular intracellular membranes *in vivo*¹¹⁴. Most of the TA proteins are first targeted to the ER to join to the secretory pathway. Later, they are

transported to their terminal destination via vesicular transport^{121,117,122,123}. While some peroxisomal TA proteins are first inserted into the ER and subsequently delivered to peroxisome¹²⁴, the majority of them are directly targeted to peroxisome¹²⁵. Likewise, mitochondrial outer membrane (MOM) proteins are also directly delivered to mitochondria from cytosol¹¹⁴. Since the majority of TA proteins are destined to go to either the ER or mitochondria, after releasing from the ribosome, they have to discriminate between the ER and mitochondria.

Experiments in which the TMD of a mitochondrial TA protein fused to cytosolic domain of an ER tail-anchored protein verified that features discriminating between the ER and mitochondria reside in the TMD region^{126,127,128,129} (Figure 2.3). In mitochondrial TA proteins, the TMD region is usually shorter than 20 residues and is flanked by basic amino acids (Figure 2.3A). Decreasing the number of the positively charged amino acids that are found in the flanking regions or enhancing the length of the TMD elucidated that these two features are doubtlessly essential for mitochondrial targeting^{130,128,131,132,133}. However, some mitochondrial TA proteins, like Bax, do not meet the short TMD criterion since TMD of Bax has ample length and hydrophobicity¹¹⁴. Furthermore, the interaction of the N-terminal cytosolic domain may have a role in targeting^{134,135}.

TA proteins that do not have precise features for targeting to the MOM are delivered to the ER, which can accept TMDs with different lengths and C-terminal regions of different charge and size (Figure 2.3B and Figure 2.3C). Mutated mitochondrial TA proteins with longer TMD or less positively charged amino acids in the flanking regions are inserted to the ER. In addition, artificial TMDs containing repeated leucines or a couple of hydrophobic amino acids are able to target TA proteins to the ER^{136,137,119}. These observations clearly show that the ER is the default harbor for TA proteins¹³⁸.

Mitochondrial targeting information is not a discrete signal; on the contrary, it is a combination of two physicochemical variables which are a degree of positive charges found in flanking regions and length of the TMD. Therefore, TA proteins with faint MOM targeting information may be inserted to both the MOM and the ER (Figure 2.3D)

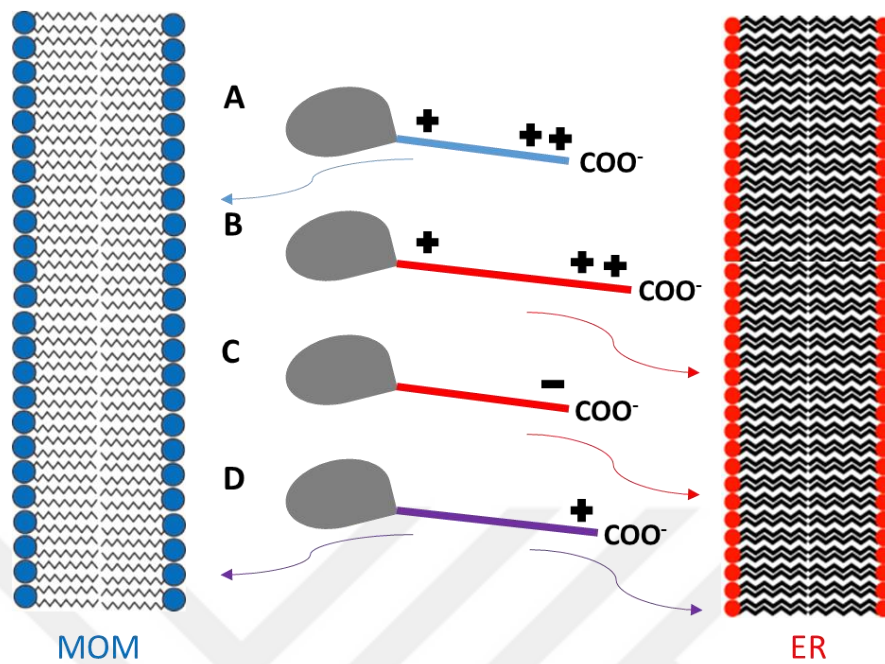


Figure 2.3. **Features that regulate targeting of TA proteins to the ER or the MOM.** The cytosolic domains of the proteins, A-D, are shown as gray while the color of the C-terminal TMD region matches with the corresponding membrane. (A) Shorter TMD compared to TMD of the ER TA proteins with positively charged amino acids at flanking regions is required for the MOM targeting. (B-C) Loss of any of these features causes insertion into the ER. (D) TMDs with intermediate features (purple), lengthened TMD and/or declined positive charge, may target a TA protein to both the ER and the MOM. Adapted from¹¹⁴

After insertion into the membrane of ER, a TA protein either stays on the ER or is transported to its final destination. During this sorting process, TMD again enacts a crucial role. Positively charged amino acids found in the luminal sequence seem to determine the targeting to peroxisomes^{124,139}. However, sorting in the secretory pathway is firmly affected by the physicochemical features of the TMD. The ER resident TA proteins contain a moderately hydrophobic and short TMD which influences the exit of the protein from the ER by slowing the entry into the transport vesicle and retrieval from the Golgi¹²⁰. Lengthening of the tail region of ubiquitin conjugating enzyme (UBC6)¹³⁷, or cytochrome b(5)¹²³, or the ER SNARE Ufe1p¹⁴⁰ causes escaping of these proteins from the ER and subsequently entry into down the secretory pathway. Hydrophobicity and length of the TMD also determine sorting of TA proteins in the secretory pathway¹⁴¹.

Besides the physicochemical features, sequence-specific characteristics of the tail region of some TA proteins may influence sorting. An essential example is the target SNAREs Syntaxins 3 and 4, which reside on the basolateral and apical plasma membrane of the polarized epithelial cells respectively¹⁴². Although TMDs of both of these proteins have nearly the same hydrophobicity, they are sorted to different membranes. GFP fusion experiments unequivocally revealed that sequence specific information within the TMD has a role in the partition of these TA proteins on the membrane of polarized epithelial cells¹⁴³. Sequence-specific features may also be essential for proper functioning of TA proteins, as in the case of SNAREs¹⁴⁴

The contribution of the cytosolic domain of some TA proteins in their sorting cannot be neglected. Targeting of some Golgi-resided TA proteins is determined by both the TMD and the cytosolic domain^{122,145,143}. In like manner, the features that affect SNARE trafficking are located both in the tail region and cytosolic domain¹⁴⁶.

2.2.2 How are tail-anchored proteins inserted into the membrane of various organelles?

TA proteins are able to translocate their C-terminus across the membrane of the ER and presumably the MOM as well even though this was not elucidated experimentally. The intriguing question here is whether the conventional translocation mechanisms, such as the Sec61 translocon of the ER translocation machinery or TOM complex of the MOM, have a role in the insertion of TA proteins.

2.2.2.1 Insertion of TA proteins into the membrane of the ER

Signal recognition particle (SRP) is the first identified cytosolic factor that is involved in the post-translational targeting of TA proteins destined to go to the ER. Crosslinking studies revealed the interaction between the TMD domain of the model TA protein and the SRP¹⁴⁷. The same interaction was also verified *in vitro* pull down experiments¹⁴⁸. Furthermore, another study demonstrated that insertion of TA proteins to the ER diminished when the SRP receptor is perturbed¹⁴⁸. On the other hand, the functional relevance of the proximity of TA proteins to the Sec61 is not clear. In addition to biochemical reconstitution

experiments²¹, studies in which conditional mutants of yeast were used revealed that Sec61 translocon is not required for insertion of TA proteins^{149,150}.

Insertion of some TA proteins involves ATP¹¹⁷. However, the function of SRP is GTP dependent^{147,151,117}, which contradicts the potential role of SRP in TA protein targeting. Hsp40/Hsc70 family molecular chaperones are ATPases and it has been proposed that these chaperones can facilitate insertion of TA proteins to the ER as they promote post-translational import of specific pre-secretory proteins into the lumen of the ER¹⁵². This proposal was supported by recapitulating the insertion of a model TA protein *in vitro* system by using purified precursor proteins with ATP and recombinant Hsp40/Hsc70¹⁵³. Although this study revealed that the presence of Hsp40/Hsc70 is sufficient for TA protein insertion into the ER, another group showed that these chaperones are solely essential for efficient insertion of some TA proteins by utilizing small molecular inhibitors of Hsp70¹⁵⁴. There is not any known receptor of Hsp40/Hsc70 at the ER and the exact mechanism by which TA proteins using these molecular chaperones are inserted into the ER is not clear. One of the suggestions is that chaperones bind to TA proteins to block their integration into inappropriate membranes, and target them to the ER where they insert themselves spontaneously in unassisted ways^{155,156}.

Identification of an ATP-dependent, novel pathway shed light on the mysterious process of TA proteins insertion into the membrane of the ER¹⁵⁷. Crosslinking experiments have demonstrated the interaction of various model TA proteins with a cytosolic, 40kDa, TMD recognition complex (TRC40)^{158,159}. TRC40 is highly conserved among species. Its yeast (*Saccharomyces cerevisiae*) homolog is termed Get3¹⁶⁰. With the identification of additional components in yeast, the investigation of the GET pathway has accelerated. A complex that functions at the upstream of TRC40 consists of TRC35, BAG6, Ubl4A (mammalian nomenclature). This complex collects TA proteins as soon as they are released from the ribosome and loads them onto TRC40 for transport to the ER^{148,161}. Sgt2, which is the yeast homolog of SGTA, interacts with TA proteins¹⁶² and serves as a scaffold protein to bring TRC35 and Ubl4A together¹⁶³. The cargo TA protein is delivered to an ER receptor which consists of tryptophan-rich basic protein (WRB) and calcium-modulating cyclophilin ligand (CAML) by TRC40. Get1 and Get2 are yeast equivalents of WRB and CAML respectively.

Several cytosolic factors and specific events on the membrane of the ER are involved in the global level tail-anchored protein insertion^{157,116}. Each of these mechanisms has been

detailed above. Indeed, these pathways are redundant, for example a yeast strain defective in GET pathway does not exhibit any growth defect^{155,164}. One possible explanation for this outcome is that Hsp40/Hsc70 can suffice for the insertion of a sufficient amount of TA protein when GET pathway is perturbed^{154,155}. It has also been proposed that a particular TA protein may prefer a specific pathway depending on distinct features like the hydrophobicity of the TMD. TA proteins with the hydrophobic tail region, such as synaptobrevin, appear to prefer TRC40 or SRP while the ones possessing a less hydrophobic TMD, like cytochrome b(5), favour specific chaperone-mediated or unaided pathways¹⁵⁵.

2.2.2.2 Insertion of TA proteins into the membrane of peroxisome

While TA proteins targeted to ER usually do not favour classical translocation machinery, peroxisomal TA proteins are inserted to peroxisomes by a mechanism which is common to the post-translational insertion of other peroxisomal membrane proteins (Class D). Insertion of class I peroxisomal proteins involves import receptor Pex19. Pex19 binds its cargo in the cytosol and delivers the cargo to peroxisome by interacting with its receptor, Pex3, found on the membrane of peroxisome^{125,165}. It has been shown that both TMD and luminal domain of Pex26 (mammalian TA protein) accommodate Pex19 recognition sequences and interaction of both of these sequences with Pex19 is necessary for targeting of Pex26 to peroxisome¹⁶⁶. If Pex26 lacks the luminal recognition sequence, it is targeted to mitochondria¹⁶⁶. Similar recognition sequences were also found in yeast Pex15 which is a functional orthologue of Pex26¹⁶⁶.

Fission protein Fis1 is another TA protein targeted to peroxisomes. Human Fis1 is mainly found on the outer membrane of mitochondria; however, a small fraction is also delivered to peroxisomes. Like Pex26, targeting of Fis1 to peroxisomes depends on the function of Pex19¹⁶⁷.

2.2.2.3 Insertion of TA proteins into the outer membrane of mitochondria

Mitochondrial TA proteins do not have sequence conservation in the TMD region; however, targeting information for mitochondria is harbored in the physicochemical features of the TMD²⁷. While ER insertion machinery can favor tail domains with various

hydrophobicity, flanking charges and length, mitochondrial TA proteins are usually characterized by TMDs with moderate hydrophobicity. Besides, the presence of positive charges at the flanking regions (on one or both sides) of the TMD is another major characteristic of mitochondrial TA proteins. Mutagenesis studies have demonstrated that perturbation of any of these physicochemical features results in the rerouting of the model TA protein to the ER^{130,168,131,79}. Even though these features are able to differentiate the population of TA proteins targeted to mitochondria from the ER counterparts, positive charge content and hydrophobicity of TMD of mitochondrial and ER TA proteins exhibit quite some overlap²⁸. However, the tendency for α -helix formation of TMD of mitochondrial TA proteins provides an additional structural feature to TMD for mitochondrial targeting¹⁶⁹. Each of these features has a distinct contribution on targeting of different TA proteins to mitochondria²⁷.

The importance of the presence of positively charged amino acids at the flanking regions of the TMD is highlighted by studies in which the intracellular localization of the Bcl-2 family proteins was shown. Bcl-2 family proteins are the major apoptosis regulators which are divided into two classes. Anti-apoptotic members, like Bcl-2 and Bcl-x_L, help cells to evade from apoptosis; on the other hand, pro-apoptotic members, such as Bak and Bax, trigger apoptosis¹⁷⁰. Bcl-x_L is solely found on the outer membrane of mitochondria¹³³ while Bcl-2 can localize on both the nuclear envelope and the membrane of the ER¹³³. Intriguingly, the TMDs of both Bcl-x_L and Bcl-2 have similar lengths and hydrophobicities. However, two positively charged amino acids that are found at either flanking region of the TMD of Bcl-x_L play an essential role in mitochondrial sorting of this protein¹³³. The lack of this signal within the TMD of Bcl-2 results in targeting of the protein to various intracellular membranes in a nonspecific manner.

Studies investigating how tail-anchored proteins are inserted into the outer membrane of mitochondria came up with contradictory results. Setoguchi et al. demonstrated that the TOM complex has no role in the insertion of three mitochondrial TA proteins (Bcl-x_L, Omp25, and Bak) in mammalian cells¹⁷¹. Likewise, TOM machinery is not involved in insertion of Fis1 (mitochondrial fission protein) *in vitro*⁷⁹. While Tom20 has been thought to participate in the import of Bcl-2^{132,172}, Tom22 was implicated as the receptor that recognizes Bax for insertion¹⁷³. Apart from Tom40, Tom20 and Tom70, all other subunits of the TOM complex (Tom5, Tom6, Tom7 and Tom22) are TA proteins even though they differ in TA sequence and structure. Insertion of Tom22 requires Tom20 and Tom70¹⁷⁴ and is promoted by

the β -barrel SAM/TOB (sorting and assembly machinery/topogenesis of β -barrel proteins) complex. All of these TOM complex TA components contain proline residue within the TMD in yeast. The presence of proline within the TMD of Tom7 is necessary for efficient insertion of the protein¹⁷⁵. The proline residue which is an α -helix breaker provides some flexibility to TMD to secure a smooth integration of the protein into the MOM¹⁷⁵. Moreover, integration of Tom6 and Tom7 into the outer membrane of isolated mitochondria was hampered when cytosolic domains of the outer membrane receptors were removed proteolytically¹⁷⁶. All these findings indicate that TA protein insertion into the outer membrane of mitochondria is controlled by more than one mechanism.

What makes the understanding of targeting of TA proteins to the MOM challenging is the moderately hydrophobic characteristic of the TMD of mitochondrial TA proteins. This feature implies that mitochondrial TA proteins should be able to integrate into the MOM without assistance. In fact, insertion of Fis1⁷⁹, Bcl-2¹⁵¹ and mitochondrial isoform of b5⁷⁹ into protein-free lipid bilayer has been validated. In addition, augmented ergosterol level in these protein-free bilayers impeded the insertion. The MOM has the lowest amount of ergosterol among all membranes that face to the cytosol in yeast⁹ and low ergosterol level elevates fluidity of a membrane⁷⁹. This characteristic of the MOM facilitates faster insertion of mitochondrial TA proteins which provides a kinetic advantage to mitochondria compared to other organelles⁷⁹. This unassisted integration shown *in vitro* may mask chaperone-mediated specific targeting occurring *in vivo*.

CHAPTER 3

MATERIAL AND METHODS

3.1 Yeast strains and plasmids

Details and associated references of strains used in this study are given in APPENDIX A. Construction details of plasmids and related references of the acquired plasmids are provided in APPENDIX B. Oligonucleotides utilized in this work are listed in APPENDIX C.

3.2 Culture conditions

Synthetic complete (SC) medium consists of 0.67% yeast nitrogen base lacking amino acids, 0.1% casamino acids, 2% dextrose, 50 µg/ml adenine hemisulfate, and either 100 µg/ml L-tryptophan (SC-Ura) or 25 µg/ml uracil (SC-Trp). Supplemental minimal medium (SMM) consists of 0.67% yeast nitrogen base lacking amino acids, 2% dextrose, 20 µg/ml adenine hemisulfate, 20 µg/ml methionine, 20 µg/ml uracil, 30 µg/ml lysine. SMM also contains 20 µg/ml histidine, 100 µg/ml leucine, and/or 20 µg/ml tryptophan depending on selection condition. SLac medium devoid of histidine consist of 0.67% yeast nitrogen base lacking amino acids, 1.2% NaOH, a volume of lactic acid to adjust the pH to 5.5, 20 µg/ml uracil, 20 µg/ml adenine hemisulfate, 20 µg/ml methionine, 20 µg/ml tryptophan, 30 µg/ml lysine, and 100 µg/ml leucine. Solid media also contain 1.7% bacteriological agar. Cells were incubated at 30°C unless indicated. For serial dilution assays, strains in logarithmic proliferation phase were diluted to an OD₆₀₀ of 0.1, and 4 µl of this dilution and three serial five-fold dilutions were spotted to a solid medium.

3.3 Microscopy

For epifluorescence microscopy studies, cells grown to logarithmic phase of proliferation were examined by using an Eclipse 80i microscope with a 100X Plan Fluor objective and linked to a DS-Qi1Mc camera (Nikon, Tokyo, Japan). Cells were grown in SMM medium suitable for plasmid selection. Images were captured using NIS-Elements version of AR 3.2 and exposure times were set automatically. The brightness of all mCherry expression images were identically adjusted in Adobe Photoshop CS5 (Adobe, San Jose, California), besides when the mCherry-BAX (TA) signal was assessed. For this case, the ‘autolevels’ adjustment was preferred. Scoring of mitochondrial morphology was performed blind to genotype. Sodium azide was used at a concentration of 500 μ M for 60 min before fluorescence microscopy to induce mitochondrial fragmentation. For staining of mitochondrial nucleoids, 4',6-diamidino-2-phenylindole (DAPI) was added to cultures at a concentration of 1 μ g/ml and cells were incubated for 15 min before analysis. Scale bars represent 5 μ m.

3.4 Fis1p TA mutant library construction

Constructs expressing Gal4-Fis1p and its mutated version at one of 27 positions within the TMD of Fis1p were generated by using recombination-based cloning¹⁷⁷. Two DNA fragments obtained by PCR were integrated in this recombination reaction. The 5' segment was generated by PCR from template plasmid b100 using primer 698 and the suitable primer (rvsposX) listed in APPENDIX C. The 3' portion was amplified from plasmid b100 using the relevant primer (fwdposX) and primer 517 listed in APPENDIX C. Two PCR products were co-transformed into the strain MaV203 with *NotI*-linearized pKS1 to recombine DNA fragments into the linearized plasmid. Each sub-library of each Fis1p TMD position was generated individually by selection of Trp⁺ clones in liquid medium. To confirm transformation and recombination efficiency, a portion of each transformation reaction was plated onto the solid SC-Trp medium. Later, equal number of cells which were determined by OD₆₀₀ measurement were collected from overnight culture of each sub-library and combined within the same liquid culture to generate the total pool prior to selection for Gal4-mediated transcription. It should be noted that all the constructs

expressing Gal4-Fis1p also have superfolder GFP in frame between the Gal4p and Fis1p segment. Labelling of sfGFP was omitted from both figure labels and the text for simplicity.

3.5 Deep mutational scanning of the Fis1p TA library

The total pool of the constructs containing Fis1p TMD mutations were grown for four generations in SC-Trp medium, SC-Ura medium and SMM-Trp-His medium with 0 mM, 5 mM, 10 mM, or 20 mM 3-AT. Later, plasmids from each culture condition were isolated from 10 OD₆₀₀ units of cells. For the isolation of the plasmids, cells were pelleted at 4,000g for 3 min. Pellets were then washed with 5 ml of 0.9 M D-sorbitol and resuspended in 1 ml of 0.9 M D-sorbitol. At this stage, one ‘‘stick-full’’ of zymolyase 20T (Amsbio, Abingdon, United Kingdom) was added, and cells were incubated at 37°C for 45 min. Cells were pelleted again at 4,000g for 3 min and processed using a plasmid purification kit (GeneJET Plasmid Miniprep Kit, Thermo Scientific, Waltham, USA) following the manufacturer’s instructions. Primers 882 and 883 were used to amplify the genomic region encoding the Fis1p TMD from each plasmid pool. By using the generated PCR products, next generation, paired-end sequencing was performed by Microsynth (Balgach, Switzerland) on a MiSeq Nano (2x150v2). FASTQ output from paired ends and lacking adaptor sequences was merged into a single segment by using the PANDAseq assembler version 2.8¹⁷⁸. To remove the flanking sequences around the Fis1p and stop codon encoding region, the TRIM function (trimmer Galaxy tool version 0.0.1) was performed using the resources of the Galaxy Project¹⁷⁹. The rest of the analysis was performed in Microsoft Excel (Redmond, USA). First, DNA sequences were converted to amino acid sequences and then TMDs with more than one amino acid mutation were eliminated. Enrichment values reflect, at a given amino acid position, the ratio of the fraction of amino acid counts following selection to the fraction of amino acid counts in the starting library. Enrichment values are not derived through comparisons across different amino acid positions. Counts for the native amino acid at each position were set as the total number of TMD counts for which all amino acids were wild-type within a given selected pool. While calculating the enrichment values, TMD amino acid replacements for which there were zero reads in the

SC-Trp sample had their value changed to one in order to allow possible detection of enrichment under selective conditions by preventing division by zero. Heat maps were generated using the Matrix2png utility¹⁸⁰ by Dr. Cory Dunn.



CHAPTER 4

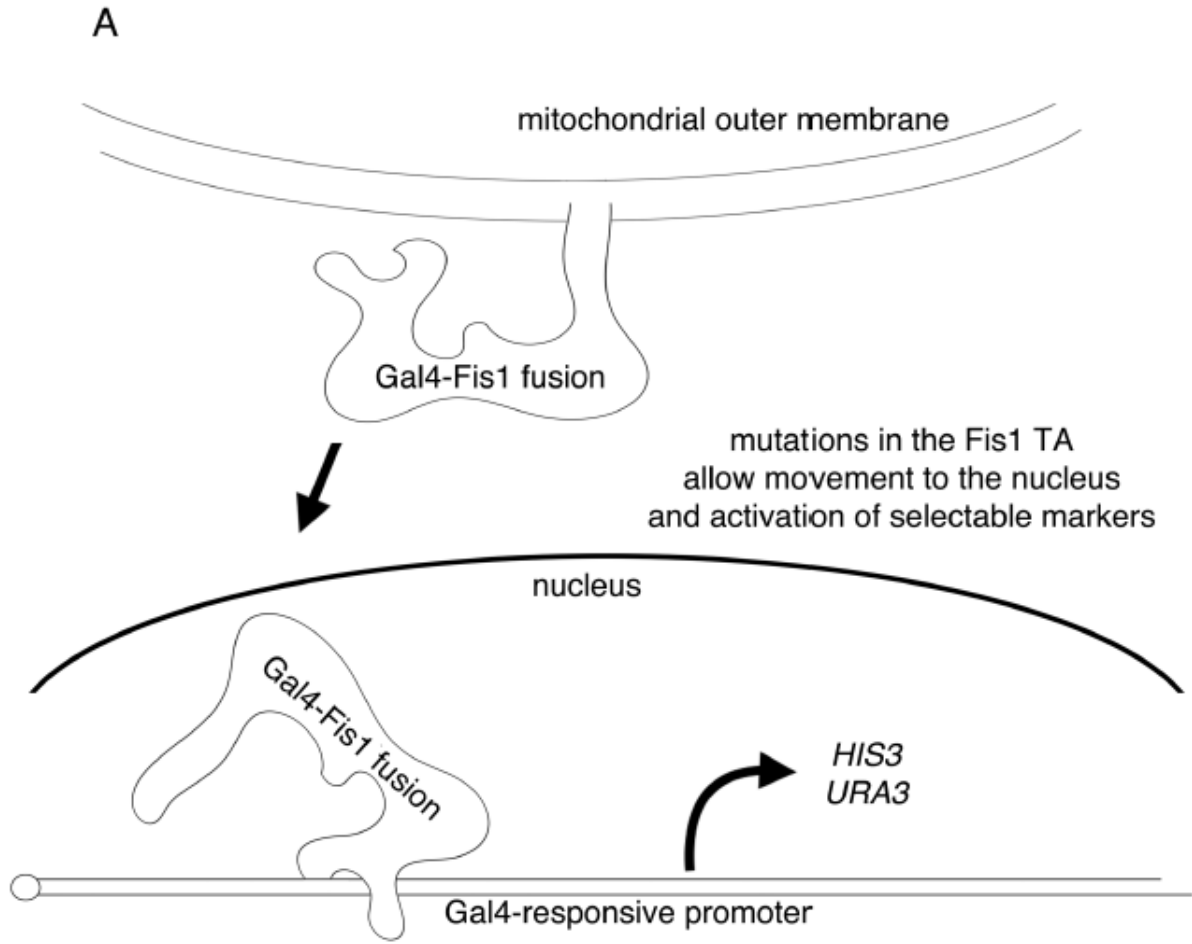
RESULTS

4.1 Targeting of the fusion protein to the outer membrane of mitochondria via the Fis1 tail anchor hampers Gal4-mediated transcription activation

It was previously shown that tail anchor (TA) of Fis1p is necessary¹⁸¹ and sufficient^{79,182} for proper insertion of this protein into the MOM. Fis1p has been proposed to settle a final topology in the MOM in which while the amino-terminal bulk of the protein faces the cytosol, positively charged amino acids found within the carboxyl-terminus protrudes into the mitochondrial intermembrane space. The two are connected by a membrane-anchoring domain (MAD) passing through the outer membrane (OM)¹⁸¹.

To identify the *trans* factors related to Fis1p insertion or to reveal *cis* mutations in the targeting sequence of Fis1p for understanding structural and sequence characteristics crucial for localization of Fis1p in *Saccharomyces cerevisiae*, we used a positive selection procedure which is based on viability following mislocalization of a chimeric protein. Similar genetic approach has been effectively utilized by different groups to isolate mutants in the yeast secretory pathway³¹ or mutants in mitochondrial import³⁵. For the screening purpose, we created a chimeric protein by fusing Gal4 transcriptional factor to the N-terminus of full-length Fis1p. According to our hypothesis, we reasoned that the chimeric protein is inserted into the mitochondrial OM in the wild type cells because of the targeting information found within the TA of Fis1p. However, *cis* or *trans* mutations will allow movement of the chimeric protein into the nucleus and result in activation of the Gal4-driven *HIS3* and *URA3* auxotrophic markers (which are inactive in the wild type cells) in MaV203, a strain commonly used for yeast-two-hybrid assays. Activation of these markers will allow us to select the *cis* or *trans* mutants under selective conditions (Figure 4.1A). We also included superfolder GFP¹⁸³ between the Gal4 and Fis1 moieties; however, the intensity of the signal was hardly discernable during the fluorescence microscopy. Only when the chimeric protein was overexpressed, GFP fluorescence was visible at

mitochondria (Figure 4.2). Therefore, we will not further refer to the presence of sfGFP while discussing Gal4-Fis1 constructs. Furthermore, we demonstrated that Gal4-Fis1p chimeric protein failed to complement the mitochondrial morphology defect of a *fis1* Δ strain (Figure 4.2 and unpublished results), which suggests that our chimeric protein is not able to interact with other mitochondrial division components that may possibly hamper nuclear localization of Gal4-Fis1p as a result of TA mutation. Like the empty vector, Gal4-Fis1p fusion protein was also incapable of providing growth on selective media; medium lacking uracil and medium lacking histidine containing 20 mM 3-aminotriazole (3-AT) which competitively inhibits His3p generated independently of Gal4p activation¹⁸⁴(Figure 4.1B). However, deletion of the TA region from the same construct [Gal4-Fis1 (Δ TA)] resulted in ample proliferation on both of the selective media. This result suggests that absence of the TA results in translocation of the chimeric protein to the nucleus and cytosolic domain of Fis1p has no role in the insertion of the protein into the MOM.



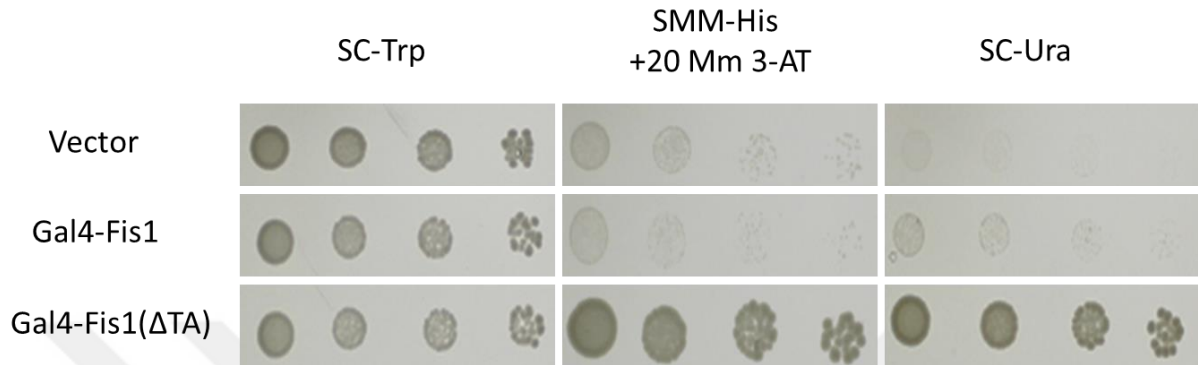
B

Figure 4.1. **A genetic selection method based on mislocalization of the Gal4-Fis1p fusion which allows identification of *cis* or *trans* mutants by blocking mitochondrial localization of the chimeric protein.** (A) A scheme for selection of *cis* or *trans* mutations that impede insertion of the chimeric protein to the mitochondrial OM. The chimeric protein consists of transcription factor Gal4 fused to full-length Fis1p (There is also sfGFP between the Gal4 and Fis1 moieties, not shown). Mutations that prevent localization of the fusion protein to mitochondria allow movement of the Gal4 containing chimeric protein to the nucleus, thereby activating *HIS3* and *URA3* reporters (Courtesy of Dr. Dunn). (B) Deletion of the TA enables cells to grow on medium involving *HIS3* or *URA3* activation. The strain MaV203 expressing Gal4-Fis1p variants from plasmids b100 (WT), b101 (ΔTA), or containing empty vector pKS1 was grown in SC-Trp medium, later, following serial dilution, spotted to SC-Trp, SMM-His + 20 mM 3-AT, or SC-Ura for 2d.

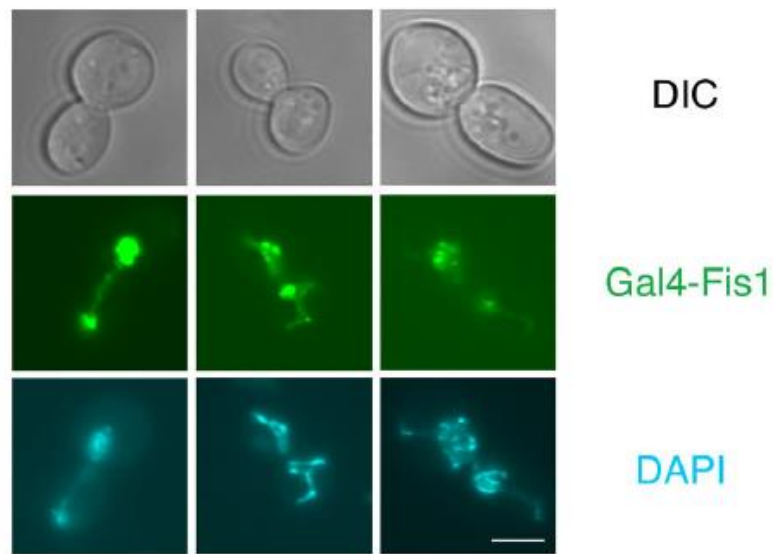


Figure 4.2. A **Gal4-Fis1 chimeric protein localizes to mitochondria.** *fis1Δ* strain CDD692 was transformed with plasmid b102, expressing a Gal4-Fis1p construct also harboring a central sfGFP domain from a high-copy plasmid. Mitochondrial DNA of live cells was stained with DAPI to reveal mitochondrial location. Mitochondrial DNA and Gal4-sfGFP-Fis1p were visualized by fluorescence microscopy.

After we show that our experimental setup is applicable, we directly started to look for *cis* or *trans* mutations that would hinder targeting of Gal4-Fis1p to the MOM by isolating colonies that are able to grow on medium lacking uracil.

4.2 Searching for the *trans* factors related to targeting of Fis1p to the outer membrane of mitochondria

We found with 33 Ura⁺ isolates which harbor either *cis* or *trans* mutation after the screen. Since our first aim is to identify *trans* factors taking a role in Fis1p targeting, we focused on selecting *trans* mutants. We mated these 33 Ura⁺ isolates (haploid) to the opposing mating type of yeast to identify recessive nuclear mutants defective in Fis1p insertion. If the trait is recessive and independent of the plasmid, the phenotype should disappear after the mating, meaning that diploids cannot survive under selective conditions. However, after sporulation, tetrad analysis should give two wild type spores and two mutant spores defective in Fis1p targeting. Following mating of these 33 Ura⁺ isolates with the opposing mating type strain (AH109), we found just one diploid strain which was unable to grow on selective medium, suggesting that the phenotype is due to a chromosomal mutation rather than being dependent on the plasmid. However, after sporulation, the phenotype had disappeared. We did not observe activation of the reporters by the wild type Gal4-Fis1p construct in any of the spores. In conclusion, we could not find any *trans* mutant strain.

We also took advantage of candidate-based approach to be able to identify any component of the mitochondrial TA protein insertion machinery. Proteomic analysis of the yeast mitochondrial outer membrane conducted by Zahedi et al.¹⁸⁵ informed us that some of the outer membrane proteins that they identified may have a role in Fis1p insertion. From the list of all proteins identified in the mitochondrial outer membrane, we picked the ones which are non-essential and may be related to the insertion of Fis1p. We also looked for some other potential proteins, unrelated to the mitochondrial outer membrane but might function in Fis1p insertion. Following selection of the potential proteins, we ordered the strains (from EUROSCARF) each of which lacks the coding sequence of one of the potential proteins playing a role in Fis1p insertion (Table 4.1). Next, we transformed these strains with b109 plasmid encoding mCherry-Fis1 TA protein. We already know that the TA of Fis1p is necessary and sufficient for mitochondrial targeting of mCherry. However, in all of the deletion strains (except *spf1Δ*), mCherry-Fis1 TA construct localized to mitochondria, suggesting that none of these proteins have an influence on insertion of

Fis1p into the MOM. It was already known that deletion of *spf1p* causes mislocalization of mitochondrial TA proteins to the ER (details were discussed in the discussion part).

Table 4.1. Potential candidate proteins playing a role in Fis1p insertion

Name of the strain	Localization of the deleted protein	Function of the deleted protein	Localization of the mCherry-Fis1 TMD construct
CDD948 (<i>get2</i> Δ)	The ER membrane	<ul style="list-style-type: none"> • Protein insertion into the ER membrane 	Mitochondria
CDD949 (<i>spf1</i> Δ)	The ER membrane	<ul style="list-style-type: none"> • Cellular calcium ion homeostasis • Cellular manganese ion homeostasis • Sterol homeostasis • Transmembrane transport 	The ER
CDD951 (<i>tom6</i> Δ)	MOM	<ul style="list-style-type: none"> • Mitochondrial outer membrane translocase complex assembly • Protein import into mitochondrial matrix 	Mitochondria
CDD952 (<i>om14</i> Δ)	MOM	<ul style="list-style-type: none"> • Protein targeting to mitochondrion • Ribosome localization 	Mitochondria

CDD953 (<i>get3Δ</i>)	Cytosol	<ul style="list-style-type: none"> • ATP-independent chaperone mediated protein folding • Pheromone-dependent signal transduction involved in conjugation with cellular fusion • Posttranslational protein targeting to the ER membrane • Protein insertion into ER membrane • Retrograde vesicle-mediated transport, Golgi to ER 	Mitochondria
CDD954 (<i>get1Δ</i>)	The ER membrane	<ul style="list-style-type: none"> • Protein insertion into ER membrane • Retrograde vesicle-mediated transport, Golgi to ER 	Mitochondria
CDD955 (<i>scm4Δ</i>)	MOM	<ul style="list-style-type: none"> • Molecular function unknown 	Mitochondria
CDD956 (<i>msp1Δ</i>)	MOM and Peroxisomal membrane	<ul style="list-style-type: none"> • ATPase activity • Protein targeting to mitochondrion 	Mitochondria
CDD957 (<i>tom7Δ</i>)	MOM	<ul style="list-style-type: none"> • Protein import into mitochondrial matrix • Protein import into mitochondrial outer membrane 	Mitochondria

Since we could not acquire any solid result related to mitochondrial TA protein insertion machinery, we focused on the understanding of the structural and sequence characteristics of the TA of Fis1p which is essential for localization of Fis1p to mitochondrial OM.

4.3 *Cis* mutations allowed us to gain insight into the structural and sequence characteristics of the TA of Fis1p

As it was mentioned before, after the screening, we came up with 33 Ura⁺ isolates and only one of them was the potential recessive nuclear mutant. Since Ura⁺ phenotype of

other 32 isolates is dependent on the plasmid encoding for Gal4-Fis1p construct, we isolated the plasmids from these isolates and sent to sequencing. Out of total 32 plasmids analyzed, at least seven of them were nonsense mutations and 19 were frameshift mutations. Nonsense mutations result in truncation of the resulting protein and frameshift mutations change amino acids sequence of the protein. These findings suggest that strong Ura⁺ phenotype requires complete destruction of the TA which would not provide any useful information regarding the sequential or structural determinants crucial for TA protein targeting.

It was previously shown that a Ura⁺ phenotype involves greater Gal4- dependent transcriptional activation than a His⁺ phenotype in the yeast two-hybrid strain that we used in this study¹⁸⁶. Therefore, we proposed that selection of TA mutants based on the His⁺ phenotype would be more informative in terms of structural features of the TA as these mutations weaken, but do not completely hinder membrane association.

As a result of the initial screen, we found 32 *cis* mutations and almost all of these mutations were located on the outside of the coding region of the TA. However, to be able to get information about structural features of the TA, we need mutations within the coding region of the TA. By taking advantage of mutagenic PCR, we induced random mutations just within the TMD of Gal4-Fis1 fusion protein. This time, we found isolates that proliferated on SMM-His+20mM AT but exhibited reduced proliferation on Sc-Ura medium compared to cells containing the Gal4-Fis1 (Δ TA) fusion protein. Sanger sequencing of the plasmids isolated from these isolates revealed that one clone has V145E mutation (amino acid numbering given in this study will correspond to that of the unmodified, full-length Fis1p protein), other two have L139P mutation, and the last one harbors two mutations: L129P and V138A. All of these substitution mutations are located within the TA of Fis1p (Table 4.2)

Table 4.2. Amino acid sequence of the TA of wild type Fis1p and the four clones

		p.139	p.145
		↓	↓
WT TMD =	LKGVVAGGVL	AGAVAVASFFLRNKRR*	
isolate1 =	LKGVVAGGVL	AGAVAEASFFLRNKRR*	
isolate2 =	LKGVVAGGV	PAGAVAVASFFLRNKRR*	
isolate3 =	LKGVVAGGV	PAGAVAVASFFLRNKRR*	
isolate4 =	PKGVVAGG	ALAGAVAVASFFLRNKRR*	

Serial dilution assays verified that V145E and L139P exhibited strong His⁺ phenotype, yet weaker but still detectable Ura⁺ phenotype. On the other hand, while the L129P/V138A mutant displayed a His⁺ phenotype, it could not exhibit uracil prototrophy (unpublished results, performed in concert with Dr. Cory Dunn) which suggests that it may show less severe localization defect compared to other two mutants. It was not surprising to see that V145E mutation hampers mitochondrial localization of the chimeric protein due to the poor accommodation of a charged amino acid within the MAD of Fis1p which consists of a hydrophobic stretch of amino acids. Furthermore, the secondary structure of the TMD of Fis1p is predicted to be mostly alpha-helical, thereby isolating the potentially helix-disrupting L139P may suggest a requirement of TA helicity for mitochondrial sorting.

As the next step, we wanted to show that these mutations preventing Gal4-Fisp targeting are not isolated solely as a result of the Gal4p-based selection method. For this purpose, we took advantage of the transcription factor Pdr1p which provides resistance to various drugs^{187,188}. Hyperactive Pdr1p is encoded by the *PDR1-249* allele and provides cycloheximide (CHX) resistance¹⁸⁹. Fusion of the wild type TA to Pdr1-249 did not provide CHX resistance. On the other hand, Pdr1-249-Fis1p (V145E) allowed CHX resistance, presumably since V145E mutation hampered insertion to the MOM, the chimeric protein entered to the nucleus and activated its targets (unpublished results, performed in concert with Dr. Cory Dunn). These findings verify that the mutations we generated by using our Gal4p-based approach are not likely to be related to the use of any specific transcriptional factor.

Our Gal4p-based approach provides indirect results on chimeric protein targeting to the MOM because of the drawbacks like mutant stability, sorting of the fusion protein to another compartment or other events unrelated to normal TA protein localization. In order to directly show that isolated TA mutations influence the MOM targeting, we hooked wild type TA and mutant TAs to the C-terminus of mCherry. We also labeled mitochondria with GFP by fusing GFP coding sequence to presequence of the Cox4 protein to demonstrate the mitochondrial localization of the chimeric proteins that we generated¹⁹⁰. It must be indicated that the TA of Fis1p is devoid of the necessary information involved in mitochondrial fragmentation¹⁹¹, thereby localization of these chimeric proteins can't be affected by interaction partners of Fis1p.

Our microscopy results which show localization of the mCherry-Fis1p TMDs faithfully recapitulated our genetic results. As expected, while mCherry fused to the wild type TA localized to mitochondria, the mCherry signal for V145E and L139P was substantially cytosolic. Moreover, the L129P/V138A showed discernable mitochondrial localization but cytosolic mCherry signal was more intense (Figure 4.3) which is consistent with the weaker activation of Gal4 targets of this fusion protein.

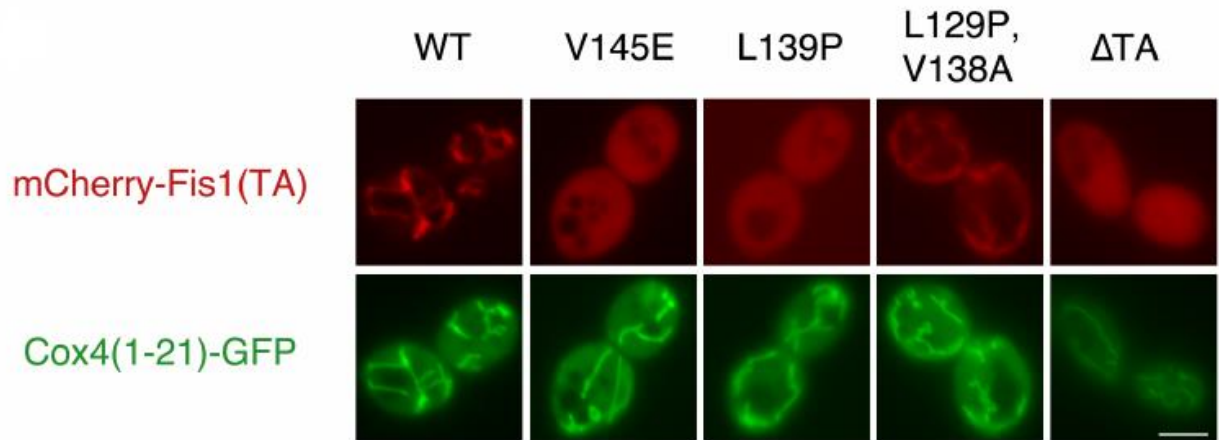


Figure 4.3. **Missense mutations within the TA of Fis1p result in cytosolic accumulation of a linked mCherry protein.** Variants of Fis1p TA fused to mCherry were expressed in the wild-type strain CDD961 from plasmids b109 (WT), b134 (V145E), b135 (L139P), b136 (L129P, V138A), or b252 (Δ TA) and imaged by fluorescence microscopy. Mitochondria were labeled with a mitochondria-targeted GFP expressed from plasmid pHS1¹⁹².

4.4 Deep mutational scanning reveals determinants of Fis1p tail-anchor targeting

After seeing the success of our genetic approach in isolation of the TA mutations which influence mitochondrial targeting, we wanted to perform more global analysis to understand structural features of the TA of Fis1p. By utilizing degenerate primers and recombination-based cloning in *S. cerevisiae*, we aimed to create a library composed of all possible codons at every single one of 27 amino acid positions within the TA of Gal4-Fisp. Later, the total pool of the constructs containing Fis1p TA mutations were grown for four generations under six possible culture conditions: no selection for *HIS3* or *URA3* reporter activation, SC-Trp medium (selecting only for plasmid maintenance); selection for *URA3* activation, SC-Ura medium; and selection for *HIS3* activation at different 3-AT concentrations, SMM-Trp-His medium with 0 mM, 5 mM, 10 mM, or 20 mM 3-AT. After isolation of plasmid DNA from each pool of mutants, TA coding sequences were amplified

by PCR and sent to next-generation sequencing. While analyzing the data, we only focused on the clones which have only zero or one amino acid change since the degenerate primers that we used can induce random substitution of just one amino acid. More than one substitution may occur as a result of any error during the PCR amplification. While all potential replacement mutations could not be detected within our starting library (Figure 4.4), and some biases existed at each TA position, most potential amino acid mutations were represented within our pool. 98.9% of potential amino acid replacements were identified in the starting pool cultured in Sc-Trp, and 95.9 % of TAs with single mutations were represented by at least 10 counts.

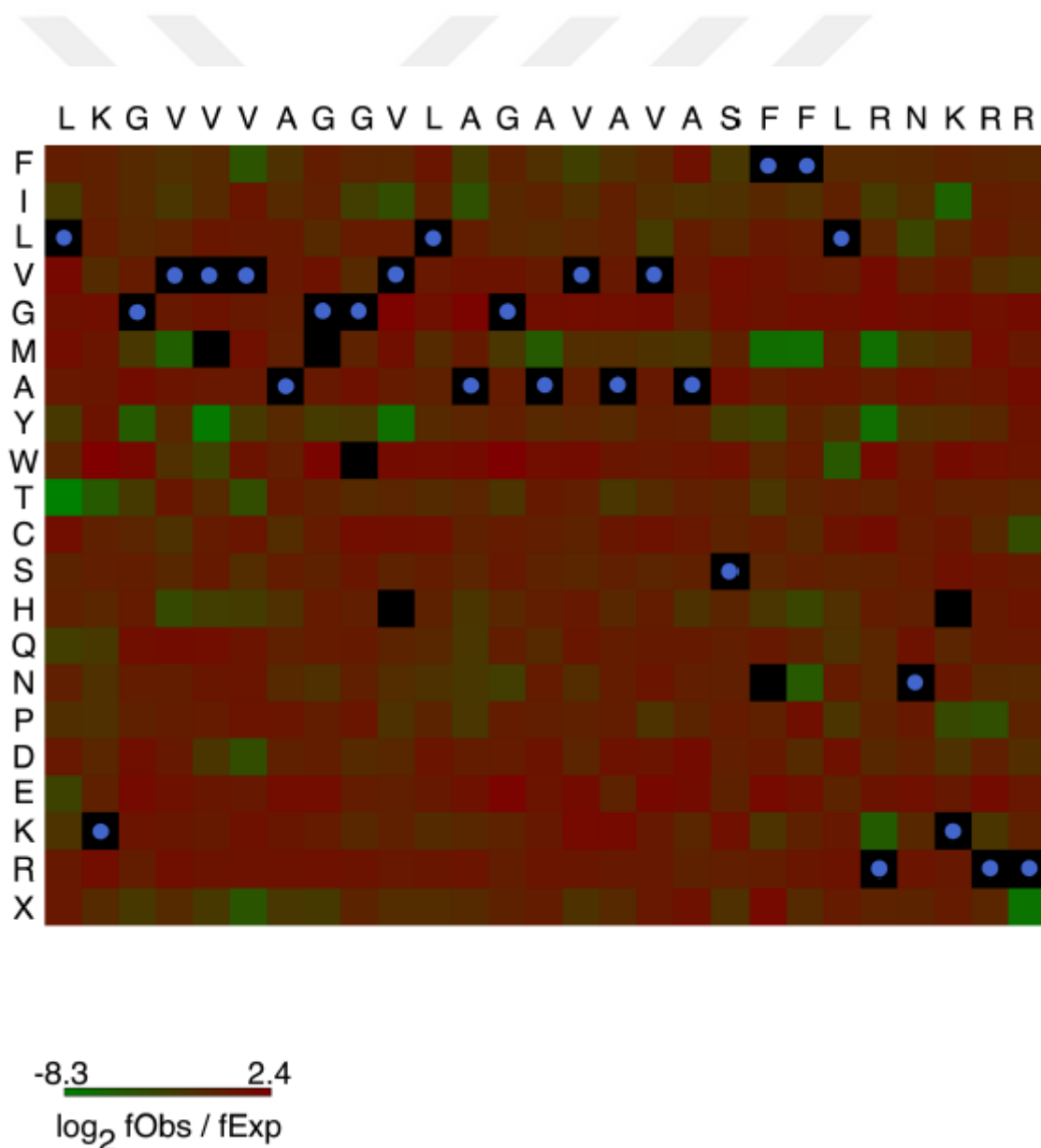


Figure 4.4. **An illustration of amino acid replacement representation within the Fis1p TA library.** The fraction of counts representing each amino acid replacement in the starting SC-Trp library was compared to the fraction that would be expected based on randomized codon values. Native amino acids are represented by a black square with a blue dot. Amino acid replacements with no representation in the library are represented by empty black squares.

There was no detectable difference in the relative abundance of the most mutants between the mutant pool grown in Sc-Trp and selective medium SMM-Trp-His with no 3-AT (Figure 4.6A). This is not surprising because of leaky expression of *HIS3* reporter independent of Gal4-mediated activation¹⁸⁴. On the other hand, addition of 3-AT at different concentrations of 5mM (Figure 4.6B), 10mM (Figure 4.6C), or 20mM (Figure 4.5) to the medium devoid of histidine, resulted in significant alteration in the distribution of the mutant pools towards to specific amino acids, urging us to do further experiments that are described below. As our initial screening performed for selection of *cis* or *trans* mutants demonstrated, the pool grown in SC-Ura medium exhibited very strong selection for nonsense mutations within the TA (Figure 4.6D), yet less marked biases among amino acids.

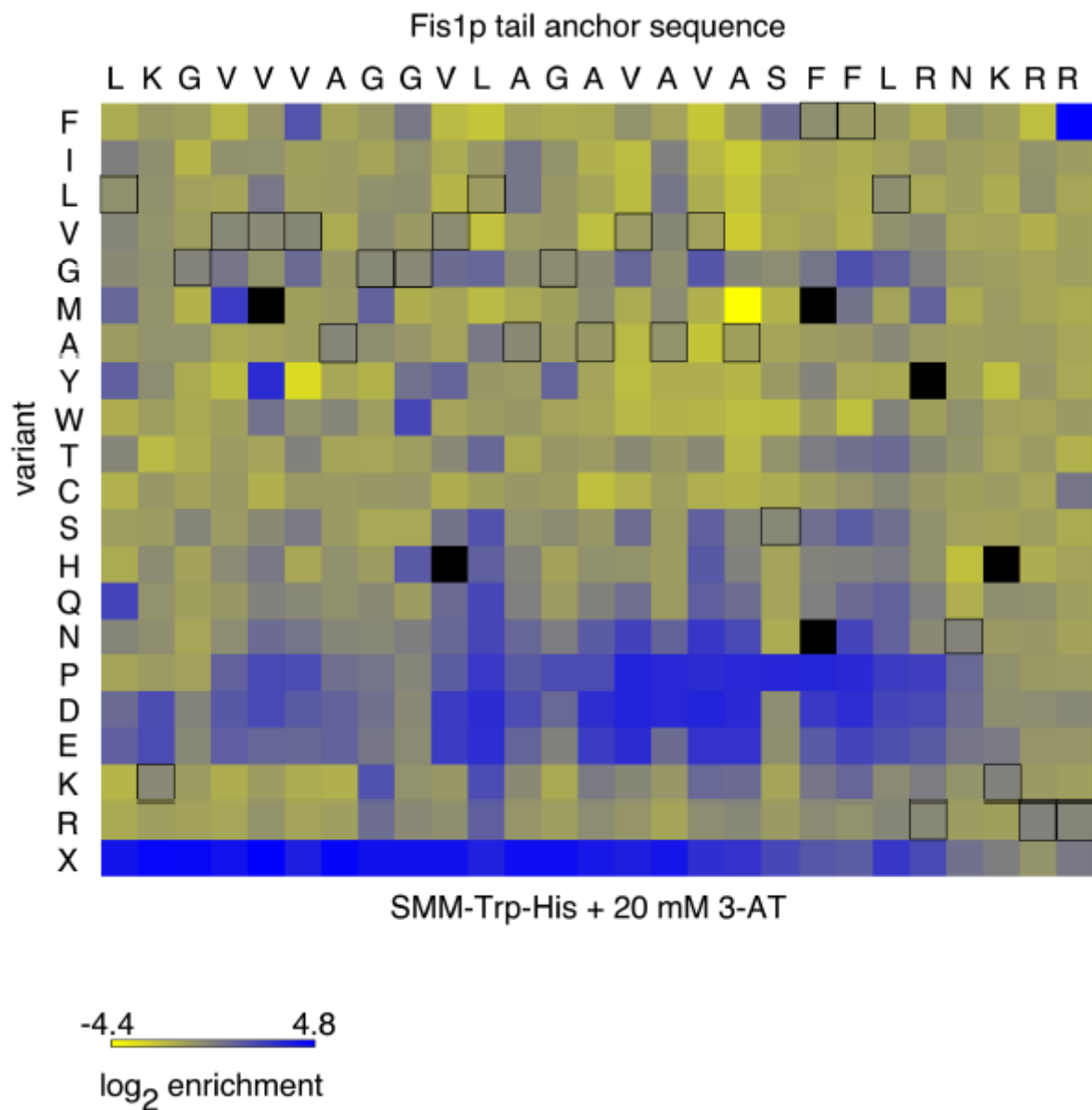


Figure 4.5. **Mutations at specific locations within the TA of the Gal4-Fis1 chimeric protein enable Gal4-driven transcription.** Log₂ of enrichment values for each amino acid were calculated for every single position following selection in SMM-Trp-His medium with 20 mM 3-AT. Enrichment values are generated for individual amino acids positions within the TMD, and not across positions. Black boxes denote the native amino acid for each position.

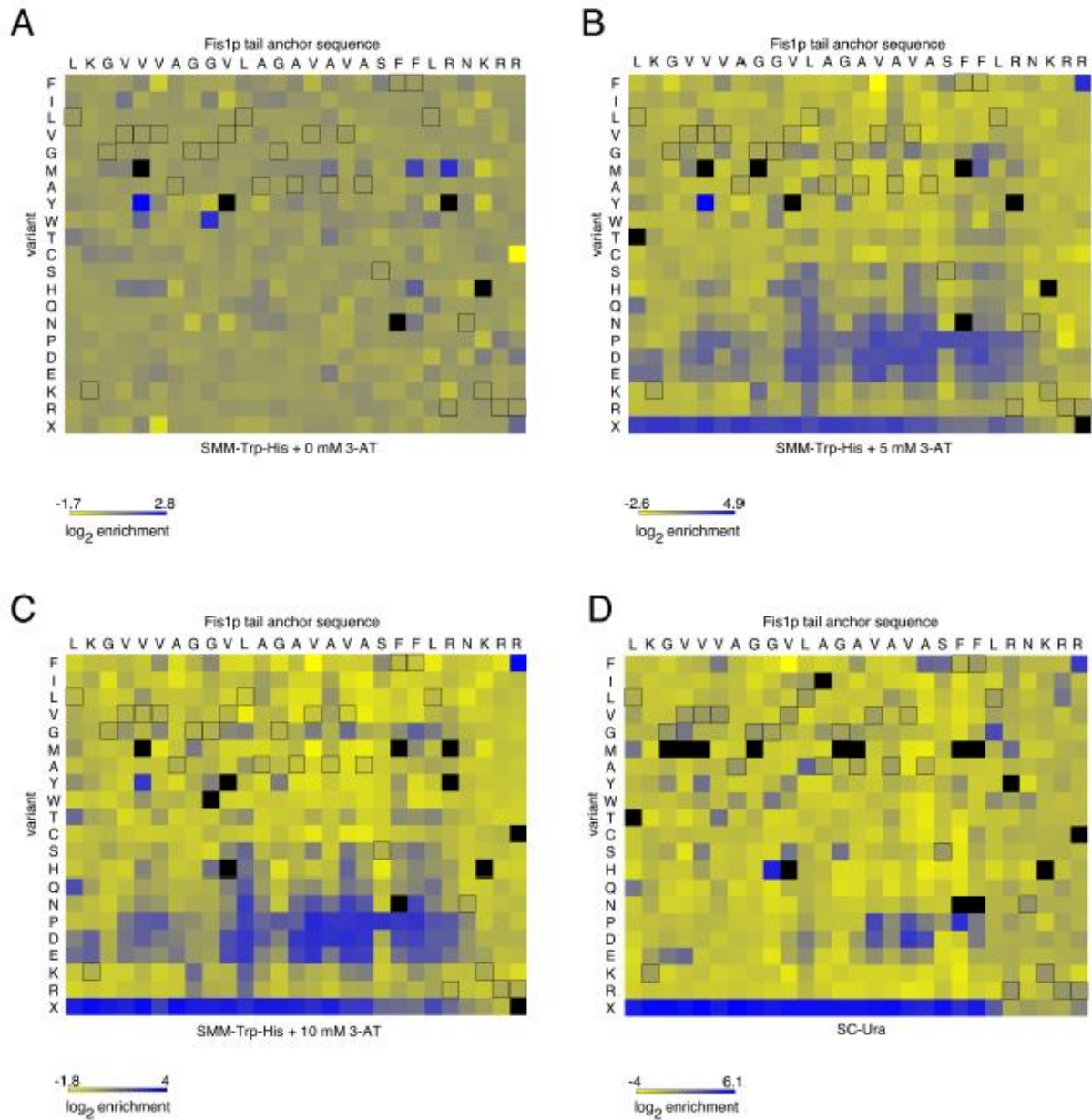


Figure 4.6. Amino acid replacement frequencies within the Fis1p TA indicate that assessing histidine auxotrophy in the presence of 3-AT may provide the most informative results regarding Gal4-Fis1p location. Quantification of replacement in SMM-Trp-His medium without 3-AT (A), containing 5 mM 3-AT (B), containing 10 mM 3-AT (C), or in SC-Ura medium (D). In all panels, black squares outline the native amino acid at each position within the Fis1p TMD.

During protein synthesis, specific codon usage can influence the translation rate and folding of the resulting polypeptide independent of the primary sequence of the protein¹⁹³. Since the length of the TA domains of TA proteins is shorter than the length of the exit tunnel of the ribosome which corresponds to 30 to 40 amino acid residues long, TA proteins must be certainly inserted post-translationally. Therefore, we investigated enrichment of codon usage of wild type amino acids at their specific positions following selection for Gal4-Fis1p localization in the nucleus. However, this examination did not exhibit any noteworthy evidence for specific codons in controlling localization of the Fis1p (Figure 4.7). Even though the data are noisy because of lack of representation of some codons at each position, same amino acids within the TA were encoded by the same codon within our selection scheme, thereby making us concentrate on the amino acid sequence rather than the codon sequence of the library variants.

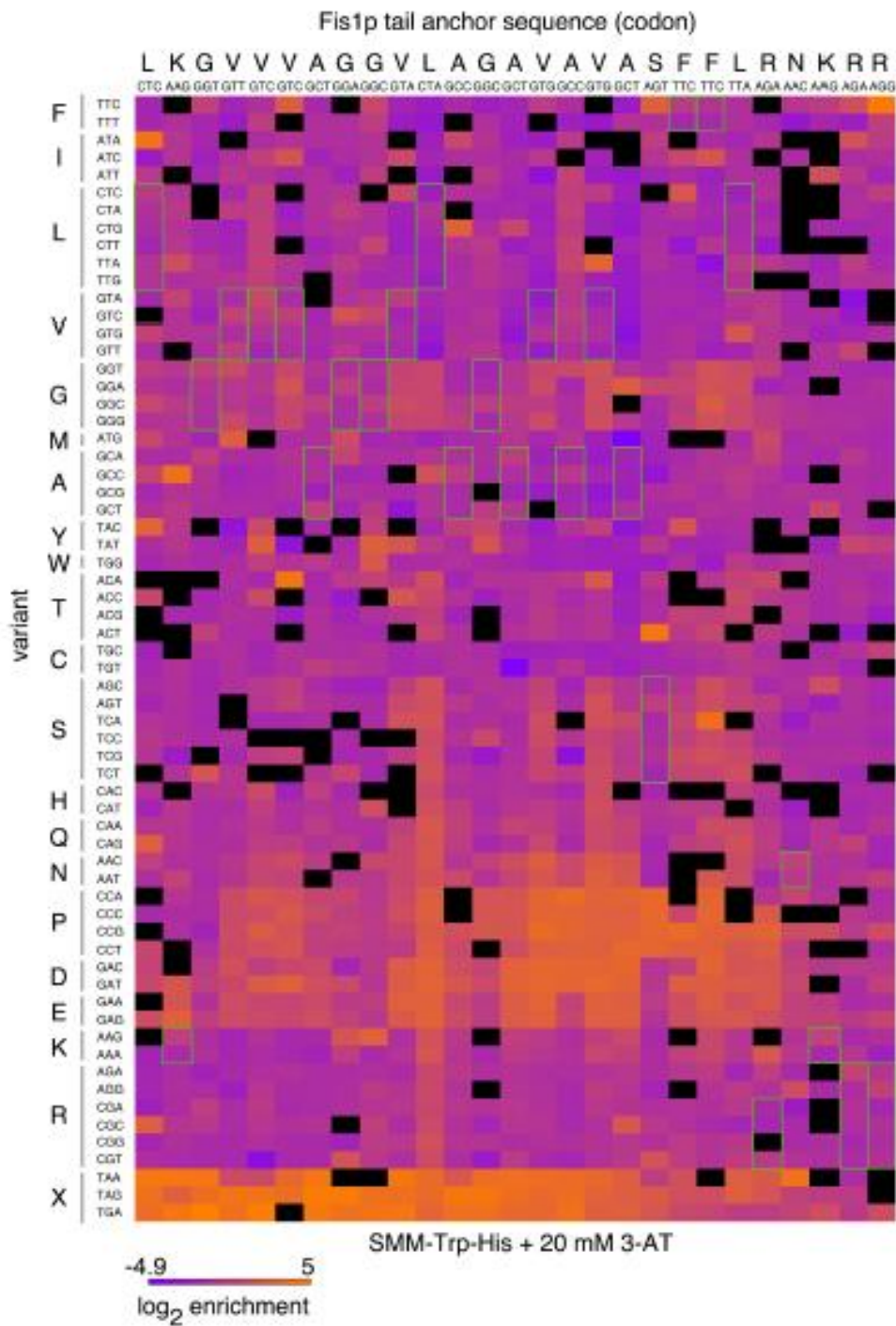


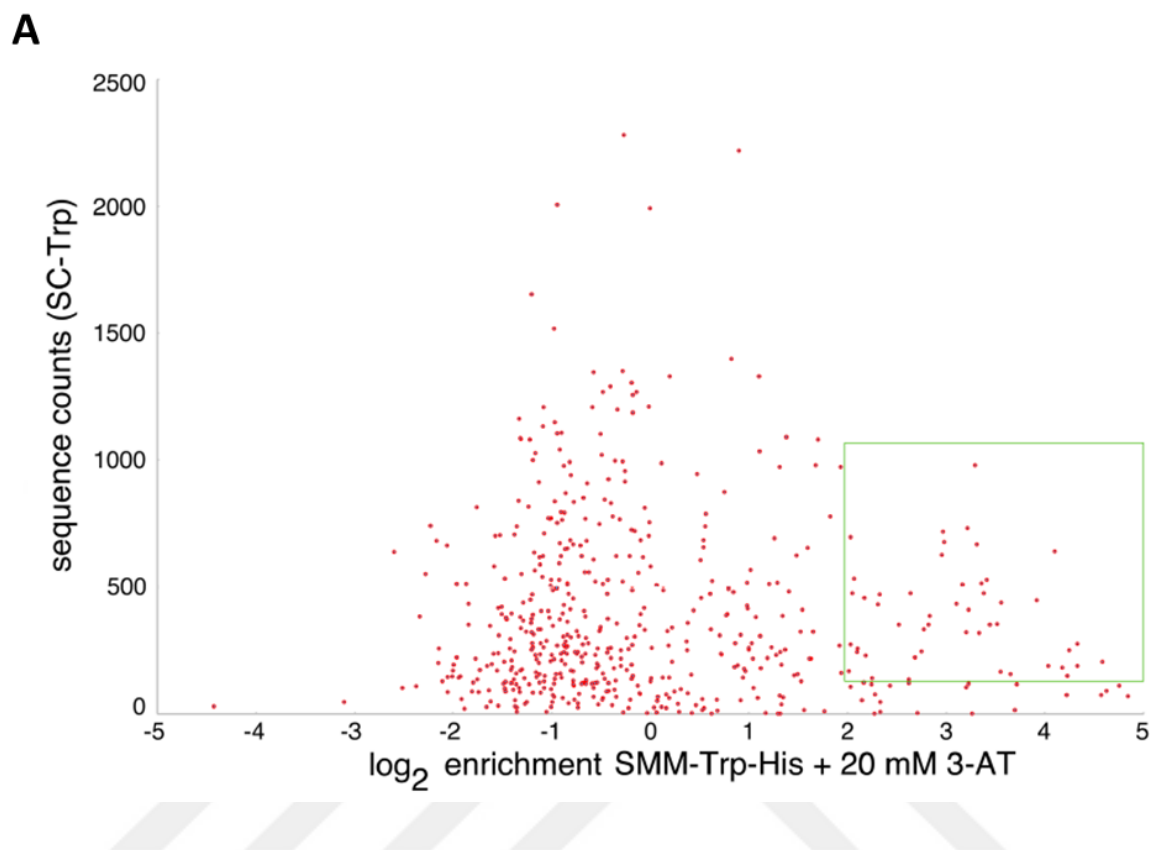
Figure 4.7. **Codon usage has no role in Gal4-Fis1p targeting.** Log₂ of enrichment values for each codon following the selection of the Fis1p TMD library in SMM-Trp-His medium

containing 20 mM 3-AT are illustrated. Green boxes denote the native amino acid at each position

4.5 Proline is not tolerated at many regions within the TA of Fis1p

As it was shown in the previous studies, there is no strict preference for a specific amino acid at a specific position within the TA of mitochondrial TA proteins for targeting to the MOM^{27,28}. Moreover, our deep mutational scanning analysis also revealed that replacement of most of the wild type amino acids within the TA did not cause activation of the reporters (Figure 4.5). Therefore, we focused on the essential mutations that result in activation of the reporters because of disruption of the structural characteristic of the TA required for proper targeting of Fis1p to the MOM.

The L139P mutation that we identified in our preliminary selection suggested that prolines might not be tolerated within the hydrophobic MAD of Fis1p. Our deep mutational scanning analysis of Fis1 TMD in SMM-Trp-His+20mM 3-AT (Figure 4.5) also suggested that proline replacement in many positions impeded mitochondrial localization of the chimeric protein. Closer examination of the mutants that were in the top 75% most frequently counted variants in the starting pool (>126 counts) and enriched at least four fold in SMM-Trp-His+20mM 3AT, 12 of 33 missense mutations of this set were proline mutations (Figure 4.8), which further affirms that mislocalization of the chimeric protein to nucleus is mostly because of proline replacements within the MAD.



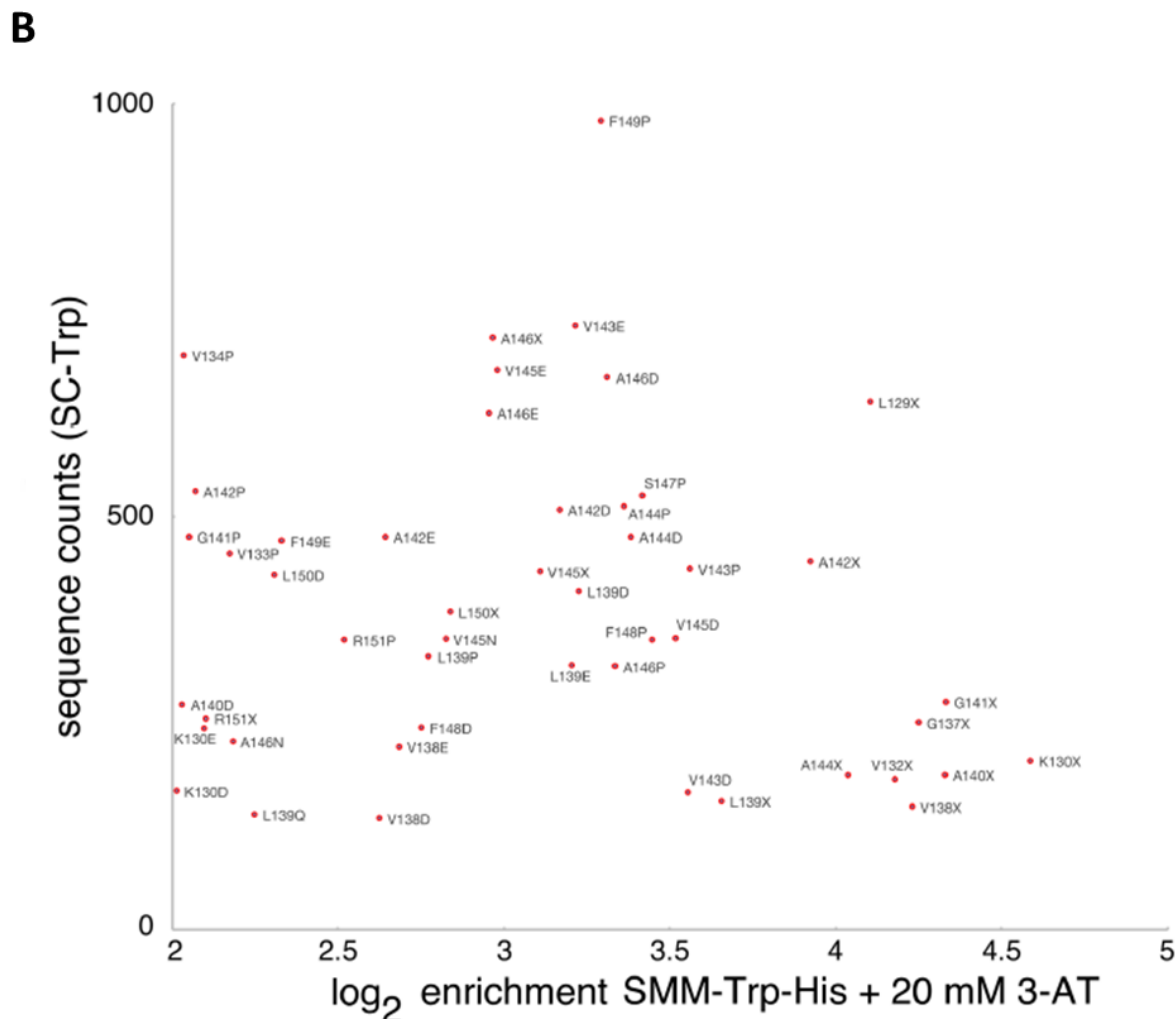


Figure 4.8. **Representation of the most abundant Gal4-Fis1p clones that are significantly enriched upon selection for nuclear translocation of the fusion protein.** TA replacement mutations are plotted. Log₂ enrichment values are given on the X-axis, and sequence counts recovered from the starting pool (SC-Trp) provided in the Y-axis. The replacement mutations which are above the 25 % percentile in mutant abundance in the starting pool and enriched at least four-fold following selection in SMM-Trp-His medium with 20 mM 3-AT are highlighted in green. (B) Expansion of the highlighted region in (A) showing specific TA mutations.

To validate what we have seen in the deep mutational scanning analysis, we mutated four positions within the TMD to proline. We also included L139P mutant that is

from our preliminary selection experiment. All proline replacement variants were tested both in the genetic assay and microscopy-based assay. Consistent with our large-scale analysis (Figure 4.5 and 4.8), V134P, L139P, A140P, and A144P mutations activated Gal4-driven reporter *HIS3* (on SMM-His+20mM 3-AT, unpublished results, performed in concert with Dr. Cory Dunn), suggesting that mitochondrial insertion did not occur. Fusion of these Fis1p TA mutants to mCherry resulted in cytosolic localization of the chimeric proteins (Figure 4.9A) meaning that these proline substitutions hampered insertion of mCherry-Fis1 TA proline mutants to the MOM. These results indicate that secondary structure of the TA of Fis1p is essential for its function and disruption of the α -helical structure at many locations may interfere with the mitochondrial targeting.

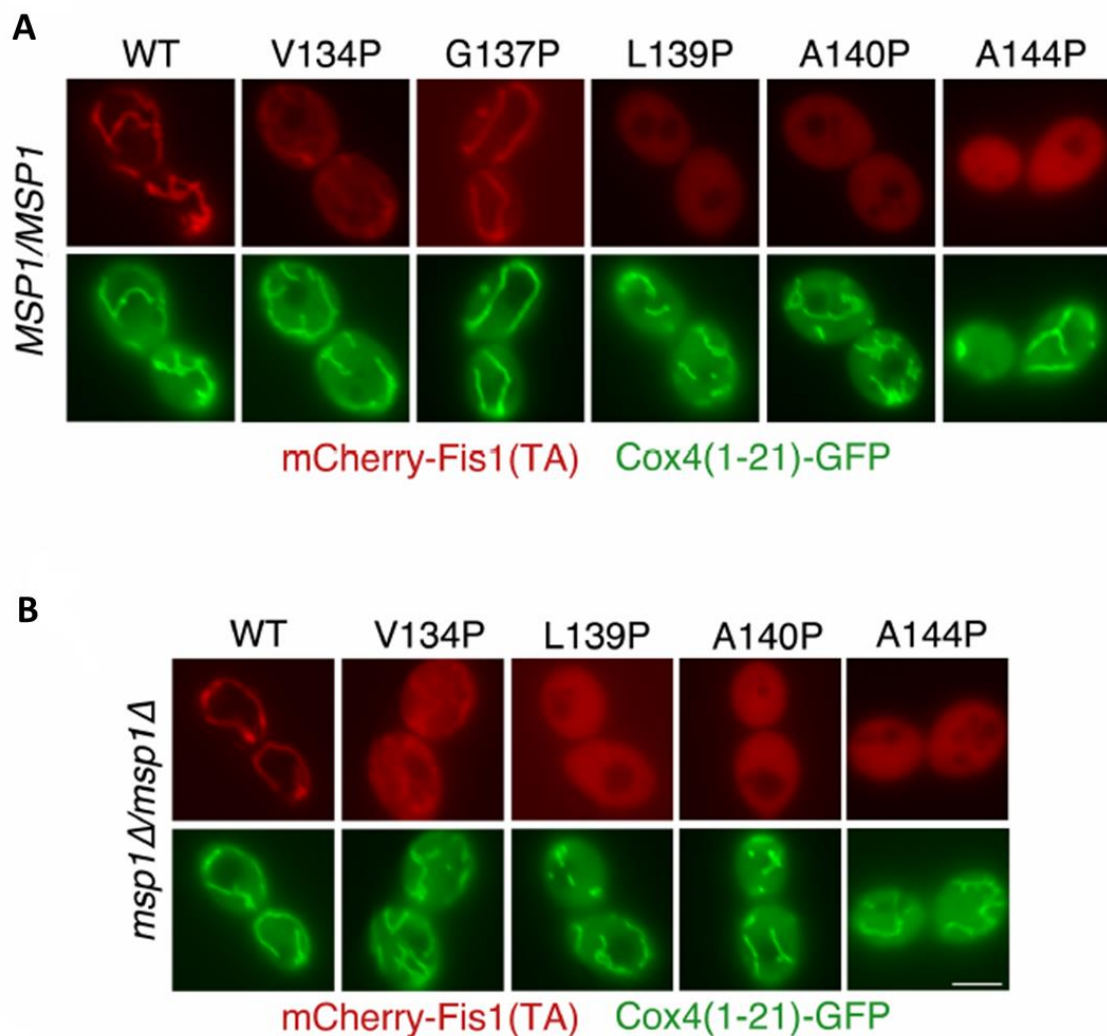


Figure 4.9. **Proline is not tolerated at many regions within the TA of Fis1p.** (A) TAs containing proline substitutions can diminish mitochondrial targeting of a linked fluorescent protein. mCherry fused to proline variants of the Fis1 TA were expressed in the wild type strain CDD961 from plasmids b109 (WT), b208 (V134P), b209 (G137P), b135 (L139P), b210 (A140P), b211 (A144P) and imaged. Mitochondria were labeled with a mitochondria-targeted GFP expressed from plasmid pHS1. (B) Deletion of the Msp1p extractase cannot reroute the mislocalized mCherry-Fis1 TA proline variants to mitochondria. Cells from *msp1Δ/msp1Δ* strain CDD1044 expressing pHS1 and plasmid b109 (WT), b208 (V134P), b135 (L139P), b210 (A140P), or b211 (A144P) were inspected as in Figure 4.3.

Intriguingly, the G137P replacement was not remarkably enriched in the large-scale analysis (Figure 4.5). Moreover, the G137P mutation containing TA fused to mCherry strongly targeted to mitochondria which suggest that proline is not universally unacceptable within the MAD of the Fis1p.

There are two possible explanations for mislocalization of the mCherry fused to mutant Fis1 TAs. First, mitochondrial targeting and insertion were hampered due to proline substitutions. Second, these mCherry-Fis1 TA variants were first inserted into the outer membrane of mitochondria; however, because of the stability problem within the lipid bilayer, these inserted fusion proteins were extracted by a quality control mechanism. It was recently identified that Msp1p is a novel mitochondrial protein quality control component in yeast. This ‘‘extractase’’ can extract improperly folded or mislocalized proteins from the MOM^{194,195}. Therefore, we hypothesized that mCherry fluorescent proteins fused to mutant TAs were first inserted to the MOM but subsequently extracted by Msp1p. However, deletion of Msp1p did not cause rerouting of the fluorescent proteins to mitochondria (Figure 4.9B) which provides no evidence for mitochondrial insertion of the mCherry-Fis1 TMDs harboring proline substitutions and then subsequent removal.

4.6 Lengthening or shortening of the TA of Fis1p does not influence targeting to mitochondria

One of the main features that affects targeting of TA to various cellular compartments is the length of the TMD^{168,196}. Our previous results demonstrated that at a specific region within the MAD, proline is tolerated. Therefore, we wondered whether this region (position 137) is amenable for deletion or insertion of new amino acids which would enable us to analyze the relationship between the length of TA of Fis1p and mitochondrial sorting. To test this, we inserted one (∇1A), two (∇2A), or three (∇3A) alanines between A135 and G136 within the TA of Gal4-Fis1p; however, any of these mutant constructs did not provide *HIS3* or *URA3* reporter activation (unpublished results, performed in concert with Dr. Cory Dunn). We also looked at localization of mCherry fused to a Fis1p TA harboring same insertions. All constructs were inserted to mitochondria (Figure 4.10A).

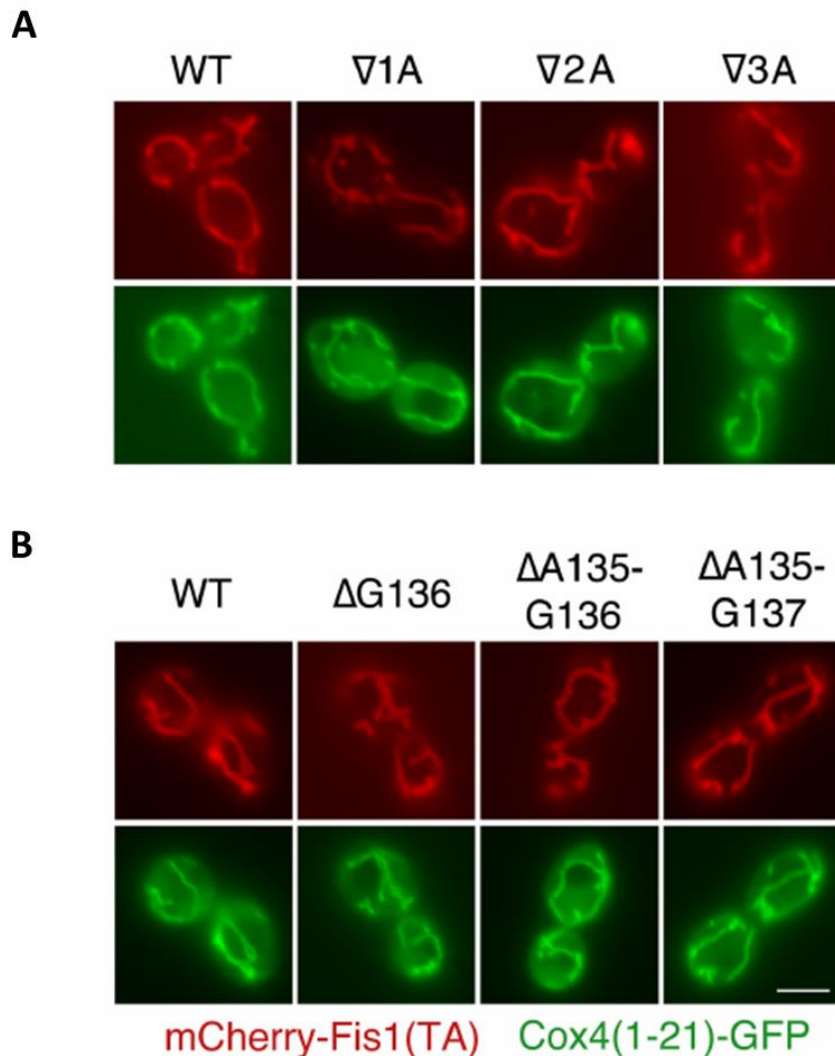


Figure 4.10. **Length of the TA of Fis1p has no influence on mitochondrial targeting.** (A) mCherry fused to a Fis1p TA harboring an insertion of up to three amino acids in length inserts into mitochondria. Strain CDD961 expressing mCherry-TA fusions from plasmid b109 (WT), b235 ($\nabla 1A$), b236 ($\nabla 2A$), or b237 ($\nabla 3A$) was visualized as in Figure 4.3. (B) mCherry fused to a Fis1p TA deleted of up to three amino acids localizes properly to mitochondria. Strain CDD961 expressing mCherry-TA fusion from plasmids b109 (WT), b232 ($\Delta G136$), b233 ($\Delta A135-G136$), or b234 ($\Delta A135-G137$) was visualized as in Figure 4.3.

Later, we deleted one (Δ G136), two (Δ A135-G136), or (Δ A135-G137) three amino acids within the TA of Fis1p and performed same analysis. Similar to insertion mutants, deletions mutants were also not able to activate *HIS3* or *URA3* reporters (unpublished results, performed in concert with Dr. Cory Dunn). Localization of mCherry fused to a Fis1 TA carrying these same deletions was mitochondrial (Figure 4.10B).

Spf1p is a P-type ATPase found in the membrane of the ER. It is involved in maintaining lipid composition of intracellular compartments. Therefore, disruption of Spf1p diminishes the contrast in ergosterol levels between the mitochondrial outer membrane and the ER. As a result of this, mitochondrial TA proteins are mislocalized to the ER¹⁹⁷. Moreover, sterol concentration of lipid bilayers can also influence the bilayer thickness¹⁹⁸, suggesting that deletions or insertions may allow mitochondrial TA proteins to relocate to mitochondria again instead of the ER in the *spf1* Δ background. However, mCherry-Fis1 TA carrying insertion or deletion mutations remained localized to the ER in the mutants lacking Spf1p (Figure 4.11).

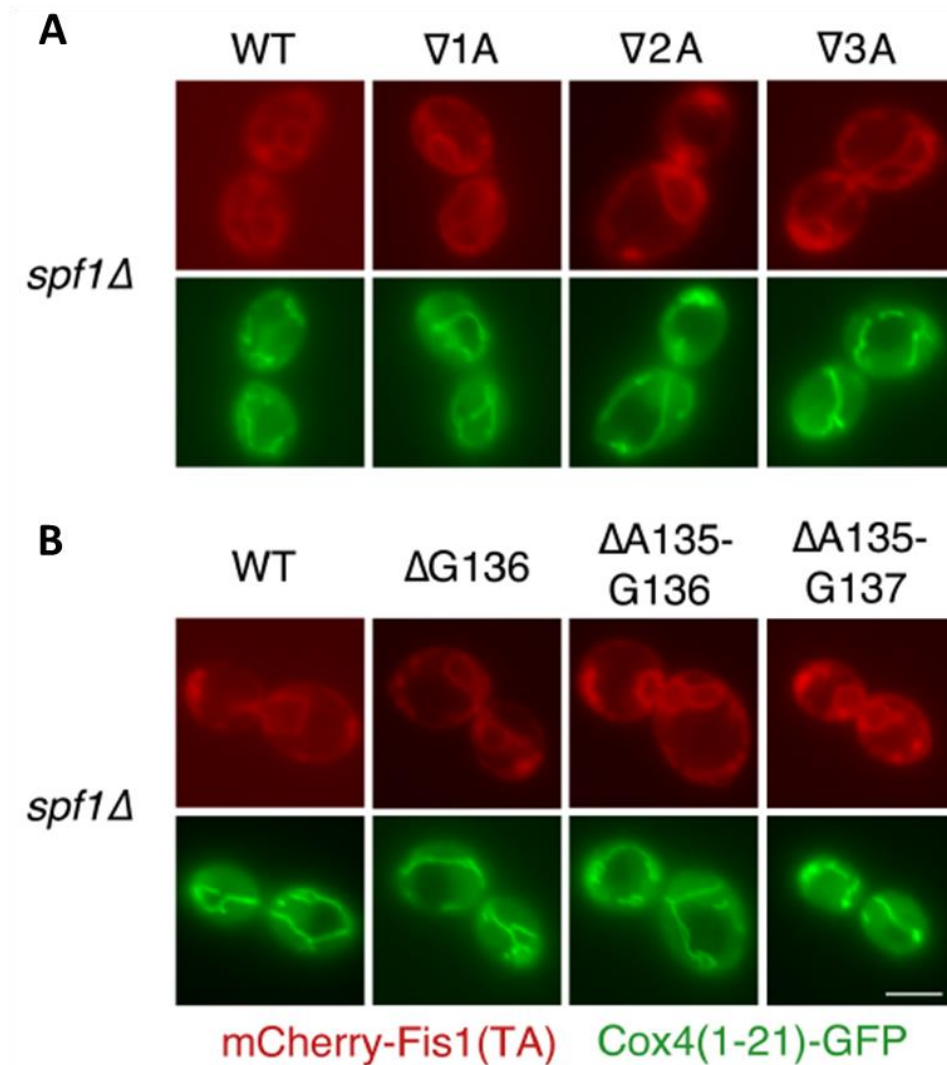


Figure 4.11. **mCherry fused to varying length of a Fis1 TA remains localized to the ER in the cells lacking Spf1p.** (A) Strain CDD1031, devoid of Spf1p and expressing mCherry-TA chimeric proteins from plasmids b109 (WT), b235 (∇1A), b236 (∇2A), or b237 (∇3A), b232 (ΔG136), b233 (ΔA135-G136), or b234 (ΔA135-G137) were visualized as in Figure 4.3.

As a general conclusion, alteration of the length of the TMD of Fis1p up to three amino acids does not affect mitochondrial targeting of itself.

4.7 The positively charged amino acids found at extreme carboxyl terminus of the Fis1p are involved in mitochondrial targeting

Closer examination of our deep mutational scanning data revealed that almost all of the nonsense mutations within the TA caused Gal4-Fis1p to move to the nucleus and activate the reporters (Figure 4.5). However, stop codon replacements within the charged RNKRR pentapeptide located at the end of the TA of Fis1p seem to allow some membrane localization. To elucidate the enigma behind this observation, we investigated the behavior of the R151X mutant which devoid of the all charged amino acids residing at the end of the TA. mCherry fused to R151X TA showed partial mitochondrial, partial the ER and some other intracellular organelles localization (Figure 4.12). Furthermore, R151X mutant of Gal4-Fis1p could not activate the Gal4-driven *URA3* reporter at all and *HIS3* reporter in the same extent of the Gal4-Fis1p lacking the entire TA (unpublished results, performed in concert with Dr. Cory Dunn).

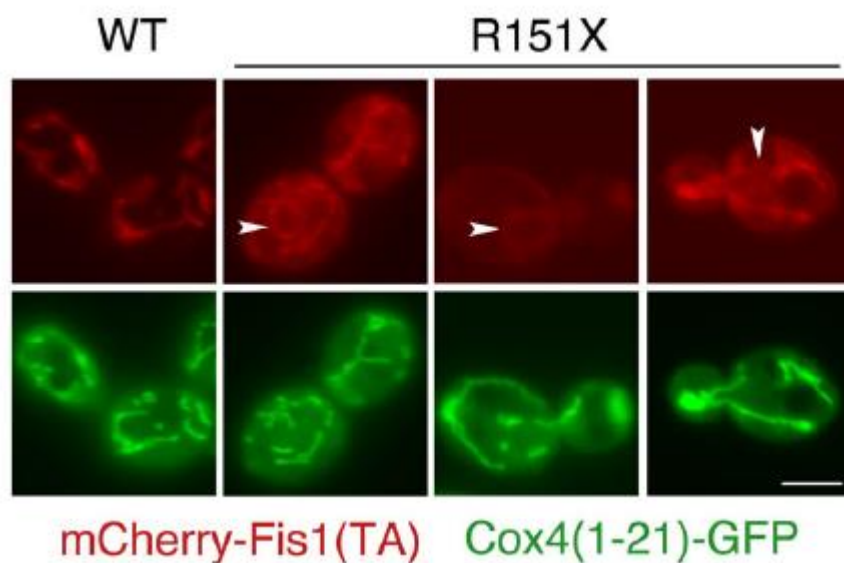


Figure 4.12. **Positively charged amino acids located at the carboxyl-terminus of the TA of Fis1p are essential for mitochondrial targeting.** Removal of the last five positively charged amino acids from the mCherry-Fis1p TA allows mislocalization to the ER and some other intracellular organelles. Strain CDD961 expressing mCherry fused to

the WT Fis1p TA (b109) or expressing mCherry linked to a truncated Fis1p TA (R151X) from plasmid b254 were examined as in Figure 4.3. White arrowheads denote mCherry localized to the ER.

Intriguingly, the ER localization of mCherry fused to the R151X TA is independent of Get3p (Figure 4.13) which is a cytosolic chaperone involved in the targeting of the ER TA proteins¹⁶⁰. This suggests that R151X TA mutant is targeted to the ER by an alternative parallel pathway.

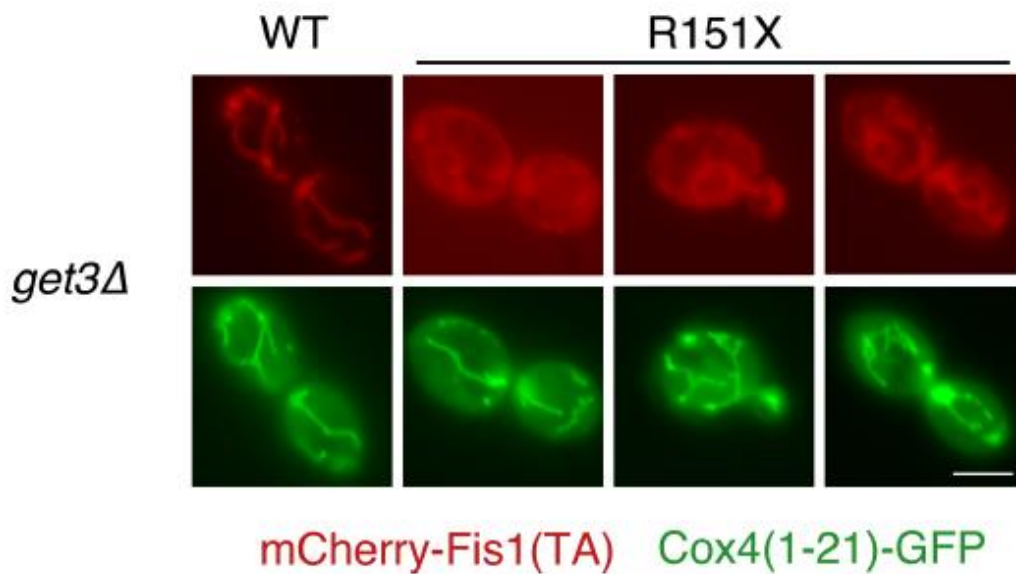


Figure 4.13. **mCherry fused to the R151X TA is targeted to the ER in Get3p independent manner.** Strain CDD1033 expressing mCherry fused to a WT Fis1p TA from plasmid b109 or expressing mCherry fused to a Fis1 TA lacking the positively charged carboxyl-terminus (R151X) from plasmid b254 were visualized as in Figure 4.3.

Our results suggested that the positively charged amino acids found at the carboxyl terminus of the TA are crucial for organelle specificity; however, not necessary for membrane localization.

We observed that R151X variant of Gal4-Fis1p activated the Gal4-driven *HIS3* reporter and mCherry carrying the same truncation was partially localized to the ER. Since the nuclear envelope is physically connected to the ER, we hypothesized that *HIS3* reporter activation by R151X variant may be a consequence of the ER localization of the chimeric

protein. To test this hypothesis, we fused the human Fis1p (hFIS1) TA to both Gal4-Fis1p (Δ TA) and mCherry since it is already known that full-length hFIS1 is targeted to the ER in *S. cerevisiae*¹⁹⁹. As expected, mCherry fused to the hFIS1 TA mostly localized to the ER (Figure 4.14A). However, Gal4 linked to the hFIS1 TA could not activate the *HIS3* reporter (unpublished results, performed in concert with Dr. Cory Dunn), suggesting that the ER localization of the R151X variant of Gal4-Fis1p is not likely to be the reason of the activation of the *HIS3* reporter.

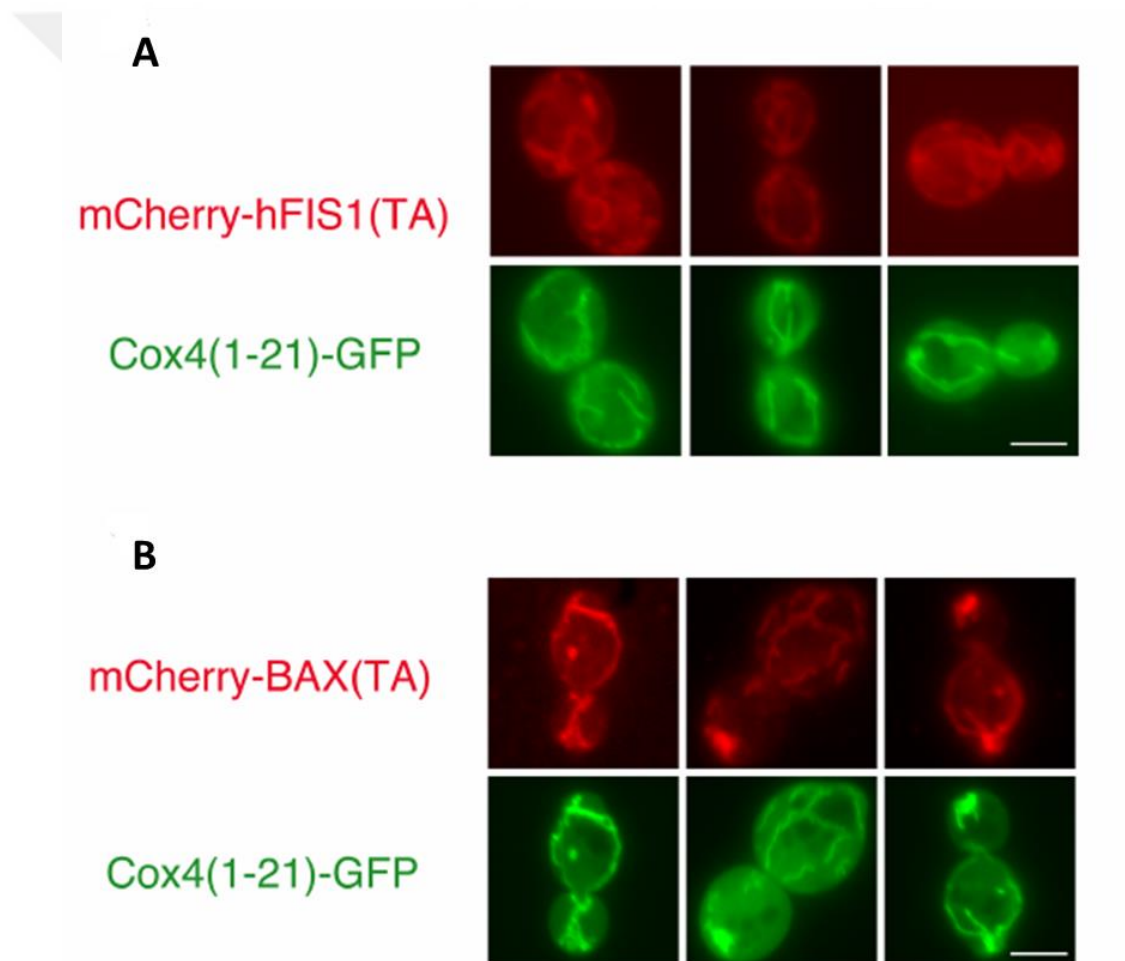


Figure 4.14. **The TAs of human proteins are not universally targeted to mitochondria in yeast.** (A) mCherry hooked to the hFIS1 TA is mislocalized to the ER in *S. cerevisiae*.

Strain CDD961 harboring plasmid b257 expressing mCherry linked to the hFIS1 TA was examined as in Figure 4.3. (B) mCherry fused to the human BAX TA is localized to mitochondria in *S. cerevisiae*. Strain CDD961 containing plasmid b255, which expresses mCherry fused to the human BAX TA, was visualized as in Figure 4.3.

After seeing mislocalization of the hFIS1 TA in *S. cerevisiae*, we wondered whether other mitochondrial human TA proteins would be targeted to mitochondria or some other compartments. Towards to this goal, we fused mCherry to the TA of human BAX protein (the domain which is sufficient for mitochondrial targeting in mammalian cells²⁰⁰). Even though the signal of mCherry reduced compared to the signal of other mCherry chimeric proteins visualized in this study and expressed under the same promoter, mCherry linked to the human BAX TA localized to mitochondria (Figure 4.14B). Moreover, Gal4-BAX TA chimeric protein did not provide reporter activation (unpublished results, performed in concert with Dr. Cory Dunn), indicating that BAX TA is sufficient for proper mitochondrial targeting in yeast.

4.8 Positively charged amino acids are more tolerated than negatively charged amino acids within the TMD of Fis1p

Our large-scale analysis demonstrated that glutamate and aspartate substitutions within the TMD of the Galp-Fis1p construct activated the selectable reporters (Figure 4.5). Indeed, a closer examination of the amino acid replacements in the top three quartiles of counts in the initial library and enriched at least four-fold upon culture in SMM-Trp-His+20mM 3-AT, native amino acids were converted to aspartate or glutamate in 18 of 33 missense mutations (Figure 4.8). Intriguingly, lysine or arginine replacements are more tolerated within the TMD of Fis1p than glutamate or aspartate. Lysine and arginine amino acids replacements were not in the high-enrichment, high count set (Figure 4.8).

To examine what we have observed in the large scale analysis, we mutated four positions within the hydrophobic stretch of the TMD of Fis1p to lysine, arginine, aspartate and glutamate. We generated aminoacid replacements at positions V132, A140, A144, and F148. While position V132 is in the close proximity to the N-terminus of the TMD, position F148 resides at the C-terminal region of the TMD. Other two positions are located in the middle region of the TMD. Later, we tested the activity of these mutants in our

genetic system, selection for Gal4-Fis1p transcriptional activity. Our results recapitulated what we have seen in our global analysis. While aspartate and glutamate mutations activated the *HIS3* reporter (on the plate containing 20 mM 3-AT), lysine and arginine were not able to provide histidine prototrophy (unpublished results, performed in concert with Dr. Cory Dunn). Only the A144D mutation could provide ample Gal4 activation for survival on SC-Ura medium (unpublished results, performed in concert with Dr. Cory Dunn), indicating a very rigorous TA localization defect originated by this TA mutation.

We later examined the localization of mCherry fused to these charge mutant containing TAs under fluorescent microscopy. Lysine and arginine substitutions at the positions V132 and F148, which are within the TMD nearer to the putative water-lipid bilayer interface, permit mCherry to localize to mitochondria (Figure 4.15A). However, negatively charged amino acid substitutions prevented mitochondrial targeting of mCherry. It is obvious that F148D and F148E mutations hampered mitochondrial targeting more rigorously than V132D and V132E. Position A144 resides in the middle region of the TMD and all charge mutations at this position hindered mitochondrial targeting of mCherry in some degree. However, A144D and A144E mutations were less able to direct mCherry to mitochondria compared to A144K or A144R mutations. Moreover, none of the charge mutants located at the position A140 could direct mCherry to mitochondria. Interestingly, A140K and A140R mutants behaved differently than A140D and 140E mCherry-TA mutants. While A140D and 140E mutants were totally localized to the cytosol, A140K and A140R mutants were inserted into other compartments in the cell, such as plasma membrane. As a general conclusion for this part, our results strongly suggested that positively charged amino acids located at various positions within the TMD of Fis1p do not prevent mitochondrial targeting and are more tolerated than the negatively charged amino acids at these same positions.

We also examined whether OM extractase Msp1 has a role in the extraction of those mislocalized charged Fis1p TAs from the outer membrane of mitochondria. However, deletion of Msp1p did not result in relocalization of previously mislocalized tail-anchored fluorescent proteins to mitochondria (Figure 4.15B). These findings suggest that charge replacements within the TMD of Fis1p inhibit insertion of Fis1p to the MOM instead of providing enhanced removal from the outer membrane of mitochondria.

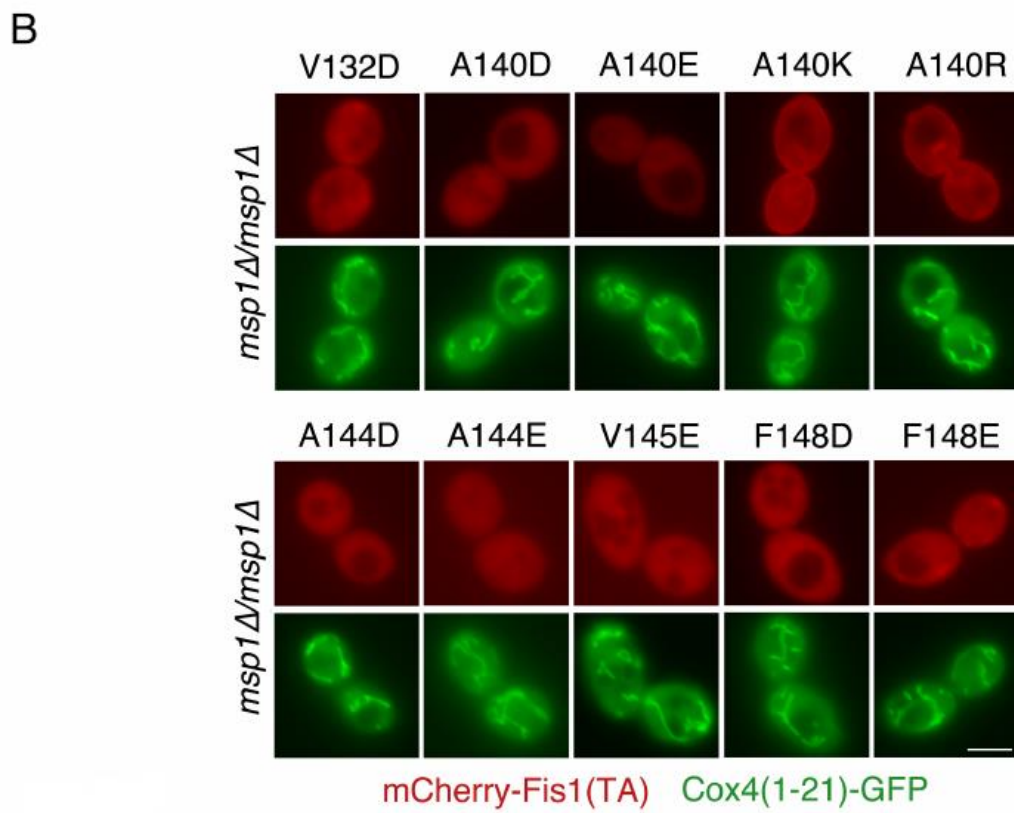
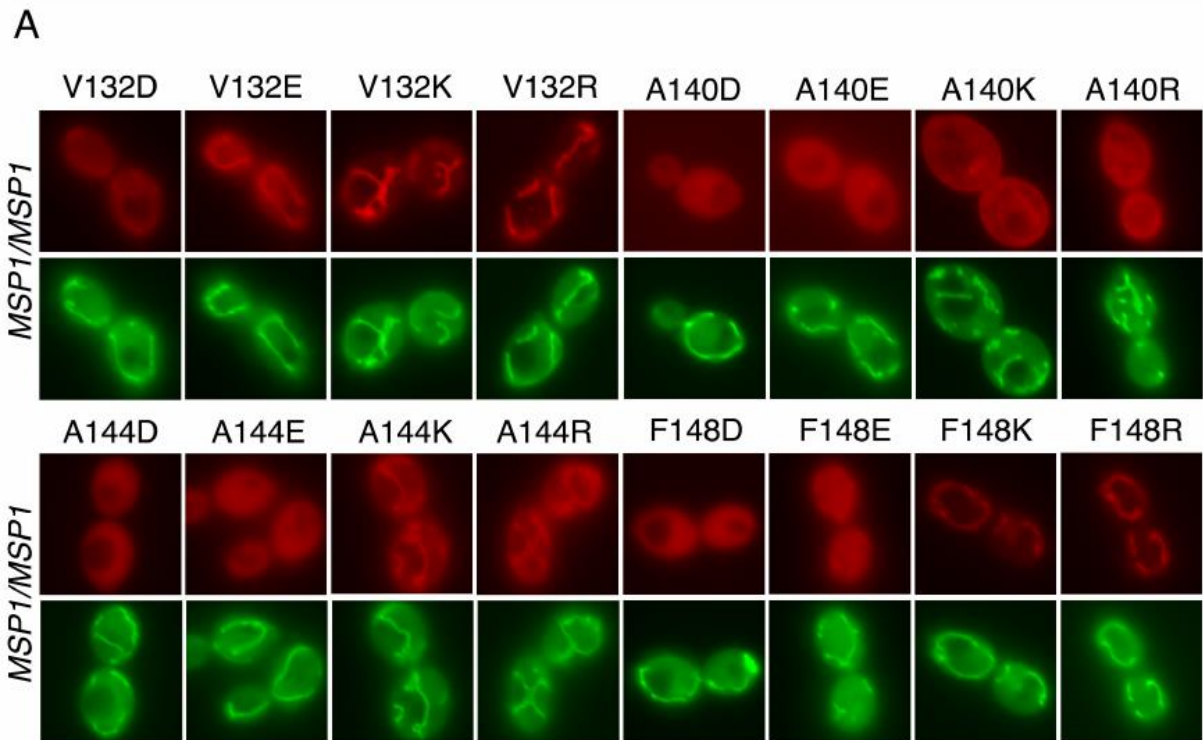


Figure 4.15. **Positively charged amino acids are more tolerated within the TMD of Fis1p for targeting to mitochondria rather than negatively charged amino acids.** (A) Visualization of localization of mCherry-TA in the cells harboring Msp1p. CDD961 strain was transformed with plasmids expressing mCherry fused to the Fis1p TA containing the indicated charge replacements from plasmids b192-b207. Cells were examined as in Figure 4.3. (B) Deletion of Msp1p does not result in relocalization of previously mislocalized tail-anchored fluorescent proteins to mitochondria. *msp1Δ/msp1Δ* strain CDD1044 was transformed with the following plasmids encoding mCherry fused to the mutant TAs: b192 (V132D), b196 (A140D), b197 (A140E), b198 (A140K), b199 (A140R), b200 (A144D), b201 (A144E), b134 (V145E), b204 (F148D), b205 (F148E). Cells were visualized as in Figure 4.3.

We have already shown that positively charged amino acids are tolerated at some positions within the TMD of Fis1 and these charge mutations do not interfere with the insertion of Fis1p. However, here the question is whether these Fis1p variants containing charged amino acid substitutions are functional or not. To determine the functionality of these Fis1p variants (V132, A144, and V148), we carried out two different assays. Even negligible Fis1p activity is sufficient for mitochondrial fission^{191,197}, which indicates that even minimal targeting of Fis1 to mitochondrial OM and related functionality of it could be observable by functional assays.

In our first functional assay, we examined whether mitochondrial morphology defect is restored upon expression of Fis1p charge variants in a strain lacking endogenous Fis1p encoding gene. Fis1p is involved in fission of mitochondria and in the absence of Fis1p, mitochondria cannot divide; however, unchecked fusion results in a unified mitochondrial network¹⁸¹. Intriguingly, all Fis1p variants containing charge substitutions (except of Fis1p- (A144P)), positive or negative, at positions V132, A144 and V148 demonstrated some Fis1p activity when they were expressed in a *fis1Δ* strain as indicated by mitochondrial morphology (Figure 4.16A). In Figure 4.15, we demonstrated that aspartate and glutamate substitutions within the TMD blocked mitochondrial targeting. However, this assay showed that even these Fis1p variants can provide some Fis1p function. Therefore, we concluded that even if mitochondrial localization of these variants is not detectable under microscope, still very little amount of Fis1p carrying negatively

charged amino acid substitution within the TMD is inserted to the MOM and this amount is sufficient for fission activity. Moreover, we can clearly state that A144D mutation inhibits mitochondrial targeting of Fis1p entirely. To further examine the activity of Fis1p, we perturbed mitochondrial morphology by treatment with sodium azide, which causes fragmentation of mitochondria that are able to divide^{201,202}, thereby making easier to visualize mitochondrial fission defects. Similar to previous results, again all Fis1p variants provided mitochondrial fission activity but the A144D mutant (Figure 4.16B and Figure 4.16C).



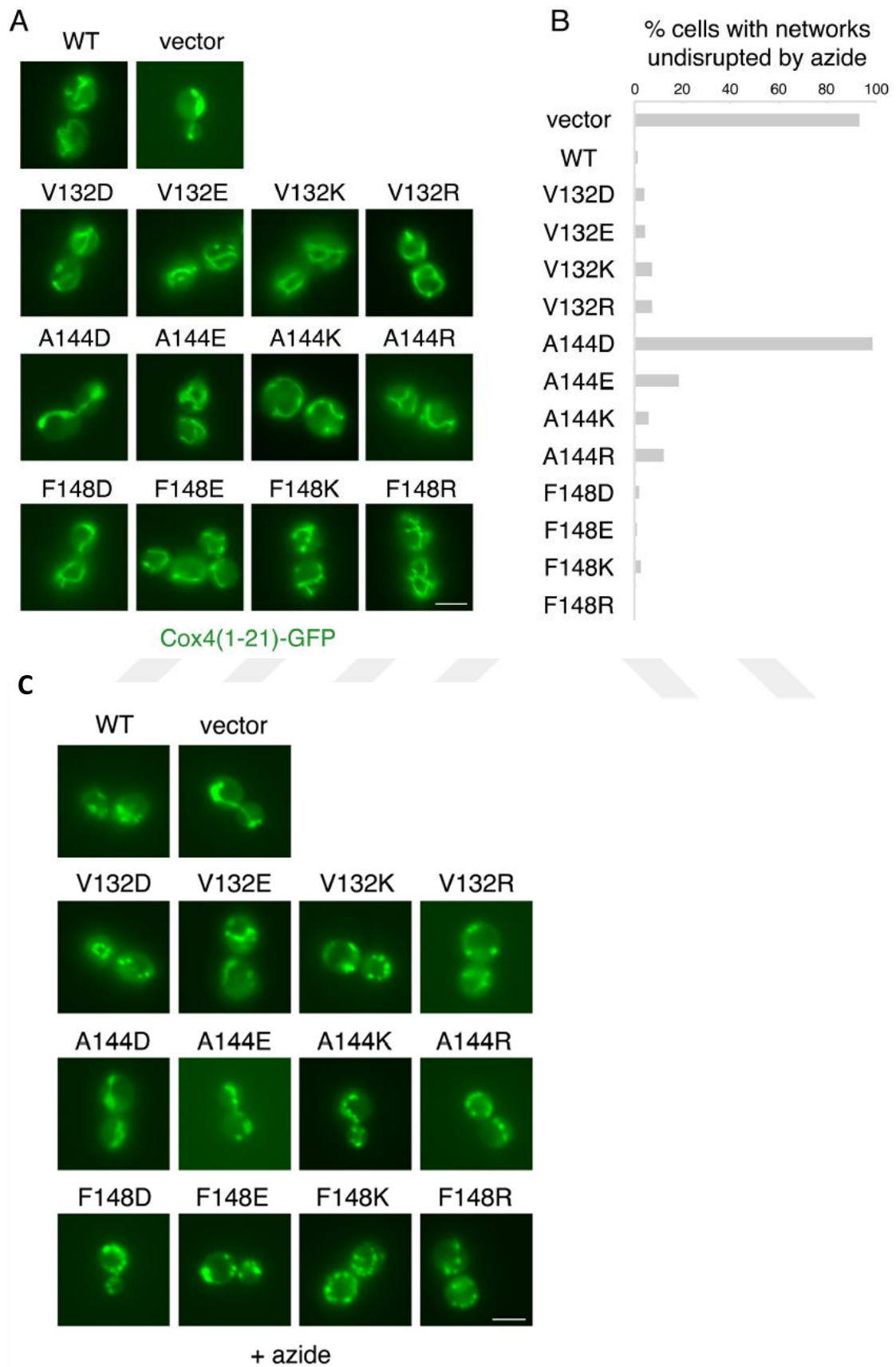


Figure 4.16. Fis1p variants containing positively or negatively charged amino acid substitutions within the TMD can promote fission activity. (A) Regular mitochondrial morphology is maintained even in the presence of positively or negatively charged amino acid substitutions within the hydrophobic TMD of Fis1p. CDD741 strain was transformed with a plasmid pRS313 expressing WT Fis1p (b239), or a plasmid expressing Fis1p containing a mutation that causes the indicated TMD alteration (plasmids b240-251). Mitochondrial morphology was examined by expression of mitochondria-targeted GFP from plasmid pHS12. (B) Induced, Fis1p-dependent mitochondrial fragmentation is allowed by charge placement within the Fis1p TMD. Transformants analyzed in (A) were treated with sodium azide to induce mitochondrial fragmentation, and cells were scored for the maintenance of a mitochondrial network. (C) Almost all charge replacements within the TMD of Fis1p allow Fis1p-dependent mitochondrial fragmentation. Images of azide-treated cells scored in (B)

We also performed a genetic assay of Fis1 function. When mitochondrial fission is blocked, as mentioned before, unchecked fusion results in a unified mitochondrial network¹⁸¹. However, mitochondrial function and mitochondrial DNA (mtDNA) are still kept. On the other hand, disruption of mitochondrial fusion, by deleting Fzo1p, results in mitochondrial fragmentation^{203,204}. As a result of fragmentation, mtDNA is lost and these cells cannot grow on the nonfermentable carbon source since they are not able to respire²⁰³. However, when both fission and fusion are defective, mtDNA is kept and cells can respire^{190,201,181,205}. As our microscopy-based analysis demonstrated, only the A144D variant of Fis1p did not show activity and let the cells keep mtDNA in the strain lacking Fzo1p (Figure 4.17). Since all other variants possessed sufficient fission activity, as a result of mitochondrial fragmentation, they lost their mtDNA in the absence of Fzo1p. In conclusion, our findings indicate that positively charged amino acid substitutions within the TMD of Fis1p can better promote mitochondrial targeting compared to negatively charged amino acids. However, it is also possible to see an accommodation of negatively charged amino acids, which may provide some low level of mitochondrial sorting, within the TMD of Fis1p.

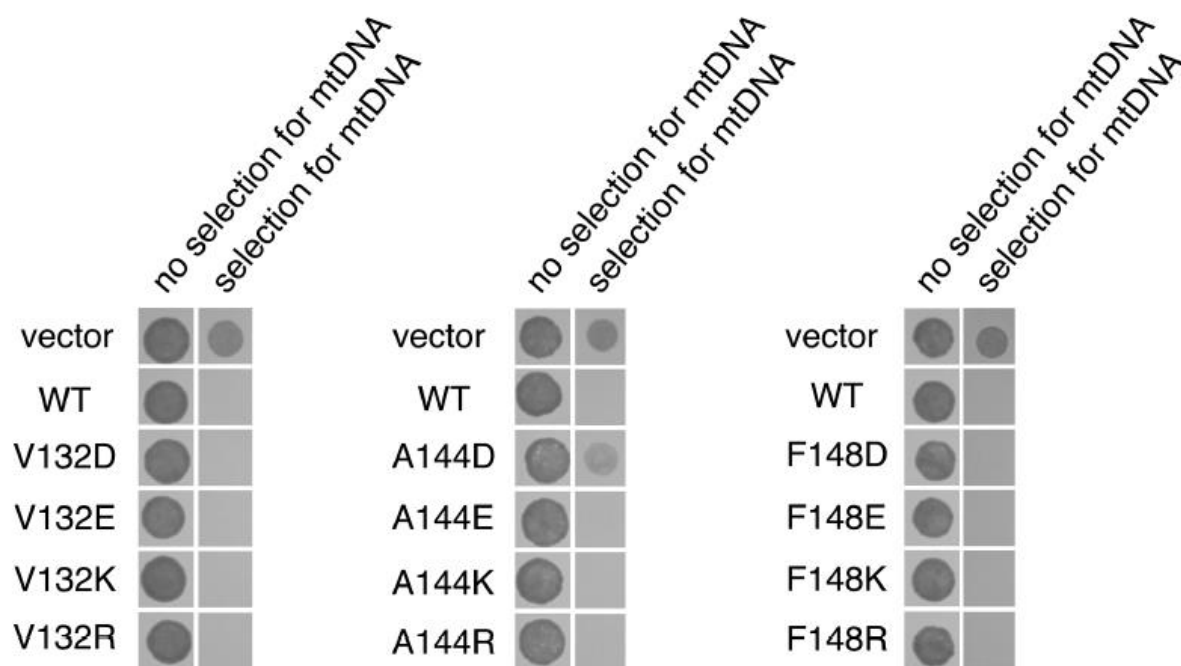


Figure 4.17. **Fis1p variants containing positively or negatively charged amino acid substitutions within the TMD can promote fission activity.** Charge substitutions within the TMD of Fis1p do not prevent the function of Fis1p variants in the genetic assay. *fzo1Δ fis1Δ* strain CDD688, carrying a CHX-counter selectable marker, *FZO1*-expressing plasmid, was transformed with the Fis1p expressing plasmids enumerated in the legend of Figure 4.16A. Transformants were grown overnight in SMM-His medium to let cells lose the *FZO1*-encoding plasmid. Serial dilutions were spotted to Slac-His+3 $\mu\text{g/ml}$ CHX and incubated for 5d to test for maintenance of mtDNA following counter selection for *FZO1*. As a control for cell proliferation under conditions not strongly selective for mtDNA maintenance, cells were also spotted to SMM-Trp-His medium and incubated for 2d.

4.9 Bacterial tail anchors insert into the various organelles in *S. cerevisiae* including mitochondria

It has been demonstrated that TA proteins are found in all domains of life and TA protein insertion mechanisms in eukaryotes may have originated from prokaryotes²⁰⁶. In the case of mitochondria, the scenario is a bit different. Because of its endosymbiotic origin, mitochondria lost or transferred a big fraction of its genome to the nuclear chromosome⁴⁵. In other words, most of the mitochondrial proteins are encoded by the

nuclear genome. Therefore, mitochondrial TA proteins have to find their way to mitochondria after they are synthesized in the cytosol. Targeting of nuclear-encoded mitochondrial TA proteins to mitochondria requires an evolved insertion mechanism or targeting can also occur in an unguided manner. To have an idea about the evolutionary perspective of the putative mitochondrial TA protein insertion machinery, we investigated whether bacterial TAs could be directed to mitochondria in *S. cerevisiae*. To analyze this, we fused TA of eight *Escherichia coli* (*E.coli*) TA proteins (Table 4.3), which were identified in a bioinformatic screen²⁰⁶, to the C-terminus of mCherry.

Table 4.3. List of the bacterial TA proteins that may potentially be targeted to various organelles in *S. cerevisiae*.

Name of the bacterial TA protein	Description of the protein
elaB	It is a membrane-anchored ribosome-binding protein. Its function is unknown.
yqjD	It is a membrane-anchored ribosome-binding protein. Its function is unknown.
tcdA	TcdA is an ATP-dependent dehydratase required to convert t(6)A37 to cyclic t(6)A37 in several tRNA species.
ygiM	ygiM has been detected as a membrane-bound homo-hexamer. It is a SH3 domain protein. Its function is unknown.
waaR	It is a lipopolysaccharide 1,2-glucosyltransferase.
djlB	DjlB is an uncharacterized DnaJ homolog (J domain-containing protein, JDP) that is a predicted HscC co-chaperone stimulating its chaperone partner's ATPase activity because of its similarities to known type III JDP DjlC HscC co-chaperone.
flk	It prevents premature secretion of FlgM and senses flagellar assembly stage.
yhdV	It is a novel verified lipoprotein, Its function is unknown.

We picked these eight bacterial TA proteins from the study of Borgese et al.²⁰⁶ just by looking whether the predicted TMD is close to the C-terminus of the TA protein. (Table 4.4). We chose the ones which may have the potential to be targeted to mitochondria in *S. cerevisiae*. As it was shown in Table 4.4, *elaB* and *yqjD* have two arginines at the extreme c-terminus of the corresponding TA, resulting mitochondrial localization of mCherry as we expected. Indeed, *elaB* and *yqjD* are paralogs²⁰⁷ which further supports mitochondrial localization of both of them. *TcdA* has a slightly longer TA than the wild type *Fis1p* TA. However, four of the last ten amino acids of *TcdA* TA are positively charged, which is obviously enough for mitochondrial targeting as our data suggested. *YgiM* TA directed mCherry to peroxisome. Even though we did not verify the identity of these structures with a peroxisome marker, from the previous studies, we know that these structures are peroxisomes. *waaR*, *djlB*, and *flk* TAs were able to localize mCherry to the ER. Indeed, ER can accept TAs with different lengths and C-terminal region of different charge and size which do not have precise features for targeting to the MOM. Despite this, we did not observe any organelle localization of *yhdV* variant (Figure 4.17).

Table 4.4. Predicted amino acid sequence of the TA of bacterial TA proteins.

Fis1 TA = LKGVVVAGGVLGAVAVASFFLRNKRR*
elaB = PWQGIGVGAAVGLVLGLLLARR*
yqjD = WTGVGIGAAIGVVLGVLLSRR*
tcdA = ASGFGAATMVTATFGFVAVSHALKKMMAKAARQG*
ygiM = WFMYG GGV LGLG LLLGLV LPHLIPSRKRKDRWMN*
waaR = LVQH H YISG I IAGVCYL CRKY YRK*
djlB = LG I I K I I F Y I F I F A G L I G K I L H L F G*
flk = PALWILLVAIILMLVWLVR*
yhdV = TAGAIAGGAAAVAGLTMGIIALSK*

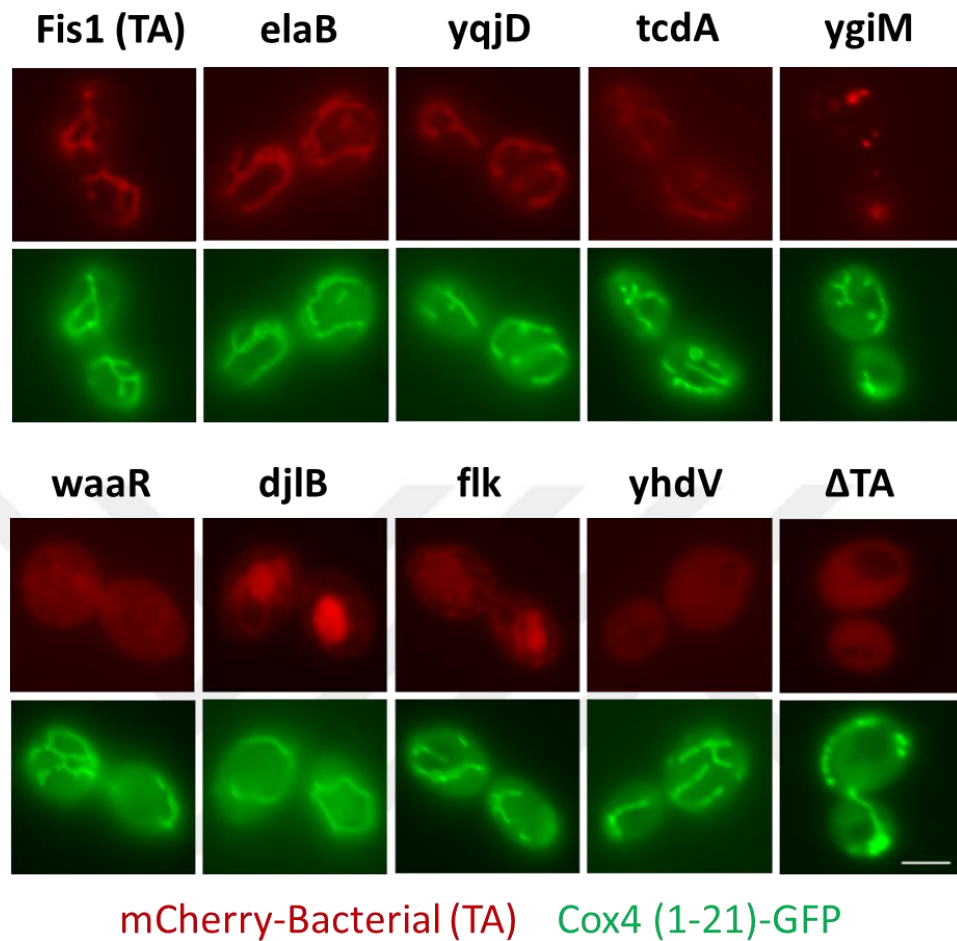


Figure 4.18. **Bacterial tail anchors are targeted to various organelles in *S. cerevisiae*.** While *elaB*, *yqjD* and *tcdA* bacterial TAs direct mCherry to mitochondria, *ygiM* TA lead to peroxisomal localization of mCherry. Other three bacterial TAs, *waaR*, *djlB* and *flk*, allow localization to the ER. *yhdV* TA is not able to sort mCherry to any compartment in yeast. mCherry linked to different bacterial TAs were expressed in wild-type strain CDD961 from plasmids b109 (WT), b273 (*flk*), b274 (*ygiM*), b275 (*elaB*), b277 (*yhdV*), b278 (*waaR*), b279 (*yqjD*), b280 (*djlB*), b281 (*TcdA*), or b252 (Δ TA) and visualized, along with mitochondrial-targeted GFP, as in Figure 4.3

CHAPTER 5

DISCUSSION

While how the ER and peroxisomal tail-anchored proteins are directed to their corresponding membranes were demonstrated, no insertion machinery has been identified for mitochondrial TA proteins. It was initially thought that the ER TA protein insertion was provided only by the SRP and Hsp40/Hsc70 family molecular chaperones. Identification of the universal ER TA protein insertion pathway, GET pathway, elucidated the mysterious process of insertion of TA proteins into the ER membrane. History of the putative machinery responsible for insertion of mitochondrial TA proteins is similar to the story of the insertion mechanism of the ER TA proteins. Investigations on the nature of the putative mitochondrial TA protein insertion machinery have yielded conflicting results. It has been shown that TOM complex does not have any role in insertion of mitochondrial TA proteins Bcl-x_L, Omp25, Bak, and Fis1^{79,208}. However, insertion of Tom22, which is also a TA protein, involves Tom20 and Tom70¹⁷⁴ and itself of Tom22 was thought as the receptor that plays a crucial role in the insertion of Bax¹⁷³. Furthermore, Tom20 is required for import of Bcl-2^{132,172}. All these results suggest that TA proteins can be targeted to the outer membrane of mitochondria by more than one mechanism. However, it is possible that a universal mitochondrial TA protein insertion machinery may exist, similar to GET pathway. In this study, our initial aim was to identify a universal machinery of mitochondrial TA protein insertion if it exists. However, we were not able to identify any *trans* factor (even though we also looked for temperature sensitive mutants by considering the possibility of being essential of the target components for survival) related to the insertion of Fis1p.

Two major drawbacks might restrict the identification of the mitochondrial TA protein insertion machinery. The first one is associated with our selection approach which

is designed to detect mutants that direct Gal4-Fis1p to the nucleus, yet mutants that are mislocalized to other organelles or are degraded, cannot be detected. A *trans* mutation within a gene coding for a *trans* factor taking a role in Fis1p insertion would prevent insertion of Gal4-Fis1p into the MOM. However, non-insertion of this chimeric to mitochondria does not mean that it would go into the nucleus and activate the selectable reporters. There are competitions between chaperones that recognize different TA proteins. The most stably and promptly binding chaperone determine the target organelle of TA protein²⁰⁹. Assuming that the mutated *trans* factor is the chaperone binding to mitochondrial TA protein, since Gal4-Fis1p would not be able to bind to right chaperone, it would be recognized by some other chaperones (due to the kinetic factors mentioned above) taking a role in insertion of other kinds of TA proteins, like the ER or peroxisomal. Because of this interaction with another chaperone, Gal4-Fis1p would be inserted into another organelle, and we would not be able to see activation of the reporters and identify this mutant strain.

The second and the most challenging problem is related to nature of mitochondrial TA protein insertion. As it is indicated before, mitochondrial TA protein insertion is controlled by more than one mechanism. Furthermore, insertion of Fis1⁷⁹, Bcl-2¹⁵¹, and mitochondrial isoform of b5⁷⁹ into protein-free lipid bilayer has been validated *in vitro*. The mitochondrial outer membrane has the lowest amount of ergosterol among all membranes presented in yeast⁹ and low ergosterol content increases the fluidity of a membrane⁷⁹. It was postulated that this nature of the MOM facilitates faster insertion of mitochondrial TA proteins which provides a kinetic advantage to mitochondria compared to other organelles⁷⁹. Because of the features that lead the unassisted integration of mitochondrial TA proteins into the MOM, identification of the chaperone-mediated specific targeting pathway may be masked in the selection approaches like ours.

Our selection method is more prone for selection of *cis* mutants rather than *trans* mutants. As our initial screening results demonstrated, only 1 of the 33 Ura⁺ isolates was a *trans* mutant. For the selection of *trans* mutants, we improved our selection method. Towards to this goal, we generated another plasmid which expresses the same Gal4-Fis1p construct and has another counter-selectable marker. Following random mutagenesis, forcing cells to lose either of the plasmids will allow us to identify *trans* mutants. A *cis*

mutation in one of the plasmids encoding for Gal4-Fis1p results in activation of the selectable markers. However, since the probability of having a *cis* mutation in both of the plasmids at the same time is low, the strain in which the selectable markers are activated after removal of one of the plasmids separately, will be the potential *trans* mutant. Indeed, we generated the required plasmid; however, we did not push too hard to find some *trans* mutants. By using this developed approach, *trans* mutants can be identified.

Kinetic factors do not affect insertion of mitochondrial TA proteins if there is no machinery. However, if there is a putative insertion machinery, insertion efficiency could be influenced since the TA protein insertion machinery may be saturable. Number of the *trans* factors and how fast a TA protein is inserted into the MOM would matter in the case of existence of a TA protein insertion machinery. We expressed mCherry-Fis1 TA construct from a plasmid in which the coding region of this construct is under the *GALI* inducible promoter. Even after induction of the culture with galactose for 5 hours, we observed strong mitochondrial localization of mCherry with no cytosolic localization (A.Keskin, unpublished results) suggesting that if there is a machinery for insertion of mitochondrial TA proteins, it is not saturable.

Indeed, in this study, we mainly focused on a revealing structural characteristic of TMD of Fis1p since mitochondrial targeting information is encoded in these structural features. By taking advantage of deep mutational scanning approach, we investigated structural characteristics of the TMD of Fis1p. This is the first fine-grained analysis of a eukaryotic organelle targeting signal in which deep mutational scanning approach has been applied, to our knowledge. Coupling a selection or screening method to deep mutational scanning is very time- and cost- effective^{210,211,212}. We completed mutant library generation, subsequent pool selection, and next generation sequencing in a few months. Deep mutational scanning has also been effectively utilized in other areas, like tumor suppressor structure and function²¹³, membrane protein insertion in bacteria²¹⁴, and the relationship between a protein's evolutionary path and present fitness^{215,216}.

5.1 Positively charged amino acids within a mitochondrial transmembrane domain may “snorkel” to the lipid bilayer.

Since placing charged residues into the lipid bilayer is energetically unfavorable²¹⁷, we were surprised to see that positively charged amino acids are tolerated within the MAD of Fis1p and do not interfere with mitochondrial targeting. Indeed, it was previously suggested that positively charged amino acids within the TA, lysine and arginine, possess relatively long aliphatic side chains which can integrate themselves into the hydrophobic milieu of the lipid bilayer. Since the aliphatic side chains of these positively charged amino acids are long enough, they are able to reach up to water-lipid bilayer interface region where positively charge head group of these amino acids can interact with negatively charged phosphate groups of the lipid bilayer. This behavior is termed as “snorkeling”^{218,219,220}. On the other hand, the shorter aliphatic side chains of aspartate and glutamate cannot reach out the membrane interface region in order to pull out the negatively charged head group from the hydrophobic environment. This property of negatively charged amino acids makes the TMD less stable within the lipid bilayer, thereby preventing insertion. Snorkeling has been observed in some other studies as well, such as structural studies of the Kv1.2 potassium channel²²¹ and integrin $\beta 3$ ²²². There was a little functional evidence of snorkeling *in vivo*; however, by taking advantage of large-scale examination of charge replacement within the given TMD, we and other groups²¹⁴ suggested snorkeling ability of positively charge amino acids. Our large-scale analysis, and subsequently performed genetic and microscopy-based analysis strongly suggested the ability of lysine or arginine to be accommodated by snorkeling at various positions within the TMD of Fis1p.

5.2 The TMD of the Fis1p may consist of two separable segments

Previous computational analysis demonstrated that TMD of Fis1p has alpha helical secondary structure in nature^{223,224}. Our results suggested that appropriate insertion of Fis1p involves an alpha-helical structure of the TMD since proline substitutions in most of the positions within the TMD blocked the insertion of Fis1p and it is known that proline is a helix breaker²²⁵. On the other hand, we observed that at the position G137, proline is more tolerated than the other proline substitutions located at the other positions tested

which indicates that TMD of Fis1p is bipartite in nature. We also did not see alteration in mitochondrial localization upon insertion of up to three alanines between A135 and G136, further supporting bipartite nature of the TMD of Fis1p. Furthermore, according to our deep mutational scanning data (Figure 4.5), it is obvious that mutations located at the carboxyl terminus end of the TMD seem to influence insertion more drastically than mutations found closer to amino terminus of the TMD. These findings indicate that those prolines may demarcate a borderline between different structural regions of the TMD.

Even though proline residue is a α -helix breaker, it provides some flexibility to TMD to secure smooth integration of TA proteins into the MOM¹⁷⁵, which suggests that presence of proline at the position G137 may further facilitate insertion of Fis1p. We just examined replacements of four proline within the TMD and three of them hindered insertion as the deep mutational scanning data suggested. However, positions A135 and G136 appear to be as tolerated as G137 for proline substitution (Figure 4.5). Testing proline replacement at these positions would also be informative about whether proline can provide some flexibility for facilitated insertion of TA proteins.

Glycine is also not tolerated within alpha-helices^{226,227} due to its conformational flexibility. However, deep mutational scanning data did not exhibit diminished Fis1p insertion when most of the amino acids within the TMD were substituted to glycine. Indeed, this was initially surprising for us after seeing severe insertion defects caused by proline substitutions. However, the presence of a glycine in an alpha-helices found within a lipid bilayer is less disruptive compared to the presence of a glycine within an alpha-helices of a soluble protein because of the ability of glycine making better intra-helical hydrogen bonding within the hydrophobic habitat of the lipid bilayer²²⁸. In fact, there are already four glycines within the TMD of *S. cerevisiae* Fis1p. Glycine is also found within the TMD of Fis1p orthologs¹⁹⁹, suggesting that glycine is not as disruptive as proline within the TMD.

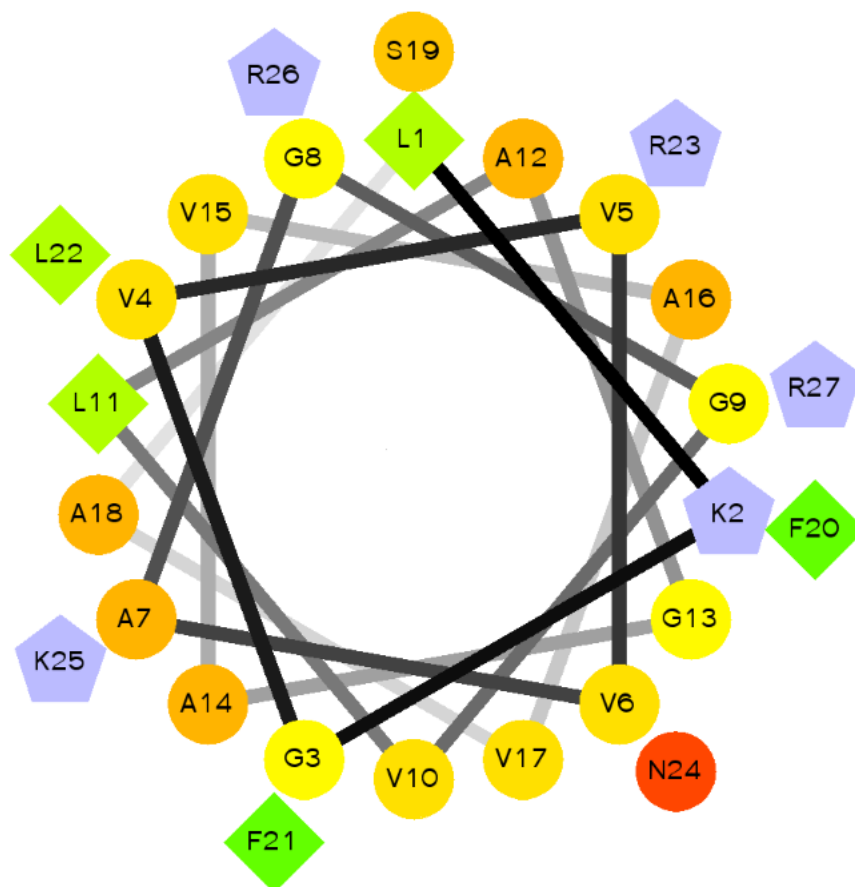


Figure 5.1. **Longer amino acids cluster at one side of the α -helix.** Amino acids having longer hydrocarbon chain, such as Leucine (L), cluster at a specific part of the α -helix while shorter amino acids, like Alanine (A), Valine (V), and Glycine (G), are distributed within the α -helix. The hydrophilic residues are presented as circles, hydrophobic residues as diamonds, and potentially positively charged as pentagons. Hydrophobicity is color coded as well: the most hydrophobic residue is green, and the amount of green is decreasing proportionally to the hydrophobicity, with zero hydrophobicity coded as yellow. Hydrophilic residues are coded red with pure red being the most hydrophilic (uncharged) residue, and the amount of red decreasing proportionally to the hydrophilicity. The potentially charged residues are light blue. The plot was generated using the Helical Wheel Projections program

We also looked at the distribution of the amino acids within the α -helix structure of the TA of Fis1 by using the Helical Wheel Projections program. The plot revealed that amino acids having longer hydrocarbon chain, like Leucine (L), are concentrated on one

side of the helix while shorter amino acids, such as Alanine (A), Valine (V), and Glycine (G) are distributed within the helix (Figure 5.1). However, we did not observe enrichment of Leucine at any specific region within the Fis1 TA in our large-scale analysis (Figure 4.5). Indeed, this is expected because the primary structure of the Fis1 TA is different from 3D (α -helix) secondary structure of the Fis1 TA. We also did not observe clustering of the positively charged amino acids. According to currently accepted Fis1p topology, positively charged amino acids found at the carboxyl-terminus of Fis1p are exposed to the mitochondrial intermembrane space. Since this charged region is not located within the MAD which gives rise to α -helix, the program is not able to place these positively charged amino acids properly.

5.3 Positively charged amino acids found at the carboxyl terminus of Fis1p are required for specific targeting to mitochondria

Four of the last five amino acids of the carboxyl terminus of Fis1p are positively charged and it was previously reported that those positively charged amino acids are essential for targeting of Fis1p and play a crucial role in insertion of TA proteins to the MOM^{168,196,199,191,229}. Our genetic selection and microscopy-based analysis also demonstrated that this highly charged region is critical for proper membrane insertion and specific targeting to mitochondria. However, how these positively charged amino acids provide organelle specificity and insertion is not clear yet.

5.4 Bacteria may have separate IM domains that might approximate the different ER and mitochondrial lipid composition

Even though there is no known identified insertion machinery for mitochondrial TA proteins, it has been experimentally shown that mitochondrial TA protein insertion can occur spontaneously. In addition to Hsp40/Hsc70 family molecular chaperones and the SRP, targeting of the ER TA proteins in eukaryotes is mainly provided by the TRC40/GET system. All of the bacterial TA proteins mentioned in this study are integrated to the inner face of the cytoplasmic membrane where they can perform a variety of functions (Table 4.3). Prokaryotic ArsA protein is a homolog of Get3p which is the chaperone binding ER TA proteins in yeast for their insertion. However, it has been shown that while archeal

Get3p homologue ArsA is involved in TA protein insertion in archaea domain, prokaryotic ArsA which is also a homolog of Get3p lacks the features required for TA insertion task²⁰⁶. Thus, GET3 targeting pathway in eukaryotes may have originated from our archeal ancestor. Therefore, since there is no known insertion machinery for bacterial TA proteins, we can suggest that insertion of all of these eight bacterial TAs discussed may occur spontaneously. However, here the question is what does promote their insertion into the various organelles in yeast?

It is known that membrane of bacteria contains domains that exhibit divergence from the surrounding membrane in terms of lipid and protein composition²³⁰. For instance, at the septal regions and cell poles, the membrane of bacteria is enriched with cardiolipin (CL)²³¹, reminiscent of the outer membrane of mitochondria. There could be some other domains on the membrane of bacteria whose lipid composition may be similar to lipid composition of the ER. In the light of this information, we thought that these various domains of the membrane of bacteria with different lipid composition may have a specific function in the cell. For example, the region similar to the membrane of the ER may exhibit similar functions to the ER. Therefore, we hypothesized that because of the lipid composition similarity, these spontaneously inserted bacterial TA proteins are targeted to a specific organelle in yeast. For instance, since *elaB* protein is possibly inserted to CL rich domain of the inner membrane of bacteria, it is directed to mitochondria in yeast due to the similarity of the lipid composition of OM of mitochondria to this CL rich domain of bacterial membrane. Indeed, physicochemical features of the TA of *elaB* also have a role in mitochondrial targeting in yeast. This can be also the case for the bacterial TA proteins targeted to the ER in yeast. However, unlike spontaneous insertion of bacterial TAs into the mitochondrial OM, the ER-targeted bacterial TAs may be recognized by Get3p to be inserted into the ER in assistant dependent manner.

Another speculation related to insertion of mitochondrial TA protein to the MOM is that the first mitochondrion translocon may have been made up of TA proteins. Because of its endosymbiotic origin, a big fraction of mitochondrial genome was transferred to the nuclear chromosome. Therefore, mitochondrial proteins encoded by the nuclear genome have to go back to mitochondria after being synthesized in the cytosol. A translocon is required for this purpose and it is possible that first mitochondrion translocon may have

been made up of TA proteins since this kind of translocon machinery would not have required a preexisting machinery.

Moreover, *ygiM* is the SRC homology 3 (SH3) domain protein and it has been previously demonstrated that *S. cerevisiae* PTS1 receptor Pex5p binds to SH3 domain of the peroxisomal membrane protein Pex13²³². Potential binding of Pex5p to SH3 domain may explain peroxisomal localization of *ygiM* in yeast.



CHAPTER 6

CONCLUSION AND OUTLOOK

In this study, one of our aims was to reveal the molecular mechanism of TA protein insertion into the MOM by utilizing a positive selection method which is based on viability following mislocalization of a chimeric protein. As a consequence of screening for *trans* mutations, we could not identify any *trans* factor taking a role in Fis1p insertion. One of the major reason of it was the limitation of our selection method. Furthermore, spontaneous insertion ability of mitochondrial TA protein makes identification of any *trans* factor really challenging. By using our developed genetic approach mentioned in discussion part, *trans* factors can be identified.

Considering these limitations, we focused on revealing the sequence and structural features of the TMD of Fis1p required for mitochondrial targeting. For this purpose, we coupled next generation sequencing to our selection method. Our deep mutational scanning analysis uncovered determinants of Fis1p tail-anchor targeting. Our results suggested that positively charged amino acids are more tolerated within the TMD of Fis1p than negatively charged residues and they do not interfere with insertion and functionality of Fis1p. Moreover, our results exhibited that length of the TMD of Fis1p does not influence targeting to mitochondria and proline is not tolerated at many positions within the TMD of Fis1p due to its helix-disrupting feature. Finally, we revealed that positively charged amino acids found at the carboxyl terminus of the Fis1p are important for organelle specificity; however, they are not required for membrane localization.

We also wanted to show whether bacterial TAs are able to localize to mitochondria in yeast. We observed that most of the bacterial TAs localized to various organelles in yeast. Preliminary results of the currently ongoing experiments are promising. We showed mitochondrial localization of some of these bacterial TAs with microscopy-based analysis. To verify the results, further experiments are needed. We can investigate whether these bacterial TAs are targeted to any membrane in yeast via our genetic approach. To understand whether bacterial TAs behave like endogenously encoded eukaryotic TAs, we

can look at localization of mCherry fused to TA of those bacterial TAs in the *spf1Δ* strain. In addition, we need to clarify that whether mitochondrially localized bacterial TAs are really inserted or merely associated with mitochondria. Sodium-carbonate extraction experiment would inform us about that. Another intriguing question, can a bacterial TA which has the ability to be targeted to mitochondria provide functionality to an endogenous TA-targeted protein? To answer this question, the functionality of a Fis1p-elaB TA construct can be tested by microscopic or genetics assays that we utilized in this study. Furthermore, is the ER targeting of waaR, djlB, and flk Get3 dependent or peroxisomal targeting of ygiM Pex5p or Pex19p dependent? All these basic questions can be elucidated with simple knock-out experiments.

This dissertation contributes to understanding of determinants of mitochondrial TA protein targeting. Systematic analyses of this kind, which give a comprehensive picture of features involved in protein targeting and which are made possible by the availability of next-generation sequencing, will probably be widely applied in the future.

BIBLIOGRAPHY

1. Wallin, E. & von Heijne, G. Genome-wide analysis of integral membrane proteins from eubacterial, archaean, and eukaryotic organisms. *Protein Sci.* **7**, 1029–38 (1998).
2. Checler, F. & Vincent, B. Alzheimer's and prion diseases: distinct pathologies, common proteolytic denominators. *Trends Neurosci.* **25**, 616–20 (2002).
3. Mailman, R., Huang, X. & Nichols, D. E. Parkinson's disease and D1 dopamine receptors. *Curr. Opin. Investig. Drugs* **2**, 1582–91 (2001).
4. Andrews, D. W. Transport across membranes: a question of navigation. *Cell* **102**, 139–44 (2000).
5. Rapoport, T. A., Jungnickel, B. & Kutay, U. Protein transport across the eukaryotic endoplasmic reticulum and bacterial inner membranes. *Annu. Rev. Biochem.* **65**, 271–303 (1996).
6. Vance, J. E., Stone, S. J. & Faust, J. R. Abnormalities in mitochondria-associated membranes and phospholipid biosynthetic enzymes in the *mnd/mnd* mouse model of neuronal ceroid lipofuscinosis. *Biochim. Biophys. Acta* **1344**, 286–99 (1997).
7. Chandra, N. C., Spiro, M. J. & Spiro, R. G. Identification of a glycoprotein from rat liver mitochondrial inner membrane and demonstration of its origin in the endoplasmic reticulum. *J. Biol. Chem.* **273**, 19715–21 (1998).
8. Titorenko, V. *et al.* Dynamics of peroxisome assembly and function. *Trends Cell Biol.* **11**, 22–29 (2001).
9. Schneiter, R. *et al.* Electrospray Ionization Tandem Mass Spectrometry (Esi-Ms/Ms) Analysis of the Lipid Molecular Species Composition of Yeast Subcellular Membranes Reveals Acyl Chain-Based Sorting/Remodeling of Distinct Molecular Species En Route to the Plasma Membrane. *J. Cell Biol.* **146**, 741–754 (1999).

10. Purdue, P. E. & Lazarow, P. B. Peroxisome biogenesis. *Annu. Rev. Cell Dev. Biol.* **17**, 701–52 (2001).
11. Subramani, S. *et al.* Components involved in peroxisome import, biogenesis, proliferation, turnover, and movement. *Physiol. Rev.* **78**, 171–88 (1998).
12. Holroyd, C. & Erdmann, R. Protein translocation machineries of peroxisomes. *FEBS Lett.* **501**, 6–10 (2001).
13. Wickner, W. & Schekman, R. Protein translocation across biological membranes. *Science* **310**, 1452–6 (2005).
14. Gould, S. J., Keller, G. A., Hosken, N., Wilkinson, J. & Subramani, S. A conserved tripeptide sorts proteins to peroxisomes. *J. Cell Biol.* **108**, 1657–1664 (1989).
15. Marzioch, M., Erdmann, R., Veenhuis, M. & Kunau, W. H. PAS7 encodes a novel yeast member of the WD-40 protein family essential for import of 3-oxoacyl-CoA thiolase, a PTS2-containing protein, into peroxisomes. *EMBO J.* **13**, 4908–18 (1994).
16. Agne, B. *et al.* Pex8p: An Intraperoxisomal Organizer of the Peroxisomal Import Machinery. *Mol. Cell* **11**, 635–646 (2003).
17. Chang, C.-C., Warren, D. S., Sacksteder, K. A. & Gould, S. J. Pex12 Interacts with Pex5 and Pex10 and Acts Downstream of Receptor Docking in Peroxisomal Matrix Protein Import. *J. Cell Biol.* **147**, 761–774 (1999).
18. Dodt, G. & Gould, S. J. Multiple PEX genes are required for proper subcellular distribution and stability of Pex5p, the PTS1 receptor: evidence that PTS1 protein import is mediated by a cycling receptor. *J. Cell Biol.* **135**, 1763–1774 (1996).
19. Miyata, N. & Fujiki, Y. Shuttling Mechanism of Peroxisome Targeting Signal Type 1 Receptor Pex5: ATP-Independent Import and ATP-Dependent Export. *Mol. Cell. Biol.* **25**, 10822–10832 (2005).
20. Götte, K. *et al.* Pex19p, a farnesylated protein essential for peroxisome biogenesis. *Mol. Cell. Biol.* **18**, 616–28 (1998).

21. Kutay, U., Hartmann, E. & Rapoport, T. A. A class of membrane proteins with a C-terminal anchor. *Trends Cell Biol.* **3**, 72–5 (1993).
22. Janiak, F., Glover, J. R., Leber, B., Rachubinski, R. a & Andrews, D. W. Targeting of passenger protein domains to multiple intracellular membranes. *Biochem. J.* **300** (Pt 1), 191–9 (1994).
23. Zhu, W., Eicher, A., Leber, B. & Andrews, D. W. At the onset of transformation polyomavirus middle-T recruits shc and src to a perinuclear compartment coincident with condensation of endosomes. *Oncogene* **17**, 565–76 (1998).
24. Wattenberg, B. & Lithgow, T. Targeting of C-terminal (tail)-anchored proteins: understanding how cytoplasmic activities are anchored to intracellular membranes. *Traffic* **2**, 66–71 (2001).
25. Lee, J., Kim, D. H. & Hwang, I. Specific targeting of proteins to outer envelope membranes of endosymbiotic organelles, chloroplasts, and mitochondria. *Front. Plant Sci.* **5**, 173 (2014).
26. A Perspective on Transport of Proteins into Mitochondria: A Myriad of Open Questions. *J. Mol. Biol.* **427**, 1135–1158 (2015).
27. Rapaport, D. Finding the right organelle. Targeting signals in mitochondrial outer-membrane proteins. *EMBO Rep.* **4**, 948–52 (2003).
28. Borgese, N., Brambillasca, S. & Colombo, S. How tails guide tail-anchored proteins to their destinations. *Curr. Opin. Cell Biol.* **19**, 368–75 (2007).
29. Denic, V., Dötsch, V. & Sinning, I. Endoplasmic reticulum targeting and insertion of tail-anchored membrane proteins by the GET pathway. *Cold Spring Harb. Perspect. Biol.* **5**, a013334 (2013).
30. Johnson, N., Powis, K. & High, S. Post-translational translocation into the endoplasmic reticulum. *Biochim. Biophys. Acta* **1833**, 2403–9 (2013).
31. Deshaies, R. J. & Schekman, R. A yeast mutant defective at an early stage in import of secretory protein precursors into the endoplasmic reticulum. *J. Cell Biol.* **105**,

- 633–645 (1987).
32. Robinson, J. S., Klionsky, D. J., Banta, L. M. & Emr, S. D. Protein sorting in *Saccharomyces cerevisiae*: isolation of mutants defective in the delivery and processing of multiple vacuolar hydrolases. *Mol. Cell. Biol.* **8**, 4936–48 (1988).
 33. Stirling, C. J., Rothblatt, J., Hosobuchi, M., Deshaies, R. & Schekman, R. Protein translocation mutants defective in the insertion of integral membrane proteins into the endoplasmic reticulum. *Mol. Biol. Cell* **3**, 129–42 (1992).
 34. Jensen, R. E., Schmidt, S. & Mark, R. J. Mutations in a 19-amino-acid hydrophobic region of the yeast cytochrome c1 presequence prevent sorting to the mitochondrial intermembrane space. *Mol. Cell. Biol.* **12**, 4677–4686 (1992).
 35. Maarse, A. C., Blom, J., Grivell, L. A. & Meijer, M. MPI1, an essential gene encoding a mitochondrial membrane protein, is possibly involved in protein import into yeast mitochondria. *EMBO J.* **11**, 3619–28 (1992).
 36. Contamine, V. & Picard, M. Maintenance and integrity of the mitochondrial genome: a plethora of nuclear genes in the budding yeast. *Microbiol. Mol. Biol. Rev.* **64**, 281–315 (2000).
 37. van der Giezen, M. Mitochondria and the Rise of Eukaryotes. *Bioscience* **61**, 594–601 (2011).
 38. Vandecasteele, G., Szabadkai, G. & Rizzuto, R. Mitochondrial Calcium Homeostasis: Mechanisms and Molecules. *IUBMB Life (International Union Biochem. Mol. Biol. Life)* **52**, 213–219 (2001).
 39. Lill, R. *et al.* The role of mitochondria in cellular iron–sulfur protein biogenesis and iron metabolism. *Biochim. Biophys. Acta - Mol. Cell Res.* **1823**, 1491–1508 (2012).
 40. Ajioka, R. S., Phillips, J. D. & Kushner, J. P. Biosynthesis of heme in mammals. *Biochim. Biophys. Acta* **1763**, 723–36 (2006).
 41. Osman, C., Voelker, D. R. & Langer, T. Making heads or tails of phospholipids in mitochondria. *J. Cell Biol.* **192**, 7–16 (2011).

42. Sickmann, A. *et al.* The proteome of *Saccharomyces cerevisiae* mitochondria. *Proc. Natl. Acad. Sci. U. S. A.* **100**, 13207–12 (2003).
43. Reinders, J., Zahedi, R. P., Pfanner, N., Meisinger, C. & Sickmann, A. Toward the complete yeast mitochondrial proteome: multidimensional separation techniques for mitochondrial proteomics. *J. Proteome Res.* **5**, 1543–54 (2006).
44. Pagliarini, D. J. *et al.* A mitochondrial protein compendium elucidates complex I disease biology. *Cell* **134**, 112–23 (2008).
45. Booth, A. & Doolittle, W. F. Eukaryogenesis, how special really? *Proc Natl Acad Sci U S A* **112**, 10278–10285 (2015).
46. Schatz, G. & Dobberstein, B. Common principles of protein translocation across membranes. *Science* **271**, 1519–26 (1996).
47. Herrmann, J. M. & Neupert, W. Protein transport into mitochondria. *Curr. Opin. Microbiol.* **3**, 210–214 (2000).
48. Pfanner, N. & Geissler, A. Versatility of the mitochondrial protein import machinery. *Nat. Rev. Mol. Cell Biol.* **2**, 339–49 (2001).
49. Huang, S., Taylor, N. L., Whelan, J. & Millar, A. H. Refining the Definition of Plant Mitochondrial Presequences through Analysis of Sorting Signals, N-Terminal Modifications, and Cleavage Motifs. *PLANT Physiol.* **150**, 1272–1285 (2009).
50. Taylor, A. B. *et al.* Crystal Structures of Mitochondrial Processing Peptidase Reveal the Mode for Specific Cleavage of Import Signal Sequences. *Structure* **9**, 615–625 (2001).
51. Mossmann, D., Meisinger, C. & Vögtle, F.-N. Processing of mitochondrial presequences. *Biochim. Biophys. Acta* **1819**, 1098–106
52. Koehler, C. M., Merchant, S. & Schatz, G. How membrane proteins travel across the mitochondrial intermembrane space. *Trends Biochem. Sci.* **24**, 428–432 (1999).
53. Pfanner, N. & Geissler, A. Versatility of the mitochondrial protein import

- machinery. *Nat. Rev. Mol. Cell Biol.* **2**, 339–49 (2001).
54. Endo, T., Yamamoto, H. & Esaki, M. Functional cooperation and separation of translocators in protein import into mitochondria, the double-membrane bounded organelles. *J. Cell Sci.* **116**, 3259–67 (2003).
55. Wiedemann, N., Frazier, A. E. & Pfanner, N. The Protein Import Machinery of Mitochondria*. (2004). doi:10.1074/jbc.R400003200
56. Hill, K. *et al.* Tom40 forms the hydrophilic channel of the mitochondrial import pore for preproteins [see comment]. *Nature* **395**, 516–21 (1998).
57. Künkele, K. P. *et al.* The preprotein translocation channel of the outer membrane of mitochondria. *Cell* **93**, 1009–19 (1998).
58. van Wilpe, S. *et al.* Tom22 is a multifunctional organizer of the mitochondrial preprotein translocase. *Nature* **401**, 485–9 (1999).
59. Abe, Y. *et al.* Structural basis of presequence recognition by the mitochondrial protein import receptor Tom20. *Cell* **100**, 551–60 (2000).
60. Brix, J., Dietmeier, K. & Pfanner, N. Differential Recognition of Preproteins by the Purified Cytosolic Domains of the Mitochondrial Import Receptors Tom20, Tom22, and Tom70. *J. Biol. Chem.* **272**, 20730–20735 (1997).
61. Meisinger, C. *et al.* Protein Import Channel of the Outer Mitochondrial Membrane: a Highly Stable Tom40-Tom22 Core Structure Differentially Interacts with Preproteins, Small Tom Proteins, and Import Receptors. *Mol. Cell. Biol.* **21**, 2337–2348 (2001).
62. Model, K. *et al.* Multistep assembly of the protein import channel of the mitochondrial outer membrane. *Nat. Struct. Biol.* **8**, 361–70 (2001).
63. Brix, J., Rüdiger, S., Bukau, B., Schneider-Mergener, J. & Pfanner, N. Distribution of binding sequences for the mitochondrial import receptors Tom20, Tom22, and Tom70 in a presequence-carrying preprotein and a non-cleavable preprotein. *J. Biol. Chem.* **274**, 16522–30 (1999).

64. Endres, M., Neupert, W. & Brunner, M. Transport of the ADP/ATP carrier of mitochondria from the TOM complex to the TIM22.54 complex. *EMBO J.* **18**, 3214–21 (1999).
65. Wiedemann, N., Pfanner, N. & Ryan, M. T. The three modules of ADP/ATP carrier cooperate in receptor recruitment and translocation into mitochondria. *EMBO J.* **20**, 951–60 (2001).
66. Young, J. C., Hoogenraad, N. J. & Hartl, F. U. Molecular chaperones Hsp90 and Hsp70 deliver preproteins to the mitochondrial import receptor Tom70. *Cell* **112**, 41–50 (2003).
67. Komiya, T. *et al.* Interaction of mitochondrial targeting signals with acidic receptor domains along the protein import pathway: evidence for the ‘acid chain’ hypothesis. *EMBO J.* **17**, 3886–98 (1998).
68. Yano, M., Terada, K. & Mori, M. AIP is a mitochondrial import mediator that binds to both import receptor Tom20 and preproteins. *J. Cell Biol.* **163**, 45–56 (2003).
69. Lesnik, C., Cohen, Y., Atir-Lande, A., Schuldiner, M. & Arava, Y. OM14 is a mitochondrial receptor for cytosolic ribosomes that supports co-translational import into mitochondria. *Nat. Commun.* **5**, 5711 (2014).
70. Knox, C., Sass, E., Neupert, W. & Pines, O. Import into Mitochondria, Folding and Retrograde Movement of Fumarase in Yeast. *J. Biol. Chem.* **273**, 25587–25593 (1998).
71. Williams, C. C., Jan, C. H. & Weissman, J. S. Targeting and plasticity of mitochondrial proteins revealed by proximity-specific ribosome profiling. *Science* **346**, 748–51 (2014).
72. Dudek, J., Rehling, P. & Van Der Laan, M. Mitochondrial protein import: Common principles and physiological networks ☆. *BBA - Mol. Cell Res.* **1833**, 274–285 (2013).
73. Becker, T. *et al.* Biogenesis of the mitochondrial TOM complex: Mim1 promotes

- insertion and assembly of signal-anchored receptors. *J. Biol. Chem.* **283**, 120–7 (2008).
74. Voulhoux, R., Bos, M. P., Geurtsen, J., Mols, M. & Tommassen, J. Role of a highly conserved bacterial protein in outer membrane protein assembly. *Science* **299**, 262–5 (2003).
75. Popov-Čeleketić, J., Waizenegger, T. & Rapaport, D. Mim1 Functions in an Oligomeric Form to Facilitate the Integration of Tom20 into the Mitochondrial Outer Membrane. *J. Mol. Biol.* **376**, 671–680 (2008).
76. Becker, T. *et al.* The mitochondrial import protein Mim1 promotes biogenesis of multispinning outer membrane proteins. *J. Cell Biol.* **194**, 387–95 (2011).
77. Papić, D., Krumpe, K., Dukanović, J., Dimmer, K. S. & Rapaport, D. Multispan mitochondrial outer membrane protein Ugo1 follows a unique Mim1-dependent import pathway. *J. Cell Biol.* **194**, 397–405 (2011).
78. Setoguchi, K., Otera, H. & Mihara, K. Cytosolic factor- and TOM-independent import of C-tail-anchored mitochondrial outer membrane proteins. *EMBO J.* **25**, 5635–47 (2006).
79. Kemper, C. *et al.* Integration of tail-anchored proteins into the mitochondrial outer membrane does not require any known import components. *J. Cell Sci.* **121**, 1990–8 (2008).
80. Geissler, A. *et al.* The mitochondrial presequence translocase: an essential role of Tim50 in directing preproteins to the import channel. *Cell* **111**, 507–18 (2002).
81. Yamamoto, H. *et al.* Tim50 is a subunit of the TIM23 complex that links protein translocation across the outer and inner mitochondrial membranes. *Cell* **111**, 519–28 (2002).
82. Truscott, K. N. *et al.* A presequence- and voltage-sensitive channel of the mitochondrial preprotein translocase formed by Tim23. *Nat. Struct. Biol.* **8**, 1074–82 (2001).

83. Bauer, M. F., Sirrenberg, C., Neupert, W. & Brunner, M. Role of Tim23 as voltage sensor and presequence receptor in protein import into mitochondria. *Cell* **87**, 33–41 (1996).
84. Chacinska, A. *et al.* Distinct forms of mitochondrial TOM-TIM supercomplexes define signal-dependent states of preprotein sorting. *Mol. Cell. Biol.* **30**, 307–18 (2010).
85. Meier, S., Neupert, W. & Herrmann, J. M. Conserved N-terminal Negative Charges in the Tim17 Subunit of the TIM23 Translocase Play a Critical Role in the Import of Preproteins into Mitochondria. *J. Biol. Chem.* **280**, 7777–7785 (2005).
86. Martinez-Caballero, S., Grigoriev, S. M., Herrmann, J. M., Campo, M. L. & Kinnally, K. W. Tim17p regulates the twin pore structure and voltage gating of the mitochondrial protein import complex TIM23. *J. Biol. Chem.* **282**, 3584–93 (2007).
87. Martin, J., Mahlke, K. & Pfanners, N. Role of an Energized Inner Membrane in Mitochondrial Protein Import **DRIVES THE MOVEMENT OF PRESEQUENCES***. *J. Biol. Chem.* **266**, 18051–18057 (1991).
88. Shariff, K., Ghosal, S. & Matouschek, A. The force exerted by the membrane potential during protein import into the mitochondrial matrix. *Biophys. J.* **86**, 3647–52 (2004).
89. Glick, B. S. *et al.* Cytochromes c1 and b2 are sorted to the intermembrane space of yeast mitochondria by a stop-transfer mechanism. *Cell* **69**, 809–22 (1992).
90. Voos, W., Gambill, B. D., Guiard, B., Pfanner, N. & Craig, E. A. Presequence and mature part of preproteins strongly influence the dependence of mitochondrial protein import on heat shock protein 70 in the matrix. *J. Cell Biol.* **123**, 119–26 (1993).
91. Matouschek, A., Pfanner, N. & Voos, W. Protein unfolding by mitochondria. *EMBO Rep.* **1**, 404–410 (2000).
92. Neupert, W. & Brunner, M. The protein import motor of mitochondria. *Nat. Rev.*

- Mol. Cell Biol.* **3**, 555–65 (2002).
93. Liu, Q., D'Silva, P., Walter, W., Marszalek, J. & Craig, E. A. Regulated cycling of mitochondrial Hsp70 at the protein import channel. *Science* **300**, 139–41 (2003).
94. Truscott, K. N. *et al.* A J-protein is an essential subunit of the presequence translocase-associated protein import motor of mitochondria. *J. Cell Biol.* **163**, 707–13 (2003).
95. Mokranjac, D., Sichting, M., Neupert, W. & Hell, K. Tim14, a novel key component of the import motor of the TIM23 protein translocase of mitochondria. *EMBO J.* **22**, 4945–4956 (2003).
96. D'Silva, P. R., Schilke, B., Walter, W. & Craig, E. A. Role of Pam16's degenerate J domain in protein import across the mitochondrial inner membrane. *Proc. Natl. Acad. Sci. U. S. A.* **102**, 12419–24 (2005).
97. Frazier, A. E. *et al.* Pam16 has an essential role in the mitochondrial protein import motor. *Nat. Struct. Mol. Biol.* **11**, 226–33 (2004).
98. Kozany, C., Mokranjac, D., Sichting, M., Neupert, W. & Hell, K. The J domain-related cochaperone Tim16 is a constituent of the mitochondrial TIM23 preprotein translocase. *Nat. Struct. Mol. Biol.* **11**, 234–41 (2004).
99. Westermann, B., Prip-Buus, C., Neupert, W. & Schwarz, E. The role of the GrpE homologue, Mge1p, in mediating protein import and protein folding in mitochondria. *EMBO J.* **14**, 3452–60 (1995).
100. Taylor, A. B. *et al.* Crystal structures of mitochondrial processing peptidase reveal the mode for specific cleavage of import signal sequences. *Structure* **9**, 615–25 (2001).
101. Bukau, B. & Horwich, A. L. The Hsp70 and Hsp60 chaperone machines. *Cell* **92**, 351–66 (1998).
102. Hartl, F. U. & Hayer-Hartl, M. Molecular chaperones in the cytosol: from nascent chain to folded protein. *Science* **295**, 1852–8 (2002).

103. Curran, S. P., Leuenberger, D., Oppliger, W. & Koehler, C. M. The Tim9p-Tim10p complex binds to the transmembrane domains of the ADP/ATP carrier. *EMBO J.* **21**, 942–953 (2002).
104. Vial, S. *et al.* Assembly of Tim9 and Tim10 into a Functional Chaperone. *J. Biol. Chem.* **277**, 36100–36108 (2002).
105. Davis, A. J., Sepuri, N. B., Holder, J., Johnson, A. E. & Jensen, R. E. Two intermembrane space TIM complexes interact with different domains of Tim23p during its import into mitochondria. *J. Cell Biol.* **150**, 1271–82 (2000).
106. Paschen, S. A. *et al.* The role of the TIM8-13 complex in the import of Tim23 into mitochondria. *EMBO J.* **19**, 6392–400 (2000).
107. Sirrenberg, C., Bauer, M. F., Guiard, B., Neupert, W. & Brunner, M. Import of carrier proteins into the mitochondrial inner membrane mediated by Tim22. *Nature* **384**, 582–585 (1996).
108. Kovermann, P. *et al.* Tim22, the essential core of the mitochondrial protein insertion complex, forms a voltage-activated and signal-gated channel. *Mol. Cell* **9**, 363–73 (2002).
109. Rehling, P. *et al.* Protein insertion into the mitochondrial inner membrane by a twin-pore translocase. *Science* **299**, 1747–51 (2003).
110. Stuart, R. Insertion of proteins into the inner membrane of mitochondria: the role of the Oxa1 complex. *Biochim. Biophys. Acta* **1592**, 79–87 (2002).
111. Herrmann, J. & Neupert, W. Protein Insertion into the Inner Membrane of Mitochondria. *IUBMB Life (International Union Biochem. Mol. Biol. Life)* **55**, 219–225 (2003).
112. Bohnert, M. *et al.* Cooperation of stop-transfer and conservative sorting mechanisms in mitochondrial protein transport. *Curr. Biol.* **20**, 1227–32 (2010).
113. Scotti, P. A. *et al.* YidC, the Escherichia coli homologue of mitochondrial Oxa1p, is a component of the Sec translocase. *EMBO J.* **19**, 542–9 (2000).

114. Borgese, N., Colombo, S. & Pedrazzini, E. The tale of tail-anchored proteins: coming from the cytosol and looking for a membrane. *J. Cell Biol.* **161**, 1013–9 (2003).
115. Blobel, G. & Sabatini, D. D. CONTROLLED PROTEOLYSIS OF NASCENT POLYPEPTIDES IN RAT LIVER CELL FRACTIONS: I. Location of the Polypeptides within Ribosomes. *J. Cell Biol.* **45**, 130–145 (1970).
116. Shao, S. & Hegde, R. S. Membrane protein insertion at the endoplasmic reticulum. *Annu. Rev. Cell Dev. Biol.* **27**, 25–56 (2011).
117. Kutay, U., Ahnert-Hilger, G., Hartmann, E., Wiedenmann, B. & Rapoport, T. A. Transport route for synaptobrevin via a novel pathway of insertion into the endoplasmic reticulum membrane. *EMBO J.* **14**, 217–23 (1995).
118. Masaki, R., Yamamoto, A. & Tashiro, Y. Membrane topology and retention of microsomal aldehyde dehydrogenase in the endoplasmic reticulum. *J. Biol. Chem.* **271**, 16939–44 (1996).
119. Honsho, M., Mitoma, J. -y. & Ito, A. Retention of Cytochrome b 5 in the Endoplasmic Reticulum Is Transmembrane and Luminal Domain-dependent. *J. Biol. Chem.* **273**, 20860–20866 (1998).
120. Pedrazzini, E., Villa, A., Longhi, R., Bulbarelli, A. & Borgese, N. Mechanism of residence of cytochrome b(5), a tail-anchored protein, in the endoplasmic reticulum. *J. Cell Biol.* **148**, 899–914 (2000).
121. Jantti, J. *et al.* Membrane insertion and intracellular-transport of yeast syntaxin sso2p in mammalian-cells . *J. Cell Sci.* **107**, 3623–3633 (1994).
122. Linstedt, A. D. *et al.* A C-terminally-anchored Golgi protein is inserted into the endoplasmic reticulum and then transported to the Golgi apparatus. *Proc. Natl. Acad. Sci. U. S. A.* **92**, 5102–5 (1995).
123. Pedrazzini, E., Villa, A. & Borgese, N. A mutant cytochrome b5 with a lengthened membrane anchor escapes from the endoplasmic reticulum and reaches the plasma

- membrane. *Proc. Natl. Acad. Sci. U. S. A.* **93**, 4207–12 (1996).
124. Elgersma, Y. *et al.* Overexpression of Pex15p, a phosphorylated peroxisomal integral membrane protein required for peroxisome assembly in *S.cerevisiae*, causes proliferation of the endoplasmic reticulum membrane. *EMBO J.* **16**, 7326–41 (1997).
125. Heiland, I. & Erdmann, R. Biogenesis of peroxisomes. *FEBS J.* **272**, 2362–2372 (2005).
126. Nguyen, M., Millar, D. G., Yong, V. W., Korsmeyer, S. J. & Shore, G. C. Targeting of Bcl-2 to the mitochondrial outer membrane by a COOH-terminal signal anchor sequence. *J. Biol. Chem.* **268**, 25265–8 (1993).
127. De Silvestris, M., D'Arrigo, A. & Borgese, N. The targeting information of the mitochondrial outer membrane isoform of cytochrome *b* 5 is contained within the carboxyl-terminal region. *FEBS Lett.* **370**, 69–74 (1995).
128. Isenmann, S., Khew-Goodall, Y., Gamble, J., Vadas, M. & Wattenberg, B. W. A splice-isoform of vesicle-associated membrane protein-1 (VAMP-1) contains a mitochondrial targeting signal. *Mol. Biol. Cell* **9**, 1649–60 (1998).
129. Nemoto, Y. & De Camilli, P. Recruitment of an alternatively spliced form of synaptojanin 2 to mitochondria by the interaction with the PDZ domain of a mitochondrial outer membrane protein. *EMBO J.* **18**, 2991–3006 (1999).
130. Kuroda, R. *et al.* Charged amino acids at the carboxyl-terminal portions determine the intracellular locations of two isoforms of cytochrome *b*5. *J. Biol. Chem.* **273**, 31097–102 (1998).
131. Borgese, N., Gazzoni, I., Barberi, M., Colombo, S. & Pedrazzini, E. Targeting of a tail-anchored protein to endoplasmic reticulum and mitochondrial outer membrane by independent but competing pathways. *Mol. Biol. Cell* **12**, 2482–96 (2001).
132. Motz, C., Martin, H., Krimmer, T. & Rassow, J. Bcl-2 and porin follow different pathways of TOM-dependent insertion into the mitochondrial outer membrane. *J.*

- Mol. Biol.* **323**, 729–38 (2002).
133. Kaufmann, T. *et al.* Characterization of the signal that directs Bcl-x(L), but not Bcl-2, to the mitochondrial outer membrane. *J. Cell Biol.* **160**, 53–64 (2003).
134. Shirane, M. & Nakayama, K. I. Inherent calcineurin inhibitor FKBP38 targets Bcl-2 to mitochondria and inhibits apoptosis. *Nat. Cell Biol.* **5**, 28–37 (2003).
135. Beilharz, T., Egan, B., Silver, P. A., Hofmann, K. & Lithgow, T. Bipartite Signals Mediate Subcellular Targeting of Tail-anchored Membrane Proteins in *Saccharomyces cerevisiae*. *J. Biol. Chem.* **278**, 8219–8223 (2003).
136. Whitley, P., Grahn, E., Kutay, U., Rapoport, T. A. & von Heijne, G. A 12-residue-long poly-leucine tail is sufficient to anchor synaptobrevin to the endoplasmic reticulum membrane. *J. Biol. Chem.* **271**, 7583–6 (1996).
137. Yang, M., Ellenberg, J., Bonifacino, J. S. & Weissman, A. M. The transmembrane domain of a carboxyl-terminal anchored protein determines localization to the endoplasmic reticulum. *J. Biol. Chem.* **272**, 1970–5 (1997).
138. Kim, P. K., Hollerbach, C., Trimble, W. S., Leber, B. & Andrews, D. W. Identification of the endoplasmic reticulum targeting signal in vesicle-associated membrane proteins. *J. Biol. Chem.* **274**, 36876–82 (1999).
139. Mullen, R. T. & Trelease, R. N. The sorting signals for peroxisomal membrane-bound ascorbate peroxidase are within its C-terminal tail. *J. Biol. Chem.* **275**, 16337–44 (2000).
140. Rayner, J. C. & Pelham, H. R. Transmembrane domain-dependent sorting of proteins to the ER and plasma membrane in yeast. *EMBO J.* **16**, 1832–41 (1997).
141. Reggiori, F., Black, M. W. & Pelham, H. R. Polar transmembrane domains target proteins to the interior of the yeast vacuole. *Mol. Biol. Cell* **11**, 3737–49 (2000).
142. Low, S. H. *et al.* Differential localization of syntaxin isoforms in polarized Madin-Darby canine kidney cells. *Mol. Biol. Cell* **7**, 2007–18 (1996).

143. Bulbarelli, A., Sprocati, T., Barberi, M., Pedrazzini, E. & Borgese, N. Trafficking of tail-anchored proteins: transport from the endoplasmic reticulum to the plasma membrane and sorting between surface domains in polarised epithelial cells. *J. Cell Sci.* **115**, 1689–702 (2002).
144. Rohde, J., Dietrich, L., Langosch, D. & Ungermann, C. The transmembrane domain of Vam3 affects the composition of cis- and trans-SNARE complexes to promote homotypic vacuole fusion. *J. Biol. Chem.* **278**, 1656–62 (2003).
145. Misumi, Y., Sohda, M., Tashiro, A., Sato, H. & Ikehara, Y. An essential cytoplasmic domain for the Golgi localization of coiled-coil proteins with a COOH-terminal membrane anchor. *J. Biol. Chem.* **276**, 6867–73 (2001).
146. Joglekar, A. P., Xu, D., Rigotti, D. J., Fairman, R. & Hay, J. C. The SNARE motif contributes to rbet1 intracellular targeting and dynamics independently of SNARE interactions. *J. Biol. Chem.* **278**, 14121–33 (2003).
147. Abell, B. M. *et al.* Signal recognition particle mediates post-translational targeting in eukaryotes. *EMBO J.* **23**, 2755–2764 (2004).
148. Leznicki, P. *et al.* Bat3 promotes the membrane integration of tail-anchored proteins. *J. Cell Sci.* **123**, 2170–8 (2010).
149. Yabal, M. *et al.* Translocation of the C Terminus of a Tail-anchored Protein across the Endoplasmic Reticulum Membrane in Yeast Mutants Defective in Signal Peptide-driven Translocation. *J. Biol. Chem.* **278**, 3489–3496 (2003).
150. Steel, G. J., Brownsword, J. & Stirling, C. J. Tail-Anchored Protein Insertion into Yeast ER Requires a Novel Posttranslational Mechanism Which Is Independent of the SEC Machinery †. *Biochemistry* **41**, 11914–11920 (2002).
151. Kim, P. K., Janiak-Spens, F., Trimble, W. S., Leber, B. & Andrews, D. W. Evidence for Multiple Mechanisms for Membrane Binding and Integration via Carboxyl-Terminal Insertion Sequences †. *Biochemistry* **36**, 8873–8882 (1997).
152. Ngosuwana, J., Wang, N. M., Fung, K. L. & Chirico, W. J. Roles of Cytosolic Hsp70

- and Hsp40 Molecular Chaperones in Post-translational Translocation of Presecretory Proteins into the Endoplasmic Reticulum. *J. Biol. Chem.* **278**, 7034–7042 (2003).
153. Abell, B. M., Rabu, C., Leznicki, P., Young, J. C. & High, S. Post-translational integration of tail-anchored proteins is facilitated by defined molecular chaperones. *J. Cell Sci.* **120**, 1743–51 (2007).
154. Rabu, C., Wipf, P., Brodsky, J. L. & High, S. A Precursor-specific Role for Hsp40/Hsc70 during Tail-anchored Protein Integration at the Endoplasmic Reticulum. *J. Biol. Chem.* **283**, 27504–27513 (2008).
155. Rabu, C., Schmid, V., Schwappach, B. & High, S. Biogenesis of tail-anchored proteins: the beginning for the end? *J. Cell Sci.* **122**, 3605–12 (2009).
156. Colombo, S. F., Longhi, R. & Borgese, N. The role of cytosolic proteins in the insertion of tail-anchored proteins into phospholipid bilayers. *J. Cell Sci.* **122**, 2383–92 (2009).
157. Denic, V. A portrait of the GET pathway as a surprisingly complicated young man. *Trends Biochem. Sci.* **37**, 411–417 (2012).
158. Favalaro, V., Spasic, M., Schwappach, B. & Dobberstein, B. Distinct targeting pathways for the membrane insertion of tail-anchored (TA) proteins. *J. Cell Sci.* **121**, 1832–40 (2008).
159. Stefanovic, S. & Hegde, R. S. Identification of a Targeting Factor for Posttranslational Membrane Protein Insertion into the ER. *Cell* **128**, 1147–1159 (2007).
160. Schuldiner, M. *et al.* The GET Complex Mediates Insertion of Tail-Anchored Proteins into the ER Membrane. *Cell* **134**, 634–645 (2008).
161. Mariappan, M. *et al.* A ribosome-associating factor chaperones tail-anchored membrane proteins. *Nature* **466**, 1120–1124 (2010).
162. Leznicki, P. *et al.* A biochemical analysis of the constraints of tail-anchored protein

- biogenesis. *Biochem. J.* **436**, 719–27 (2011).
163. Leznicki, P. & High, S. SGTA antagonizes BAG6-mediated protein triage. *Proc. Natl. Acad. Sci.* **109**, 19214–19219 (2012).
164. Schuldiner, M. *et al.* Exploration of the Function and Organization of the Yeast Early Secretory Pathway through an Epistatic Miniarray Profile. *Cell* **123**, 507–519 (2005).
165. van der Zand, A., Braakman, I. & Tabak, H. F. Peroxisomal Membrane Proteins Insert into the Endoplasmic Reticulum. *Mol. Biol. Cell* **21**, 2057–2065 (2010).
166. Halbach, A. *et al.* Targeting of the tail-anchored peroxisomal membrane proteins PEX26 and PEX15 occurs through C-terminal PEX19-binding sites. *J. Cell Sci.* **119**, 2508–17 (2006).
167. Delille, H. K. & Schrader, M. Targeting of hFis1 to peroxisomes is mediated by Pex19p. *J. Biol. Chem.* **283**, 31107–15 (2008).
168. Isenmann, S., Khew-Goodall, Y., Gamble, J., Vadas, M. & Wattenberg, B. W. A Splice-Isoform of Vesicle-associated Membrane Protein-1 (VAMP-1) Contains a Mitochondrial Targeting Signal. *Mol. Biol. Cell* **9**, 1649–1660 (1998).
169. Wattenberg, B. W., Clark, D. & Brock, S. An artificial mitochondrial tail signal/anchor sequence confirms a requirement for moderate hydrophobicity for targeting. *Biosci. Rep.* **27**, 385–401 (2007).
170. Cory, S. & Adams, J. M. The Bcl2 family: regulators of the cellular life-or-death switch. *Nat. Rev. Cancer* **2**, 647–56 (2002).
171. Setoguchi, K., Otera, H. & Mihara, K. Cytosolic factor- and TOM-independent import of C-tail-anchored mitochondrial outer membrane proteins. *EMBO J.* **25**, 5635–47 (2006).
172. Schleiff, E., Shore, G. C. & Goping, I. S. Human mitochondrial import receptor, Tom20p. Use of glutathione to reveal specific interactions between Tom20-glutathione S-transferase and mitochondrial precursor proteins. *FEBS Lett.* **404**,

- 314–318 (1997).
173. Bellot, G. *et al.* TOM22, a core component of the mitochondria outer membrane protein translocation pore, is a mitochondrial receptor for the proapoptotic protein Bax. *Cell Death Differ.* **14**, 785–794 (2007).
174. Keil, P. & Pfanner, N. Insertion of MOM22 into the mitochondrial outer membrane strictly depends on surface receptors. *FEBS Lett.* **321**, 197–200 (1993).
175. Allen, R., Egan, B., Gabriel, K., Beilharz, T. & Lithgow, T. A conserved proline residue is present in the transmembrane-spanning domain of Tom7 and other tail-anchored protein subunits of the TOM translocase. *FEBS Lett.* **514**, 347–50 (2002).
176. Dembowski, M., Kunkele, K. P., Nargang, F. E., Neupert, W. & Rapaport, D. Assembly of Tom6 and Tom7 into the TOM core complex of *Neurospora crassa*. *J. Biol. Chem.* **276**, 17679–85 (2001).
177. Oldenburg, K. R., Vo, K. T., Michaelis, S. & Paddon, C. Recombination-mediated PCR-directed plasmid construction *in vivo* in yeast. *Nucleic Acids Res.* **25**, 451–2 (1997).
178. Masella, A. P., Bartram, A. K., Truszkowski, J. M., Brown, D. G. & Neufeld, J. D. PANDAseq: paired-end assembler for illumina sequences. *BMC Bioinformatics* **13**, 31 (2012).
179. Goecks, J. *et al.* Galaxy: a comprehensive approach for supporting accessible, reproducible, and transparent computational research in the life sciences. *Genome Biol.* **11**, R86 (2010).
180. Pavlidis, P. & Noble, W. S. Matrix2png: a utility for visualizing matrix data. *Bioinformatics* **19**, 295–6 (2003).
181. Mozdy, A. D., McCaffery, J. M. & Shaw, J. M. Dnm1p GTPase-mediated mitochondrial fission is a multi-step process requiring the novel integral membrane component Fis1p. *J. Cell Biol.* **151**, 367–80 (2000).
182. Förtsch, J., Hummel, E., Krist, M. & Westermann, B. The myosin-related motor

- protein Myo2 is an essential mediator of bud-directed mitochondrial movement in yeast. *J. Cell Biol.* **194**, 473–88 (2011).
183. Pédelacq, J.-D., Cabantous, S., Tran, T., Terwilliger, T. C. & Waldo, G. S. Engineering and characterization of a superfolder green fluorescent protein. *Nat. Biotechnol.* **24**, 79–88 (2006).
184. Durfee, T. *et al.* The retinoblastoma protein associates with the protein phosphatase type 1 catalytic subunit. *Genes Dev.* **7**, 555–69 (1993).
185. Zahedi, R. P. *et al.* Proteomic analysis of the yeast mitochondrial outer membrane reveals accumulation of a subclass of preproteins. *Mol. Biol. Cell* **17**, 1436–50 (2006).
186. Vidal, M., Braun, P., Chen, E., Boeke, J. D. & Harlow, E. Genetic characterization of a mammalian protein-protein interaction domain by using a yeast reverse two-hybrid system. *Proc. Natl. Acad. Sci. U. S. A.* **93**, 10321–6 (1996).
187. Meyers, S. *et al.* Interaction of the yeast pleiotropic drug resistance genes PDR1 and PDR5. *Curr. Genet.* **21**, 431–6 (1992).
188. Prasad, R. & Goffeau, A. Yeast ATP-binding cassette transporters conferring multidrug resistance. *Annu. Rev. Microbiol.* **66**, 39–63 (2012).
189. Mutlu, N., Garipler, G., Akdoğan, E. & Dunn, C. D. Activation of the pleiotropic drug resistance pathway can promote mitochondrial DNA retention by fusion-defective mitochondria in *Saccharomyces cerevisiae*. *G3 (Bethesda)*. **4**, 1247–58 (2014).
190. Sesaki, H. & Jensen, R. E. Division versus fusion: Dnm1p and Fzo1p antagonistically regulate mitochondrial shape. *J. Cell Biol.* **147**, 699–706 (1999).
191. Habib, S. J., Vasiljev, A., Neupert, W. & Rapaport, D. Multiple functions of tail-anchor domains of mitochondrial outer membrane proteins. *FEBS Lett.* **555**, 511–515 (2003).
192. Sesaki, H. & Jensen, R. E. Division versus fusion: Dnm1p and Fzo1p

- antagonistically regulate mitochondrial shape. *J. Cell Biol.* **147**, 699–706 (1999).
193. Yu, C.-H. *et al.* Codon Usage Influences the Local Rate of Translation Elongation to Regulate Co-translational Protein Folding. *Mol. Cell* **59**, 744–754 (2015).
194. Chen, Y.-C. *et al.* Msp1/ATAD1 maintains mitochondrial function by facilitating the degradation of mislocalized tail-anchored proteins. *EMBO J.* **33**, 1548–64 (2014).
195. Okreglak, V. & Walter, P. The conserved AAA-ATPase Msp1 confers organelle specificity to tail-anchored proteins. *Proc. Natl. Acad. Sci.* **111**, 8019–8024 (2014).
196. Horie, C., Suzuki, H., Sakaguchi, M. & Mihara, K. Characterization of signal that directs C-tail-anchored proteins to mammalian mitochondrial outer membrane. *Mol. Biol. Cell* **13**, 1615–25 (2002).
197. Krumpe, K. *et al.* Ergosterol content specifies targeting of tail-anchored proteins to mitochondrial outer membranes. *Mol. Biol. Cell* **23**, 3927–35 (2012).
198. Dufourc, E. J. Sterols and membrane dynamics. *J. Chem. Biol.* **1**, 63–77 (2008).
199. Stojanovski, D., Koutsopoulos, O. S., Okamoto, K. & Ryan, M. T. Levels of human Fis1 at the mitochondrial outer membrane regulate mitochondrial morphology. *J. Cell Sci.* **117**, 1201–10 (2004).
200. Schinzel, A. *et al.* Conformational control of Bax localization and apoptotic activity by Pro168. *J. Cell Biol.* **164**, 1021–32 (2004).
201. Fekkes, P., Shepard, K. A. & Yaffe, M. P. Gag3p, an outer membrane protein required for fission of mitochondrial tubules. *J. Cell Biol.* **151**, 333–40 (2000).
202. Klecker, T. *et al.* Interaction of MDM33 with mitochondrial inner membrane homeostasis pathways in yeast. *Sci. Rep.* **5**, 18344 (2015).
203. Hermann, G. J. *et al.* Mitochondrial fusion in yeast requires the transmembrane GTPase Fzo1p. *J. Cell Biol.* **143**, 359–73 (1998).
204. Rapaport, D., Brunner, M., Neupert, W. & Westermann, B. Fzo1p Is a

- Mitochondrial Outer Membrane Protein Essential for the Biogenesis of Functional Mitochondria in *Saccharomyces cerevisiae*. *J. Biol. Chem.* **273**, 20150–20155 (1998).
205. Tieu, Q. & Nunnari, J. Mdv1p is a WD repeat protein that interacts with the dynamin-related GTPase, Dnm1p, to trigger mitochondrial division. *J. Cell Biol.* **151**, 353–66 (2000).
206. Borgese, N. & Righi, M. Remote origins of tail-anchored proteins. *Traffic* **11**, 877–85 (2010).
207. Luirink, J., Yu, Z., Wagner, S. & de Gier, J.-W. Biogenesis of inner membrane proteins in *Escherichia coli*. *Biochim. Biophys. Acta - Bioenerg.* **1817**, 965–976 (2012).
208. Setoguchi, K. *et al.* Cytosolic factor- and TOM-independent import of C-tail-anchored mitochondrial outer membrane proteins. *EMBO J.* **25**, 5635–5647 (2006).
209. Borgese, N. & Fasana, E. Targeting pathways of C-tail-anchored proteins. *Biochim. Biophys. Acta - Biomembr.* **1808**, 937–946 (2011).
210. Boucher, J. I. *et al.* Viewing protein fitness landscapes through a next-gen lens. *Genetics* **198**, 461–71 (2014).
211. Fowler, D. M. & Fields, S. Deep mutational scanning: a new style of protein science. *Nat. Methods* **11**, 801–807 (2014).
212. Araya, C. L. & Fowler, D. M. Deep mutational scanning: assessing protein function on a massive scale. *Trends Biotechnol.* **29**, 435–442 (2011).
213. Starita, L. M. *et al.* Massively Parallel Functional Analysis of BRCA1 RING Domain Variants. *Genetics* **200**, 413–22 (2015).
214. Elazar, A. A. *et al.* Mutational scanning reveals the determinants of protein insertion and association energetics in the plasma membrane. *J. Chem. Inf. Model.* **53**, 1689–1699 (2013).

215. Hietpas, R. T., Jensen, J. D. & Bolon, D. N. A. Experimental illumination of a fitness landscape. *Proc. Natl. Acad. Sci. U. S. A.* **108**, 7896–901 (2011).
216. Melamed, D., Young, D. L., Gamble, C. E., Miller, C. R. & Fields, S. Deep mutational scanning of an RRM domain of the *Saccharomyces cerevisiae* poly(A)-binding protein. *RNA* **19**, 1537–51 (2013).
217. Cymer, F., von Heijne, G. & White, S. H. Mechanisms of Integral Membrane Protein Insertion and Folding. *J. Mol. Biol.* **427**, 999–1022 (2015).
218. Segrest, J. P., De Loof, H., Dohlman, J. G., Brouillette, C. G. & Anantharamaiah, G. M. Amphipathic helix motif: Classes and properties. *Proteins Struct. Funct. Genet.* **8**, 103–117 (1990).
219. de Planque, M. R. *et al.* Different membrane anchoring positions of tryptophan and lysine in synthetic transmembrane alpha-helical peptides. *J. Biol. Chem.* **274**, 20839–46 (1999).
220. Schow, E. V *et al.* Arginine in membranes: the connection between molecular dynamics simulations and translocon-mediated insertion experiments. *J. Membr. Biol.* **239**, 35–48 (2011).
221. Long, S. B., Campbell, E. B. & Mackinnon, R. Voltage sensor of Kv1.2: structural basis of electromechanical coupling. *Science* **309**, 903–8 (2005).
222. Kim, C. *et al.* Basic amino-acid side chains regulate transmembrane integrin signalling. *Nature* **481**, 209–13 (2012).
223. Drozdetskiy, A., Cole, C., Procter, J. & Barton, G. J. JPred4: a protein secondary structure prediction server. *Nucleic Acids Res.* **43**, W389–94 (2015).
224. Buchan, D. W. A., Minnici, F., Nugent, T. C. O., Bryson, K. & Jones, D. T. Scalable web services for the PSIPRED Protein Analysis Workbench. *Nucleic Acids Res.* **41**, W349–57 (2013).
225. Senes, A., Engel, D. E. & DeGrado, W. F. Folding of helical membrane proteins: the role of polar, GxxxG-like and proline motifs. *Curr. Opin. Struct. Biol.* **14**, 465–

- 479 (2004).
226. Chou, P. Y. & Fasman, G. D. Conformational parameters for amino acids in helical, beta-sheet, and random coil regions calculated from proteins. *Biochemistry* **13**, 211–22 (1974).
227. O’Neil, K. T. & DeGrado, W. F. A thermodynamic scale for the helix-forming tendencies of the commonly occurring amino acids. *Science* **250**, 646–51 (1990).
228. Dong, H., Sharma, M., Zhou, H.-X. & Cross, T. A. Glycines: role in α -helical membrane protein structures and a potential indicator of native conformation. *Biochemistry* **51**, 4779–89 (2012).
229. Yoon, Y., Krueger, E. W., Oswald, B. J. & McNiven, M. A. The mitochondrial protein hFis1 regulates mitochondrial fission in mammalian cells through an interaction with the dynamin-like protein DLP1. *Mol. Cell. Biol.* **23**, 5409–20 (2003).
230. Ridgway, N. & McLeod, R. *Biochemistry of lipids, lipoproteins and membranes*.
231. Oliver, P. M. *et al.* Localization of Anionic Phospholipids in Escherichia coli Cells. doi:10.1128/JB.01877-14
232. Bottger, G. *et al.* Saccharomyces cerevisiae PTS1 receptor Pex5p interacts with the SH3 domain of the peroxisomal membrane protein Pex13p in an unconventional, non-PXXP-related manner. *Mol. Biol. Cell* **11**, 3963–76 (2000).

VITA

Abdurrahman Keskin was born in Bursa, Turkey on February 12, 1990. He received his Bachelor of Science degree in Molecular Biology and Genetics from Middle East Technical University, Ankara, in 2013. Between September 2014 and July 2016, he worked as a teaching and research assistant at Koç University, Istanbul, Turkey. His M.S. study is titled as ‘‘A genetic approach to reveal determinants of mitochondrial tail-anchored protein targeting’’.

APPENDIX A: Details of strains used in this study

Strain	Genotype	Source	Parental strain(s)	Method Used
BY4741	<i>MATa his3Δ1 leu2Δ0 met15Δ0 ura3Δ0</i>	EUROSCARF Y00000		
BY4742	<i>MATa his3Δ1 leu2Δ0 lys2Δ0 ura3Δ0</i>	EUROSCARF Y10000		
BY4743	<i>MATa/a his3Δ1/ his3Δ1 leu2Δ0/leu2Δ0 met15Δ0/MET15 LYS2/lys2Δ0 ura3Δ0/ura3Δ0</i>	EUROSCARF Y20000		
RJ1578	<i>MATa opl1 ade1 p+</i>	(Dunn and Jensen, 2003)		
CDD463	<i>MATa leu2Δ0 his3Δ200 met15Δ0 trp1Δ63 ura3Δ0</i>	(Garipler <i>et al.</i> , 2014)		
CDD688	<i>MATa ura3-1 trp1Δ2 ade2-1 leu2-3,112 his3-11,15 can1-100 cyh2 fzo1Δ::LEU2 fis1Δ::kanMX4 + plasmid b19 [pFZO1-CYH2-TRP1]</i>	(Mutlu <i>et al.</i> , 2014)		
CDD692	<i>MATa ura3-1 trp1Δ2 ade2-1 leu2-3,112 his3-11,15 can1-100 fis1Δ::kanMX4</i>	(Mutlu <i>et al.</i> , 2014)		
CDD741	<i>MATa ura3-1 trp1Δ2 ade2-1 leu2-3,112 his3-11,15 can1-100 fis1Δ::kanMX4 + plasmid pHS12 [pCOX4(1-21)-GFP-LEU2]</i>	This study	CDD692	Transformation with plasmid pHS12.
MaV203	<i>MATa leu2-3,112; trp1-901; his3Δ200; ade2-101 (?); cyh2; can1; gal4Δ; gal80Δ; GAL1::lacZ; HIS3^{UASGALI}::HIS3@LYS2; SPAL10^{UASGALI}::URA3</i>	Invitrogen		
AH109	<i>MATa trp1-901 leu2-3,112; ura3-52 his3Δ200 gal4Δ gal80Δ, LYS2::GAL1^{UAS}GAL1^{TATA}- HIS3, GAL2^{UAS}-GAL2^{TATA}-ADE2 URA3::MEL1^{UAS}-MEL1^{TATA}-lacZ</i>	Clontech		

CDD846	<i>MATα leu2-3,112; trp1-901; his3Δ200; ade2-101 (?); cyh2; can1; gal4Δ; gal80Δ; GAL1::lacZ; HIS3_{UASGALI}::HIS3@LYS2; SPAL10_{UASGALI}::URA3 + plasmid pKS1</i>	This study		
CDD847	<i>MATα leu2-3,112; trp1-901; his3Δ200; ade2-101 (?); cyh2; can1; gal4Δ; gal80Δ; GAL1::lacZ; HIS3_{UASGALI}::HIS3@LYS2; SPAL10_{UASGALI}::URA3 + plasmid b100 [pCYH2-TRP1-GAL4-sfGFP-FIS1]</i>	This study		
CDD948	<i>MATα yero83cΔ::KanMX4</i>	EUROSCARF Y10223		
CDD949	<i>MATα ye1031wΔ::KanMX4</i>	EUROSCARF Y10272		
CDD951	<i>MATα yor045wΔ::KanMX4</i>	EUROSCARF Y11821		
CDD952	<i>MATα ybr230cΔ::KanMX4</i>	EUROSCARF Y13370		
CDD953	<i>MATα ydl100cΔ::KanMX4</i>	EUROSCARF Y13797		
CDD954	<i>MATα ygl020cΔ::KanMX4</i>	EUROSCARF Y14388		
CDD955	<i>MATα ygr049uΔ::KanMX4</i>	EUROSCARF Y14679		
CDD956	<i>MATα his3Δ1 leu2Δ0 lys2Δ0 ura3Δ0 msp1Δ::kanMX4</i>	EUROSCARF Y16978		
CDD957	<i>MATα ynl070wΔ::KanMX4</i>	EUROSCARF Y17217		
CDD961	<i>MATα/α his3Δ1/his3Δ1 leu2Δ0/leu2Δ0 met15Δ0/MET15 LYS2/lys2Δ0 ura3Δ0/ura3Δ0 + plasmid pHS1 [pCOX4(1-21)-GFP-HIS3]</i>	This study	BY4743	Transformation with plasmid pHS1.

CDD974	<i>MATα his3Δ1 leu2Δ0 lys2Δ0 ura3Δ0 ydr329cΔ::kanMX4</i>	EUROSCARF Y13688		
CDD975	<i>MATα his3Δ1 leu2Δ0 lys2Δ0 ura3Δ0 ydl065cΔ::kanMX4</i>	EUROSCARF Y13762		
CDD994	<i>MATα/α his3Δ1/ his3Δ1 leu2Δ0/leu2Δ0 met15Δ0/MET15 LYS2/lys2Δ0 ura3Δ0/ura3Δ0 ylr324wΔ::hphNT1/YLR324 msp1Δ::kanMX4/MSP1</i>	This study	BY4741, CDD956	<i>YLR324W</i> was disrupted with <i>hphNT1</i> using primers 1006/1007 and template pRS306H (Taxis and Knop, 2006).
CDD1012	<i>MATα/α his3Δ1/ his3Δ1 leu2Δ0/leu2Δ0 met15Δ0/MET15 LYS2/lys2Δ0 ura3Δ0/ura3Δ0 msp1Δ::kanMX4/MSP1</i>	This study	CDD994, BY4742	CDD994 was sporulated, and a G418-resistant and hygromycin-sensitive spore was mated to BY4742.
CDD1028	<i>MATα/α his3Δ1/ his3Δ1 leu2Δ0/leu2Δ0 met15Δ0/MET15 LYS2/lys2Δ0 ura3Δ0/ura3Δ0 ydr329cΔ::kanMX4/YDR329C get3Δ::hphNT1/GET3</i>	This study	BY4741, CDD974	Strains BY4741 and CDD974 were mated. <i>GET3</i> was disrupted with <i>hphNT1</i> using primers 1051/1052 and template pRS306H (Taxis and Knop, 2006).
CDD1029	<i>MATα/α his3Δ1/ his3Δ1 leu2Δ0/leu2Δ0 met15Δ0/MET15 LYS2/lys2Δ0 ura3Δ0/ura3Δ0 ydl065cΔ::kanMX4/YDL065C get3Δ::hphNT1/GET3</i>	This study	BY4741, CDD975	Strains BY4741 and CDD975 were mated. <i>GET3</i> was disrupted with <i>hphNT1</i> using primers 1051/1052 and template pRS306H (Taxis and Knop, 2006).
CDD1031	<i>MATα/α his3Δ1/ his3Δ1 leu2Δ0/leu2Δ0 met15Δ0/MET15 LYS2/lys2Δ0 ura3Δ0/ura3Δ0 spf1Δ::hphNT1/spf1Δ::hphNT1</i>	This study	CDD1012	<i>SPF1</i> was disrupted with <i>hphNT1</i> using primers 749/750 and template pRS306H (Taxis and Knop, 2006). The resulting strain was sporulated, and two hygromycin-resistant, G418-sensitive spores of opposite mating type were mated.
CDD1033	<i>MATα/α his3Δ1/ his3Δ1 leu2Δ0/leu2Δ0 met15Δ0/MET15 LYS2/lys2Δ0 ura3Δ0/ura3Δ0 get3Δ::hphNT1/get3Δ::hphNT1</i>	This study	CDD1028, CDD1029	CDD1028 and CDD1029 were sporulated. Hygromycin-resistant, G418-sensitive spores of opposite mating type were mated.

CDD1040	<i>MATa/α his3Δ1/ his3Δ1 leu2Δ0/leu2Δ0 met15Δ0/MET15 LYS2/lys2Δ0 ura3Δ0/ura3Δ0 msp1Δ::kanMX4/msp1Δ::kanMX4</i>	This study	CDD1012	<i>SPF1</i> was disrupted with <i>hphNT1</i> using primers 749/750 and template pRS306H (Taxis and Knop, 2006). The resulting strain was sporulated, and two hygromycin-sensitive, G418-resistant colonies of opposite mating type were mated.
CDD1044	<i>MATa/α his3Δ1/ his3Δ1 leu2Δ0/leu2Δ0 met15Δ0/MET15 LYS2/lys2Δ0 ura3Δ0/ura3Δ0 msp1Δ::kanMX4/msp1Δ::kanMX4 + plasmid pHS1 [pCOX4(1-21)- GFP-HIS3]</i>	This study	CDD1040	Transformation with plasmid pHS1.

APPENDIX B: Plasmids used for experiments during this study

Plasmid	Name	Construction details or source
pKS1	pCYH2-TRP1	(Ryan <i>et al.</i> , 1998)
pRS313	pARS-CEN-HIS3	(Sikorski and Hieter, 1989)
pRS316	pARS-CEN-URA3	(Sikorski and Hieter, 1989)
b19	pFZO1-CYH2-TRP1	(Mutlu <i>et al.</i> , 2014)
pHS1	pCOX4(1-21)-GFP-HIS3	(Sesaki and Jensen, 1999)
pHS12	pCOX4(1-21)-GFP-LEU2	(Sesaki and Jensen, 1999)
b100	pCYH2-TRP1-GAL4-sfGFP-FIS1	The <i>FIS1</i> promoter was amplified from the gDNA of strain CDD48 using primers 698 and 699. The <i>GAL4</i> ORF was amplified from CDD48 gDNA using primers 700 and 701. The superfolderGFP ORF was amplified using primers 702 and 703 and plasmid pFA6a-link-yoSuperfolderGFP-Kan (Lee <i>et al.</i> , 2013). The <i>FIS1</i> ORF was amplified from CDD48 gDNA using primers 704 and 705. The <i>ADHI</i> 3' UTR was amplified from CDD48 gDNA using primers 706 and 517. PCR products were co-transformed with <i>NotI</i> -cut pKS1 into strain MaV203.
b101	pCYH2-TRP1-GAL4-sfGFP-FIS1(Δ TA)	The <i>FIS1</i> promoter was amplified from the gDNA of strain CDD48 using primers 698 and 699. The <i>GAL4</i> ORF was amplified from CDD48 gDNA using primers 700 and 701. The superfolderGFP ORF was amplified using primers 702 and 703 and plasmid pFA6a-link-yoSuperfolderGFP-Kan (Lee <i>et al.</i> , 2013). The <i>FIS1</i> ORF lacking the portion encoding the tail anchor was amplified from CDD48 gDNA using primers 704 and 707. The <i>ADHI</i> 3' UTR was amplified from CDD48 gDNA using primers 708 and 517. PCR products were co-transformed with <i>NotI</i> -cut pKS1 into strain MaV203.
b102	2 μ -TRP1-GAL4-sfGFP-FIS1	The <i>GAL4-sfGFP-FIS1</i> fusion and control sequences were amplified from plasmid b100 using primers 738 and 739. The PCR product was co-transformed with <i>NotI</i> -cut pRS424 (Sikorski and Hieter, 1989) into strain CDD836.
b109	pLEU2-mCherry-FIS1-TA	The <i>ADHI</i> promoter was amplified from the gDNA of strain CDD847 using primers 531 and 762. The mCherry ORF was amplified from plasmid pHS12-mCherry [Addgene #25444, provided by Dr. Benjamin Glick, University of Chicago] using primers 763 and 764. The genomic region encoding the <i>FIS1</i> tail anchor the and <i>ADHI</i> 3' UTR were together amplified from plasmid b100 using primers 765 and 517. PCR products were co-transformed with <i>NotI</i> -cut pRS315 (Sikorski and Hieter, 1989) into strain CDD847.

b128	pCYH2-TRP1-GAL4-sfGFP-FIS1 (VI45E)	A product containing the <i>FIS1</i> promoter, the <i>GAL4</i> ORF, the superfolderGFP ORF, and a portion of <i>FIS1</i> was amplified from plasmid b100 using primers 698 and 776. A second product containing a portion of <i>FIS1</i> and the <i>ADHI</i> 3' UTR was amplified from plasmid b100 using primers 773 and 517 and using a lower fidelity polymerase. PCR products were co-transformed into strain MaV203 with <i>NotI</i> -cut pKS1. Selection was performed on a SMM plate lacking histidine and including 20mM 3-AT.
b129	pCYH2-TRP1-GAL4-sfGFP-FIS1 (LI39P)	A product containing the <i>FIS1</i> promoter, the <i>GAL4</i> ORF, the superfolderGFP ORF, and a portion of <i>FIS1</i> was amplified from plasmid b100 using primers 698 and 776. A second product containing a portion of <i>FIS1</i> and the <i>ADHI</i> 3' UTR was amplified from plasmid b100 using primers 773 and 517 and using a lower fidelity polymerase. PCR products were co-transformed into strain MaV203 with <i>NotI</i> -cut pKS1. Selection was performed on a SMM plate lacking histidine and including 20mM 3-AT.
b130	pCYH2-TRP1-GAL4-sfGFP-FIS1 (LI29P,VI38A)	A product containing the <i>FIS1</i> promoter, the <i>GAL4</i> ORF, the superfolderGFP ORF, and a portion of <i>FIS1</i> was amplified from plasmid b100 using primers 698 and 776. A second product containing a portion of <i>FIS1</i> and the <i>ADHI</i> 3' UTR was amplified using a lower fidelity polymerase from plasmid b100 using primers 773 and 517. 300 μ M MnCl ₂ included in this PCR reaction. PCR products were co-transformed into strain MaV203 with <i>NotI</i> -cut pKS1. Selection was performed on a SMM plate lacking histidine and including 20mM 3-AT.
b134	pLEU2-mCherry-FIS1-TA (VI45E)	The <i>ADHI</i> promoter was amplified from gDNA (CDD847) using primers 531 and 762. The mCherry ORF was amplified from pHS12-mCherry [Addgene #25444, provided by Dr. Benjamin Glick, University of Chicago] using primers 763 and 764. The region encoding the Fis1p tail anchor and the 3' UTR of <i>ADHI</i> was amplified from plasmid b128 using primers 765 and 517. PCR products were co-transformed into strain BY4743 with <i>NotI</i> -cut pRS315 (Sikorski and Hieter, 1989). A product containing the <i>ADHI</i> promoter, the mCherry ORF, and the tail anchor of <i>FIS1</i> was amplified from the resulting plasmid using primers 531 and 774. A second product containing the <i>ADHI</i> 3' UTR was amplified from the gDNA of strain CDD846 using primers 775 and 517. PCR products were co-transformed into strain BY4743 with <i>NotI</i> -cut pRS315 (Sikorski and Hieter, 1989).
b135	pLEU2-mCherry-FIS1-TA (LI39P)	The <i>ADHI</i> promoter was amplified from gDNA (CDD847) using primers 531 and 762. The mCherry ORF was amplified from plasmid pHS12-mCherry [Addgene #25444, provided by Dr. Benjamin Glick, University of Chicago] using primers 763 and 764. The region encoding the <i>FIS1</i> tail anchor and the 3' UTR of <i>ADHI</i> was amplified from plasmid b129 using primers 765 and 517. PCR products were co-transformed into strain BY4743 with <i>NotI</i> -HF cut pRS315 (Sikorski and Hieter, 1989). A product containing the <i>ADHI</i> promoter, the mCherry ORF, and the tail anchor of <i>FIS1</i> was amplified from the resulting plasmid using primers 531 and 774. A second product containing the <i>ADHI</i> 3' UTR was amplified from the gDNA of strain CDD846 using primers 775 and 517. PCR products were co-transformed into strain BY4743 with <i>NotI</i> -cut pRS315 (Sikorski and Hieter, 1989).
b136	pLEU2-mCherry-FIS1-TA (LI29P, VI38A)	The <i>ADHI</i> promoter was amplified from gDNA (CDD847) using primers 531 and 762. The mCherry ORF was amplified from plasmid pHS12-mCherry [Addgene #25444, provided by Dr. Benjamin Glick, University of Chicago] using primers 763 and 764. The region encoding the <i>FIS1</i> tail anchor and the 3' UTR of <i>ADHI</i> was amplified from plasmid b130 using primers 765 and 517. PCR products were co-transformed into strain BY4743 with <i>NotI</i> -cut pRS315 (Sikorski & Hieter, 1989). A product containing

		the <i>ADHI</i> promoter, the mCherry ORF, and the tail anchor of <i>FIS1</i> was amplified from the resulting plasmid using primers 531 and 774. A second product containing the <i>ADHI</i> 3' UTR was amplified from the gDNA of strain CDD846 using primers 775 and 517. PCR products were co-transformed into strain BY4743 with <i>NotI</i> -cut pRS315 (Sikorski and Hieter, 1989).
b158	p <i>URA3-PDR1-mCherry-FIS1-TA</i>	The <i>PDR1</i> promoter and <i>PDR1</i> ORF were amplified from plasmid b60 (Mutlu <i>et al.</i> , 2014) using primers 11 and 900. The mCherry ORF, the sequence encoding the Fis1p tail anchor, and the <i>ADHI</i> 3' UTR were amplified together from plasmid b109 using primers 899 and 12. PCR products were co-transformed into strain BY4743 with <i>NotI</i> -cut pRS316 (Sikorski and Hieter, 1989).
b159	p <i>URA3-PDR1-mCherry-FIS1-TA (V145E)</i>	The <i>PDR1</i> promoter and <i>PDR1</i> ORF were amplified from plasmid b60 (Mutlu <i>et al.</i> , 2014) using primers 11 and 900. The mCherry ORF, the sequence encoding the Fis1p tail anchor, and the <i>ADHI</i> 3' UTR were amplified together from plasmid b134 using primers 899 and 12. PCR products were co-transformed into strain BY4743 with <i>NotI</i> -cut pRS316 (Sikorski and Hieter, 1989).
b160	p <i>URA3-PDR1-249-mCherry-FIS1-TA</i>	The <i>PDR1</i> promoter and <i>PDR1-249</i> ORF were amplified from plasmid b65 (Mutlu <i>et al.</i> , 2014) using primers 11 and 900. The mCherry ORF, the sequence encoding the Fis1p tail anchor, and the <i>ADHI</i> 3' UTR were amplified together from plasmid b109 using primers 899 and 12. PCR products were co-transformed into strain BY4743 with <i>NotI</i> -cut pRS316 (Sikorski and Hieter, 1989).
b165	p <i>URA3-PDR1-249-mCherry-FIS1-TA (V145E)</i>	The <i>PDR1</i> promoter and <i>PDR1-249</i> ORF were amplified from plasmid b65 (Mutlu <i>et al.</i> , 2014) using primers 11 and 900. The mCherry ORF, the sequence encoding the Fis1p tail anchor, and the <i>ADHI</i> 3' UTR were amplified together from plasmid b134 using primers 899 and 12. PCR products were co-transformed into strain BY4743 with <i>NotI</i> -cut pRS316 (Sikorski and Hieter, 1989).
b172	p <i>CYH2-TRP1-GAL4-sfGFP-FIS1 (V132D)</i>	A product containing the <i>FIS1</i> promoter, the <i>GAL4</i> ORF, the superfolderGFP ORF, and a portion of <i>FIS1</i> was amplified from plasmid b100 using primers 11 and <i>rvspos4</i> . A second product containing a portion of <i>FIS1</i> and the <i>ADHI</i> 3' UTR was amplified from plasmid b100 using primers 906 and 12. PCR products were co-transformed into strain CDD463 with <i>NotI</i> -cut pKS1.
b173	p <i>CYH2-TRP1-GAL4-sfGFP-FIS1 (V132E)</i>	A product containing the <i>FIS1</i> promoter, the <i>GAL4</i> ORF, the superfolderGFP ORF, and a portion of <i>FIS1</i> was amplified from plasmid b100 using primers 11 and <i>rvspos4</i> . A second product containing a portion of <i>FIS1</i> and the <i>ADHI</i> 3' UTR was amplified from plasmid b100 using primers 907 and 12. PCR products were co-transformed into strain CDD463 with <i>NotI</i> -cut pKS1.
b174	p <i>CYH2-TRP1-GAL4-sfGFP-FIS1 (V132K)</i>	A product containing the <i>FIS1</i> promoter, the <i>GAL4</i> ORF, the superfolderGFP ORF, and a portion of <i>FIS1</i> was amplified from plasmid b100 using primers 11 and <i>rvspos4</i> . A second product containing a portion of <i>FIS1</i> and the <i>ADHI</i> 3' UTR was amplified from plasmid b100 using primers 908 and 12. PCR products were co-transformed into strain CDD463 with <i>NotI</i> -cut pKS1.
b175	p <i>CYH2-TRP1-GAL4-sfGFP-FIS1 (V132R)</i>	A product containing the <i>FIS1</i> promoter, the <i>GAL4</i> ORF, the superfolderGFP ORF, and a portion of <i>FIS1</i> was amplified from plasmid b100 using primers 11 and <i>rvspos4</i> . A second product containing a portion of <i>FIS1</i> and the <i>ADHI</i> 3' UTR was amplified from plasmid b100 using primers 909 and 12. PCR products were co-transformed into strain CDD463 with <i>NotI</i> -cut pKS1.

b176	pCYH2-TRP1-GAL4-sfGFP-FIS1 (A140D)	A product containing the <i>FIS1</i> promotor, the <i>GAL4</i> ORF, the superfolderGFP ORF, and a portion of <i>FIS1</i> was amplified from plasmid b100 using primers 11 and rvspos12. A second product containing a portion of <i>FIS1</i> and the <i>ADHI</i> 3' UTR was amplified from plasmid b100 using primers 910 and 12. PCR products were co-transformed into strain CDD463 with <i>NotI</i> -cut pKS1.
b177	pCYH2-TRP1-GAL4-sfGFP-FIS1 (A140E)	A product containing the <i>FIS1</i> promotor, the <i>GAL4</i> ORF, the superfolderGFP ORF, and a portion of <i>FIS1</i> was amplified from plasmid b100 using primers 11 and rvspos12. A second product containing a portion of <i>FIS1</i> and the <i>ADHI</i> 3' UTR was amplified from plasmid b100 using primers 911 and 12. PCR products were co-transformed into strain CDD463 with <i>NotI</i> -cut pKS1.
b178	pCYH2-TRP1-GAL4-sfGFP-FIS1 (A140K)	A product containing the <i>FIS1</i> promotor, the <i>GAL4</i> ORF, the superfolderGFP ORF, and a portion of <i>FIS1</i> was amplified from plasmid b100 using primers 11 and rvspos12. A second product containing a portion of <i>FIS1</i> and the <i>ADHI</i> 3' UTR was amplified from plasmid b100 using primers 912 and 12. PCR products were co-transformed into strain CDD463 with <i>NotI</i> -cut pKS1.
b179	pCYH2-TRP1-GAL4-sfGFP-FIS1 (A140R)	A product containing the <i>FIS1</i> promotor, the <i>GAL4</i> ORF, the superfolderGFP ORF, and a portion of <i>FIS1</i> was amplified from plasmid b100 using primers 11 and rvspos12. A second product containing a portion of <i>FIS1</i> and the <i>ADHI</i> 3' UTR was amplified from plasmid b100 using primers 913 and 12. PCR products were co-transformed into strain CDD463 with <i>NotI</i> -cut pKS1.
b180	pCYH2-TRP1-GAL4-sfGFP-FIS1 (A144D)	A product containing the <i>FIS1</i> promotor, the <i>GAL4</i> ORF, the superfolderGFP ORF, and a portion of <i>FIS1</i> was amplified from plasmid b100 using primers 11 and rvspos16. A second product containing a portion of <i>FIS1</i> and the <i>ADHI</i> 3' UTR was amplified from plasmid b100 using primers 914 and 12. PCR products were co-transformed into strain CDD463 with <i>NotI</i> -cut pKS1.
b181	pCYH2-TRP1-GAL4-sfGFP-FIS1 (A144E)	A product containing the <i>FIS1</i> promotor, the <i>GAL4</i> ORF, the superfolderGFP ORF, and a portion of <i>FIS1</i> was amplified from plasmid b100 using primers 11 and rvspos16. A second product containing a portion of <i>FIS1</i> and the <i>ADHI</i> 3' UTR was amplified from plasmid b100 using primers 915 and 12. PCR products were co-transformed into strain CDD463 with <i>NotI</i> -cut pKS1.
b182	pCYH2-TRP1-GAL4-sfGFP-FIS1 (A144K)	A product containing the <i>FIS1</i> promotor, the <i>GAL4</i> ORF, the superfolderGFP ORF, and a portion of <i>FIS1</i> was amplified from plasmid b100 using primers 11 and rvspos16. A second product containing a portion of <i>FIS1</i> and the <i>ADHI</i> 3' UTR was amplified from plasmid b100 using primers 916 and 12. PCR products were co-transformed into strain CDD463 with <i>NotI</i> -cut pKS1.
b183	pCYH2-TRP1-GAL4-sfGFP-FIS1 (A144R)	A product containing the <i>FIS1</i> promotor, the <i>GAL4</i> ORF, the superfolderGFP ORF, and a portion of <i>FIS1</i> was amplified from plasmid b100 using primers 11 and rvspos16. A second product containing a portion of <i>FIS1</i> and the <i>ADHI</i> 3' UTR was amplified from plasmid b100 using primers 917 and 12. PCR products were co-transformed into strain CDD463 with <i>NotI</i> -cut pKS1.
b184	pCYH2-TRP1-GAL4-sfGFP-FIS1 (F148D)	A product containing the <i>FIS1</i> promotor, the <i>GAL4</i> ORF, the superfolderGFP ORF, and a portion of <i>FIS1</i> was amplified from plasmid b100 using primers 11 and rvspos20. A second product containing a portion of <i>FIS1</i> and the <i>ADHI</i> 3' UTR was amplified from plasmid b100 using primers 918 and 12. PCR products were co-transformed into strain CDD463 with <i>NotI</i> -cut pKS1.

b185	pCYH2-TRP1-GAL4-sfGFP-FIS1 (F148E)	A product containing the <i>FIS1</i> promotor, the <i>GAL4</i> ORF, the superfolderGFP ORF, and a portion of <i>FIS1</i> was amplified from plasmid b100 using primers 11 and rvspos20. A second product containing a portion of <i>FIS1</i> and the <i>ADHI</i> 3' UTR was amplified from plasmid b100 using primers 919 and 12. PCR products were co-transformed into strain CDD463 with <i>NotI</i> -cut pKS1.
b186	pCYH2-TRP1-GAL4-sfGFP-FIS1 (F148K)	A product containing the <i>FIS1</i> promotor, the <i>GAL4</i> ORF, the superfolderGFP ORF, and a portion of <i>FIS1</i> was amplified from plasmid b100 using primers 11 and rvspos20. A second product containing a portion of <i>FIS1</i> and the <i>ADHI</i> 3' UTR was amplified from plasmid b100 using primers 920 and 12. PCR products were co-transformed into strain CDD463 with <i>NotI</i> -cut pKS1.
b187	pCYH2-TRP1-GAL4-sfGFP-FIS1 (F148R)	A product containing the <i>FIS1</i> promotor, the <i>GAL4</i> ORF, the superfolderGFP ORF, and a portion of <i>FIS1</i> was amplified from plasmid b100 using primers 11 and rvspos20. A second product containing a portion of <i>FIS1</i> and the <i>ADHI</i> 3' UTR was amplified from plasmid b100 using primers 921 and 12. PCR products were co-transformed into strain CDD463 with <i>NotI</i> -cut pKS1.
b188	pCYH2-TRP1-GAL4-sfGFP-FIS1 (V134P)	A product containing the <i>FIS1</i> promotor, the <i>GAL4</i> ORF, the superfolderGFP ORF, and a portion of <i>FIS1</i> was amplified from plasmid b100 using primers 11 and rvspos6. A second product containing a portion of <i>FIS1</i> and the <i>ADHI</i> 3' UTR was amplified from plasmid b100 using primers 969 and 12. PCR products were co-transformed into strain CDD463 with <i>NotI</i> -cut pKS1.
b189	pCYH2-TRP1-GAL4-sfGFP-FIS1 (G137P)	A product containing the <i>FIS1</i> promotor, the <i>GAL4</i> ORF, the superfolderGFP ORF, and a portion of <i>FIS1</i> was amplified from plasmid b100 using primers 11 and rvspos9. A second product containing a portion of <i>FIS1</i> and the <i>ADHI</i> 3' UTR was amplified from plasmid b100 using primers 970 and 12. PCR products were co-transformed into strain CDD463 with <i>NotI</i> -cut pKS1.
b190	pCYH2-TRP1-GAL4-sfGFP-FIS1 (A140P)	A product containing the <i>FIS1</i> promotor, the <i>GAL4</i> ORF, the superfolderGFP ORF, and a portion of <i>FIS1</i> was amplified from plasmid b100 using primers 11 and rvspos12. A second product containing a portion of <i>FIS1</i> and the <i>ADHI</i> 3' UTR was amplified from plasmid b100 using primers 971 and 12. PCR products were co-transformed into strain CDD463 with <i>NotI</i> -cut pKS1.
b191	pCYH2-TRP1-GAL4-sfGFP-FIS1 (A144P)	A product containing the <i>FIS1</i> promotor, the <i>GAL4</i> ORF, the superfolderGFP ORF, and a portion of <i>FIS1</i> was amplified from plasmid b100 using primers 11 and rvspos16. A second product containing a portion of <i>FIS1</i> and the <i>ADHI</i> 3' UTR was amplified from plasmid b100 using primers 972 and 12. PCR products were co-transformed into strain CDD463 with <i>NotI</i> -cut pKS1.
b192	pLEU2-mCherry-FIS1-TA (V132D)	A product containing the <i>ADHI</i> promotor, the mCherry ORF, and a portion of <i>FIS1</i> was amplified from plasmid b109 using primers 11 and 764. A second product containing a portion of <i>FIS1</i> and the <i>ADHI</i> 3' UTR was amplified from plasmid b172 using primers 765 and 12. PCR products were co-transformed into strain BY4743 with <i>NotI</i> -cut pRS315 (Sikorski and Hieter, 1989).
b193	pLEU2-mCherry-FIS1-TA (V132E)	A product containing the <i>ADHI</i> promotor, the mCherry ORF, and a portion of <i>FIS1</i> was amplified from plasmid b109 using primers 11 and 764. A second product containing a portion of <i>FIS1</i> and the <i>ADHI</i> 3' UTR was amplified from plasmid b173 using primers 765 and 12. PCR products were co-transformed into strain BY4743 with <i>NotI</i> -cut pRS315 (Sikorski and Hieter, 1989).

b194	pLEU2- mCherry-FIS1- TA (V132K)	A product containing the <i>ADHI</i> promotor, the mCherry ORF, and a portion of <i>FIS1</i> was amplified from plasmid b109 using primers 11 and 764. A second product containing a portion of <i>FIS1</i> and the <i>ADHI</i> 3' UTR was amplified from plasmid b174 using primers 765 and 12. PCR products were co-transformed into strain BY4743 with <i>NotI</i> -cut pRS315 (Sikorski and Hieter, 1989).
b195	pLEU2- mCherry-FIS1- TA (V132R)	A product containing the <i>ADHI</i> promotor, the mCherry ORF, and a portion of <i>FIS1</i> was amplified from plasmid b109 using primers 11 and 764. A second product containing a portion of <i>FIS1</i> and the <i>ADHI</i> 3' UTR was amplified from plasmid b175 using primers 765 and 12. PCR products were co-transformed into strain BY4743 with <i>NotI</i> -cut pRS315 (Sikorski and Hieter, 1989).
b196	pLEU2- mCherry-FIS1- TA (A140D)	A product containing the <i>ADHI</i> promotor, the mCherry ORF, and a portion of <i>FIS1</i> was amplified from plasmid b109 using primers 11 and 764. A second product containing a portion of <i>FIS1</i> and the <i>ADHI</i> 3' UTR was amplified from plasmid b176 using primers 765 and 12. PCR products were co-transformed into strain BY4743 with <i>NotI</i> -cut pRS315 (Sikorski and Hieter, 1989).
b197	pLEU2- mCherry-FIS1- TA (A140E)	A product containing the <i>ADHI</i> promotor, the mCherry ORF, and a portion of <i>FIS1</i> was amplified from plasmid b109 using primers 11 and 764. A second product containing a portion of <i>FIS1</i> and the <i>ADHI</i> 3' UTR was amplified from plasmid b177 using primers 765 and 12. PCR products were co-transformed into strain BY4743 with <i>NotI</i> -cut pRS315 (Sikorski and Hieter, 1989).
b198	pLEU2- mCherry-FIS1- TA (A140K)	A product containing the <i>ADHI</i> promotor, the mCherry ORF, and a portion of <i>FIS1</i> was amplified from plasmid b109 using primers 11 and 764. A second product containing a portion of <i>FIS1</i> and the <i>ADHI</i> 3' UTR was amplified from plasmid b178 using primers 765 and 12. PCR products were co-transformed into strain BY4743 with <i>NotI</i> -cut pRS315 (Sikorski and Hieter, 1989).
b199	pLEU2- mCherry-FIS1- TA (A140R)	A product containing the <i>ADHI</i> promotor, the mCherry ORF, and a portion of <i>FIS1</i> was amplified from plasmid b109 using primers 11 and 764. A second product containing a portion of <i>FIS1</i> and the <i>ADHI</i> 3' UTR was amplified from plasmid b179 using primers 765 and 12. PCR products were co-transformed into strain BY4743 with <i>NotI</i> -cut pRS315 (Sikorski and Hieter, 1989).
b200	pLEU2- mCherry-FIS1- TA (A144D)	A product containing the <i>ADHI</i> promotor, the mCherry ORF, and a portion of <i>FIS1</i> was amplified from plasmid b109 using primers 11 and 764. A second product containing a portion of <i>FIS1</i> and the <i>ADHI</i> 3' UTR was amplified from plasmid b180 using primers 765 and 12. PCR products were co-transformed into strain BY4743 with <i>NotI</i> -cut pRS315 (Sikorski and Hieter, 1989).
b201	pLEU2- mCherry-FIS1- TA (A144E)	A product containing the <i>ADHI</i> promotor, the mCherry ORF, and a portion of <i>FIS1</i> was amplified from plasmid b109 using primers 11 and 764. A second product containing a portion of <i>FIS1</i> and the <i>ADHI</i> 3' UTR was amplified from plasmid b181 using primers 765 and 12. PCR products were co-transformed into strain BY4743 with <i>NotI</i> -cut pRS315 (Sikorski and Hieter, 1989).
b202	pLEU2- mCherry-FIS1- TA (A144K)	A product containing the <i>ADHI</i> promotor, the mCherry ORF, and a portion of <i>FIS1</i> was amplified from plasmid b109 using primers 11 and 764. A second product containing a portion of <i>FIS1</i> and the <i>ADHI</i> 3' UTR was amplified from plasmid b182 using primers 765 and 12. PCR products were co-transformed into strain BY4743 with <i>NotI</i> -cut pRS315 (Sikorski and Hieter, 1989).

b203	pLEU2- mCherry-FIS1- TA (A144R)	A product containing the <i>ADHI</i> promotor, the mCherry ORF, and a portion of <i>FIS1</i> was amplified from plasmid b109 using primers 11 and 764. A second product containing a portion of <i>FIS1</i> and the <i>ADHI</i> 3' UTR was amplified from plasmid b183 using primers 765 and 12. PCR products were co-transformed into strain BY4743 with <i>NotI</i> -cut pRS315 (Sikorski and Hieter, 1989).
b204	pLEU2- mCherry-FIS1- TA (F148D)	A product containing the <i>ADHI</i> promotor, the mCherry ORF, and a portion of <i>FIS1</i> was amplified from plasmid b109 using primers 11 and 764. A second product containing a portion of <i>FIS1</i> and the <i>ADHI</i> 3' UTR was amplified from plasmid b184 using primers 765 and 12. PCR products were co-transformed into strain BY4743 with <i>NotI</i> -cut pRS315 (Sikorski and Hieter, 1989).
b205	pLEU2- mCherry-FIS1- TA (F148E)	A product containing the <i>ADHI</i> promotor, the mCherry ORF, and a portion of <i>FIS1</i> was amplified from plasmid b109 using primers 11 and 764. A second product containing a portion of <i>FIS1</i> and the <i>ADHI</i> 3' UTR was amplified from plasmid b185 using primers 765 and 12. PCR products were co-transformed into strain BY4743 with <i>NotI</i> -cut pRS315 (Sikorski and Hieter, 1989).
b206	pLEU2- mCherry-FIS1- TA (F148K)	A product containing the <i>ADHI</i> promotor, the mCherry ORF, and a portion of <i>FIS1</i> was amplified from plasmid b109 using primers 11 and 764. A second product containing a portion of <i>FIS1</i> and the <i>ADHI</i> 3' UTR was amplified from plasmid b186 using primers 765 and 12. PCR products were co-transformed into strain BY4743 with <i>NotI</i> -cut pRS315 (Sikorski and Hieter, 1989).
b207	pLEU2- mCherry-FIS1- TA (F148R)	A product containing the <i>ADHI</i> promotor, the mCherry ORF, and a portion of <i>FIS1</i> was amplified from plasmid b109 using primers 11 and 764. A second product containing a portion of <i>FIS1</i> and the <i>ADHI</i> 3' UTR was amplified from plasmid b187 using primers 765 and 12. PCR products were co-transformed into strain BY4743 with <i>NotI</i> -cut pRS315 (Sikorski and Hieter, 1989).
b208	pLEU2- mCherry-FIS1- TA (V134P)	A product containing the <i>ADHI</i> promotor, the mCherry ORF, and a portion of <i>FIS1</i> was amplified from plasmid b109 using primers 11 and rvspos6. A second product containing a portion of <i>FIS1</i> and the <i>ADHI</i> 3' UTR was amplified from plasmid b109 using primers 969 and 12. PCR products were co-transformed into strain BY4743 with <i>NotI</i> -cut pRS315 (Sikorski and Hieter, 1989).
b209	pLEU2- mCherry-FIS1- TA (G137P)	A product containing the <i>ADHI</i> promotor, the mCherry ORF, and a portion of <i>FIS1</i> was amplified from plasmid b109 using primers 11 and rvspos9. A second product containing a portion of <i>FIS1</i> and the <i>ADHI</i> 3' UTR was amplified from plasmid b109 using primers 970 and 12. PCR products were co-transformed into strain BY4743 with <i>NotI</i> -cut pRS315 (Sikorski and Hieter, 1989).
b210	pLEU2- mCherry-FIS1- TA (A140P)	A product containing the <i>ADHI</i> promotor, the mCherry ORF, and a portion of <i>FIS1</i> was amplified from plasmid b109 using primers 11 and rvspos12. A second product containing a portion of <i>FIS1</i> and the <i>ADHI</i> 3' UTR was amplified from plasmid b109 using primers 971 and 12. PCR products were co-transformed into strain BY4743 with <i>NotI</i> -cut pRS315 (Sikorski and Hieter, 1989).
b211	pLEU2- mCherry-FIS1- TA (A144P)	A product containing the <i>ADHI</i> promotor, the mCherry ORF, and a portion of <i>FIS1</i> was amplified from plasmid b109 using primers 11 and rvspos16. A second product containing a portion of <i>FIS1</i> and the <i>ADHI</i> 3' UTR was amplified from plasmid b109 using primers 972 and 12. PCR products were co-transformed into strain BY4743 with <i>NotI</i> -cut pRS315 (Sikorski and Hieter, 1989).

b226	pCYH2-TRP1-GAL4-sfGFP-FIS1 (Δ G136)	A product containing the <i>FIS1</i> promotor, the <i>GAL4</i> ORF, the superfolderGFP ORF, and a portion of <i>FIS1</i> was amplified from plasmid b100 using primers 11 and rvspos9. A second product containing a portion of <i>FIS1</i> and the <i>ADHI</i> 3' UTR was amplified from plasmid b100 using primers 1059 and 12. PCR products were co-transformed into strain CDD463 with <i>NotI</i> -cut pKS1.
b227	pCYH2-TRP1-GAL4-sfGFP-FIS1 (Δ A135-G136)	A product containing the <i>FIS1</i> promotor, the <i>GAL4</i> ORF, the superfolderGFP ORF, and a portion of <i>FIS1</i> was amplified from plasmid b100 using primers 11 and rvspos7. A second product containing a portion of <i>FIS1</i> and the <i>ADHI</i> 3' UTR was amplified from plasmid b100 using primers 1058 and 12. PCR products were co-transformed into strain CDD463 with <i>NotI</i> -cut pKS1.
b228	pCYH2-TRP1-GAL4-sfGFP-FIS1 (Δ A135-G137)	A product containing the <i>FIS1</i> promotor, the <i>GAL4</i> ORF, the superfolderGFP ORF, and a portion of <i>FIS1</i> was amplified from plasmid b100 using primers 11 and rvspos7. A second product containing a portion of <i>FIS1</i> and the <i>ADHI</i> 3' UTR was amplified from plasmid b100 using primers 1057 and 12. PCR products were co-transformed into strain CDD463 with <i>NotI</i> -cut pKS1.
b229	pCYH2-TRP1-GAL4-sfGFP-FIS1 (∇ IA)	A product containing the <i>FIS1</i> promotor, the <i>GAL4</i> ORF, the superfolderGFP ORF, and a portion of <i>FIS1</i> was amplified from plasmid b100 using primers 11 and rvspos8. A second product containing a portion of <i>FIS1</i> and the <i>ADHI</i> 3' UTR was amplified from plasmid b100 using primers 1060 and 12. PCR products were co-transformed into strain CDD463 with <i>NotI</i> -cut pKS1.
b230	pCYH2-TRP1-GAL4-sfGFP-FIS1 (∇ 2A)	A product containing the <i>FIS1</i> promotor, the <i>GAL4</i> ORF, the superfolderGFP ORF, and a portion of <i>FIS1</i> was amplified from plasmid b100 using primers 11 and rvspos8. A second product containing a portion of <i>FIS1</i> and the <i>ADHI</i> 3' UTR was amplified from plasmid b100 using primers 1061 and 12. PCR products were co-transformed into strain CDD463 with <i>NotI</i> -cut pKS1.
b231	pCYH2-TRP1-GAL4-sfGFP-FIS1 (∇ 3A)	A product containing the <i>FIS1</i> promotor, the <i>GAL4</i> ORF, the superfolderGFP ORF, and a portion of <i>FIS1</i> was amplified from plasmid b100 using primers 11 and rvspos8. A second product containing a portion of <i>FIS1</i> and the <i>ADHI</i> 3' UTR was amplified from plasmid b100 using primers 1062 and 12. PCR products were co-transformed into strain CDD463 with <i>NotI</i> -cut pKS1.
b232	pLEU2-mCherry-FIS1-TA (Δ G136)	A product containing the <i>ADHI</i> promotor, the mCherry ORF, and a portion of <i>FIS1</i> was amplified from plasmid b109 using primers 11 and rvspos9. A second product containing a portion of <i>FIS1</i> and the <i>ADHI</i> 3' UTR was amplified from plasmid b109 using primers 1059 and 12. PCR products were co-transformed into strain BY4743 with <i>NotI</i> -cut pRS315 (Sikorski and Hieter, 1989).
b233	pLEU2-mCherry-FIS1-TA (Δ A135-G136)	A product containing the <i>ADHI</i> promotor, the mCherry ORF, and a portion of <i>FIS1</i> was amplified from plasmid b109 using primers 11 and rvspos7. A second product containing a portion of <i>FIS1</i> and the <i>ADHI</i> 3' UTR was amplified from plasmid b109 using primers 1058 and 12. PCR products were co-transformed into strain BY4743 with <i>NotI</i> -cut pRS315 (Sikorski and Hieter, 1989).
b234	pLEU2-mCherry-FIS1-TA (Δ A135-G137)	A product containing the <i>ADHI</i> promotor, the mCherry ORF, and a portion of <i>FIS1</i> was amplified from plasmid b109 using primers 11 and rvspos7. A second product containing a portion of <i>FIS1</i> and the <i>ADHI</i> 3' UTR was amplified from plasmid b109 using primers 1057 and 12. PCR products were co-transformed into strain BY4743 with <i>NotI</i> -cut pRS315 (Sikorski and Hieter, 1989).

b235	pLEU2- mCherry-FIS1- TA (V1A)	A product containing the <i>ADHI</i> promotor, the mCherry ORF, and a portion of <i>FIS1</i> was amplified from plasmid b109 using primers 11 and rvspos8. A second product containing a portion of <i>FIS1</i> and the <i>ADHI</i> 3' UTR was amplified from plasmid b109 using primers 1060 and 12. PCR products were co-transformed into strain BY4743 with <i>NotI</i> -cut pRS315 (Sikorski and Hieter, 1989).
b236	pLEU2- mCherry-FIS1- TA (V2A)	A product containing the <i>ADHI</i> promotor, the mCherry ORF, and a portion of <i>FIS1</i> was amplified from plasmid b109 using primers 11 and rvspos8. A second product containing a portion of <i>FIS1</i> and the <i>ADHI</i> 3' UTR was amplified from plasmid b109 using primers 1061 and 12. PCR products were co-transformed into strain BY4743 with <i>NotI</i> -cut pRS315 (Sikorski and Hieter, 1989).
b237	pLEU2- mCherry-FIS1- TA (V3A)	A product containing the <i>ADHI</i> promotor, the mCherry ORF, and a portion of <i>FIS1</i> was amplified from plasmid b109 using primers 11 and rvspos8. A second product containing a portion of <i>FIS1</i> and the <i>ADHI</i> 3' UTR was amplified from plasmid b109 using primers 1062 and 12. PCR products were co-transformed into strain BY4743 with <i>NotI</i> -cut pRS315 (Sikorski and Hieter, 1989).
b238	pCYH2-TRP1- FIS1	The <i>FIS1</i> promoter was amplified from the yeast genomic DNA of strain CDD847 using primers 698 and 974. The <i>FIS1</i> ORF and <i>ADHI</i> 3' UTR were amplified from plasmid b100 using primers 973 and 517. PCR products were co-transformed into strain CDD463 with <i>NotI</i> -cut pKS1.
b239	pHIS3-FIS1	The <i>FIS1</i> promoter, <i>FIS1</i> ORF, and <i>ADHI</i> 3' UTR were amplified from plasmid b238 using primers 11 and 12, then co-transformed into strain BY4743 with <i>NotI</i> -cut pRS313 (Sikorski and Hieter, 1989).
b240	pHIS3-FIS1 (V132D)	The <i>FIS1</i> promoter was amplified from the yeast genomic DNA of strain CDD847 using primers 698 and 974. The <i>FIS1</i> ORF and <i>ADHI</i> 3' UTR were amplified from plasmid b172 using primers 973 and 517. PCR products were co-transformed into strain CDD463 with <i>NotI</i> -cut pKS1. The <i>FIS1</i> promoter, <i>FIS1</i> ORF, and <i>ADHI</i> 3' UTR were amplified from the resulting plasmid using primers 11 and 12, then co-transformed into strain BY4743 with <i>NotI</i> -cut pRS313 (Sikorski and Hieter, 1989).
b241	pHIS3-FIS1 (V132E)	The <i>FIS1</i> promoter was amplified from the yeast genomic DNA of strain CDD847 using primers 698 and 974. The <i>FIS1</i> ORF and <i>ADHI</i> 3' UTR were amplified from plasmid b173 using primers 973 and 517. PCR products were co-transformed into strain CDD463 with <i>NotI</i> -cut pKS1. The <i>FIS1</i> promoter, <i>FIS1</i> ORF, and <i>ADHI</i> 3' UTR were amplified from the resulting plasmid using primers 11 and 12, then co-transformed into strain BY4743 with <i>NotI</i> -cut pRS313 (Sikorski and Hieter, 1989).
b242	pHIS3-FIS1 (V132K)	The <i>FIS1</i> promoter was amplified from the yeast genomic DNA of strain CDD847 using primers 698 and 974. The <i>FIS1</i> ORF and <i>ADHI</i> 3' UTR were amplified from plasmid b174 using primers 973 and 517. PCR products were co-transformed into strain CDD463 with <i>NotI</i> -cut pKS1. The <i>FIS1</i> promoter, <i>FIS1</i> ORF, and <i>ADHI</i> 3' UTR were amplified from the resulting plasmid using primers 11 and 12, then co-transformed into strain BY4743 with <i>NotI</i> -cut pRS313 (Sikorski and Hieter, 1989).
b243	pHIS3-FIS1 (V132R)	The <i>FIS1</i> promoter was amplified from the yeast genomic DNA of strain CDD847 using primers 698 and 974. The <i>FIS1</i> ORF and <i>ADHI</i> 3' UTR were amplified from plasmid b175 using primers 973 and 517. PCR products were co-transformed into strain CDD463 with <i>NotI</i> -cut pKS1. The <i>FIS1</i> promoter, <i>FIS1</i> ORF, and <i>ADHI</i> 3' UTR were amplified from the resulting plasmid using primers 11 and 12, then co-transformed into strain BY4743 with <i>NotI</i> -cut pRS313 (Sikorski and Hieter, 1989).

b244	p <i>HIS3-FIS1</i> (A144D)	The <i>FIS1</i> promoter was amplified from the yeast genomic DNA of strain CDD847 using primers 698 and 974. The <i>FIS1</i> ORF and <i>ADHI</i> 3' UTR were amplified from plasmid b180 using primers 973 and 517. PCR products were co-transformed into strain BY4743 with <i>NotI</i> -cut pRS313 (Sikorski and Hieter, 1989).
b245	p <i>HIS3-FIS1</i> (A144E)	The <i>FIS1</i> promoter was amplified from the yeast genomic DNA of strain CDD847 using primers 698 and 974. The <i>FIS1</i> ORF and <i>ADHI</i> 3' UTR were amplified from plasmid b181 using primers 973 and 517. PCR products were co-transformed into strain BY4743 with <i>NotI</i> -cut pRS313 (Sikorski and Hieter, 1989).
b246	p <i>HIS3-FIS1</i> (A144K)	The <i>FIS1</i> promoter was amplified from the yeast genomic DNA of strain CDD847 using primers 698 and 974. The <i>FIS1</i> ORF and <i>ADHI</i> 3' UTR were amplified from plasmid b182 using primers 973 and 517. PCR products were co-transformed into strain BY4743 with <i>NotI</i> -cut pRS313 (Sikorski and Hieter, 1989).
b247	p <i>HIS3-FIS1</i> (A144R)	The <i>FIS1</i> promoter was amplified from the yeast genomic DNA of strain CDD847 using primers 698 and 974. The <i>FIS1</i> ORF and <i>ADHI</i> 3' UTR were amplified from plasmid b183 using primers 973 and 517. PCR products were co-transformed into strain BY4743 with <i>NotI</i> -cut pRS313 (Sikorski and Hieter, 1989).
b248	p <i>HIS3-FIS1</i> (F148D)	The <i>FIS1</i> promoter was amplified from the yeast genomic DNA of strain CDD847 using primers 698 and 974. The <i>FIS1</i> ORF and <i>ADHI</i> 3' UTR were amplified from plasmid b184 using primers 973 and 517. PCR products were co-transformed into strain CDD463 with <i>NotI</i> -cut pKS1. The <i>FIS1</i> promoter, <i>FIS1</i> ORF, and <i>ADHI</i> 3' UTR were amplified from the resulting plasmid using primers 11 and 12, then co-transformed into strain BY4743 with <i>NotI</i> -cut pRS313 (Sikorski and Hieter, 1989).
b249	p <i>HIS3-FIS1</i> (F148E)	The <i>FIS1</i> promoter was amplified from the yeast genomic DNA of strain CDD847 using primers 698 and 974. The <i>FIS1</i> ORF and <i>ADHI</i> 3' UTR were amplified from plasmid b185 using primers 973 and 517. PCR products were co-transformed into strain CDD463 with <i>NotI</i> -cut pKS1. The <i>FIS1</i> promoter, <i>FIS1</i> ORF, and <i>ADHI</i> 3' UTR were amplified from the resulting plasmid using primers 11 and 12, then co-transformed into strain BY4743 with <i>NotI</i> -cut pRS313 (Sikorski and Hieter, 1989).
b250	p <i>HIS3-FIS1</i> (F148K)	The <i>FIS1</i> promoter was amplified from the yeast genomic DNA of strain CDD847 using primers 698 and 974. The <i>FIS1</i> ORF and <i>ADHI</i> 3' UTR were amplified from plasmid b186 using primers 973 and 517. PCR products were co-transformed into strain CDD463 with <i>NotI</i> -cut pKS1. The <i>FIS1</i> promoter, <i>FIS1</i> ORF, and <i>ADHI</i> 3' UTR were amplified from the resulting plasmid using primers 11 and 12, then co-transformed into strain BY4743 with <i>NotI</i> -cut pRS313 (Sikorski and Hieter, 1989).
b251	p <i>HIS3-FIS1</i> (F148R)	The <i>FIS1</i> promoter was amplified from the yeast genomic DNA of strain CDD847 using primers 698 and 974. The <i>FIS1</i> ORF and <i>ADHI</i> 3' UTR were amplified from plasmid b187 using primers 973 and 517. PCR products were co-transformed into strain CDD463 with <i>NotI</i> -cut pKS1. The <i>FIS1</i> promoter, <i>FIS1</i> ORF, and <i>ADHI</i> 3' UTR were amplified from the resulting plasmid using primers 11 and 12, then co-transformed into strain BY4743 with <i>NotI</i> -cut pRS313 (Sikorski and Hieter, 1989).
b252	p <i>LEU2-mCherry-ΔTA</i>	A PCR product containing the <i>ADHI</i> promoter, the mCherry ORF, and a small portion of <i>FIS1</i> lacking the region encoding the Fis1p tail anchor was amplified from plasmid b109 using primers 11 and 707. A second product containing the <i>ADHI</i> 3' UTR was amplified from plasmid b109 using primers 708 and 12. PCR products were co-transformed into strain BY4743 with <i>NotI</i> -cut pRS315 (Sikorski and Hieter, 1989).

b253	pCYH2-TRP1-GAL4-sfGFP-FIS1 (R151X)	The <i>FIS1</i> promoter, <i>GAL4</i> ORF, superfolderGFP ORF, and a portion of the region encoding the Fis1p tail anchor up to and including the 150th amino acid were amplified from plasmid b100 using primers 11 and rvspos23. The <i>ADHI</i> 3' UTR was amplified from plasmid b100 using primers 903 and 12. PCR products were co-transformed into strain CDD463 with <i>NotI</i> -cut pKS1.
b254	pLEU2-mCherry-FIS1-TA (R151X)	A PCR product containing the <i>ADHI</i> promoter, the mCherry ORF, and a portion of the region encoding the Fis1p tail anchor up to and including the 150th amino acid was amplified from plasmid b109 using primers 11 and rvspos23. A second product containing the <i>ADHI</i> 3' UTR was amplified from plasmid b109 using primers 903 and 12. PCR products were co-transformed into strain BY4743 with <i>NotI</i> -cut pRS315 (Sikorski and Hieter, 1989).
b255	pLEU2-mCherry-BAX-TA	The <i>ADHI</i> promoter and the mCherry ORF were amplified from plasmid b109 using primers 11 and 764. The genomic region encoding the tail anchor of human BAX was amplified from plasmid pBM272-BAX (Gross <i>et al.</i> , 2000) using primers 922 and 923. The <i>ADHI</i> 3' UTR was amplified from plasmid b100 using primers 775 and 517. PCR products were co-transformed with <i>NotI</i> -cut pRS315 (Sikorski and Hieter, 1989) into strain CDD463.
b257	pLEU2-mCherry-hFIS1-TA	The <i>ADHI</i> promoter and the mCherry ORF were amplified from plasmid b109 using primers 11 and 764. The genomic region encoding the human <i>FIS1</i> tail anchor was amplified from human cell line genomic DNA using primers 924 and 925. The <i>ADHI</i> 3' UTR was amplified from plasmid b100 using primers 775 and 517. PCR products were co-transformed with <i>NotI</i> -cut pRS315 (Sikorski and Hieter, 1989) into strain CDD463.
b258	pCYH2-TRP1-GAL4-sfGFP-hFIS1-TA	The <i>FIS1</i> promoter, <i>GAL4</i> ORF, superfolderGFP ORF, and a genomic region of <i>FIS1</i> not encoding the tail anchor were amplified from plasmid b100 using primers 11 and 984. The genomic region encoding the human <i>FIS1</i> tail anchor was amplified from plasmid b257 using primers 924 and 925. The <i>ADHI</i> 3' UTR was amplified from plasmid b109 using primers 775 and 12. PCR products were co-transformed into strain CDD463 with <i>NotI</i> -cut pKS1.
b273	pLEU2-mCherry-flk-TA	The <i>ADHI</i> promoter and the mCherry ORF were amplified from plasmid b152 using primers 11 and 764. The genomic region encoding the tail anchor of bacterial flk was amplified from <i>E.coli</i> (DH5 α) gDNA using primers 955 and 956. The <i>ADHI</i> 3' UTR was amplified from plasmid b152 using primers 775 and 12. PCR products were co-transformed with <i>NotI</i> -cut pRS315 (Sikorski and Hieter, 1989) into strain CDD3.
b274	pLEU2-mCherry-ygiM-TA	The <i>ADHI</i> promoter and the mCherry ORF were amplified from plasmid b152 using primers 11 and 764. The genomic region encoding the tail anchor of bacterial ygiM was amplified from <i>E.coli</i> (DH5 α) gDNA using primers 963 and 964. The <i>ADHI</i> 3' UTR was amplified from plasmid b152 using primers 775 and 12. PCR products were co-transformed with <i>NotI</i> -cut pRS315 (Sikorski and Hieter, 1989) into strain CDD3.
b275	pLEU2-mCherry-elaB-TA	The <i>ADHI</i> promoter and the mCherry ORF were amplified from plasmid b152 using primers 11 and 764. The genomic region encoding the tail anchor of bacterial elaB was amplified from <i>E.coli</i> (DH5 α) gDNA using primers 953 and 954. The <i>ADHI</i> 3' UTR was amplified from plasmid b152 using primers 775 and 12. PCR products were co-transformed with <i>NotI</i> -cut pRS315 (Sikorski and Hieter, 1989) into strain CDD3.
b277	pLEU2-mCherry-yhdV-TA	The <i>ADHI</i> promoter and the mCherry ORF were amplified from plasmid b152 using primers 11 and 764. The genomic region encoding the tail anchor of bacterial yhdV was amplified from <i>E.coli</i> (DH5 α) gDNA using primers 965 and 966. The <i>ADHI</i> 3' UTR

		was amplified from plasmid b152 using primers 775 and 12. PCR products were co-transformed with <i>NotI</i> -cut pRS315 (Sikorski and Hieter, 1989) into strain CDD3.
b278	pLEU2- mCherry- waaR-TA	The <i>ADHI</i> promoter and the mCherry ORF were amplified from plasmid b152 using primers 11 and 764. The genomic region encoding the tail anchor of bacterial waaR was amplified from <i>E.coli</i> (DH5 α) gDNA using primers 959 and 960. The <i>ADHI</i> 3' UTR was amplified from plasmid b152 using primers 775 and 12. PCR products were co-transformed with <i>NotI</i> -cut pRS315 (Sikorski and Hieter, 1989) into strain CDD3.
b279	pLEU2- mCherry-yqjD- TA	The <i>ADHI</i> promoter and the mCherry ORF were amplified from plasmid b152 using primers 11 and 764. The genomic region encoding the tail anchor of bacterial yqjD was amplified from <i>E.coli</i> (DH5 α) gDNA using primers 967 and 968. The <i>ADHI</i> 3' UTR was amplified from plasmid b152 using primers 775 and 12. PCR products were co-transformed with <i>NotI</i> -cut pRS315 (Sikorski and Hieter, 1989) into strain CDD3.
b280	pLEU2- mCherry-djlB- TA	The <i>ADHI</i> promoter and the mCherry ORF were amplified from plasmid b152 using primers 11 and 764. The genomic region encoding the tail anchor of bacterial djlB was amplified from <i>E.coli</i> (DH5 α) gDNA using primers 951 and 952. The <i>ADHI</i> 3' UTR was amplified from plasmid b152 using primers 775 and 12. PCR products were co-transformed with <i>NotI</i> -cut pRS315 (Sikorski and Hieter, 1989) into strain CDD3.
b281	pLEU2- mCherry-tcdA- TA	The <i>ADHI</i> promoter and the mCherry ORF were amplified from plasmid b152 using primers 11 and 764. The genomic region encoding the tail anchor of bacterial tcdA was amplified from <i>E.coli</i> (DH5 α) gDNA using primers 957 and 958. The <i>ADHI</i> 3' UTR was amplified from plasmid b152 using primers 775 and 12. PCR products were co-transformed with <i>NotI</i> -cut pRS315 (Sikorski and Hieter, 1989) into strain CDD3.

APPENDIX C: List of primers used in this study

Name	Sequence
11	GTAAAACGACGGCCAGTGAATTG
12	CGCCAAGCTCGGAATTAACCCTCAC
517	ATATCGAATTCCTGCAGCCCGGGGGATCCATGCCGGTAGAGGTGTGGTCAAT AAGAGCGA
531	GACTCACTATAGGGCGAATTGGAGCTCCACATCCTTTTGTGTTTCCGGGTG TAC
698	GACTCACTATAGGGCGAATTGGAGCTCCACCAGTTCAAATAACATGTGTCCA TTACCTGT
699	TGCTTGTTCGATAGAAGACAGTAGCTTCATACTTATGTTGTATGGCTGTGCTC TGATCTG
700	CAGATCAGAGCACAGCCATACAACATAAGTATGAAGCTACTGTCTTCTATCG ACAAGCA
701	ACCTGTAAACAATTCCTCGCCTTTAGACATCTCTTTTTTTGGGTTTGGTGGGG TATCTTC
702	GAAGATACCCACCAAACCCAAAAAAGAGATGTCTAAAGGCGAGGAATTG TTACAGGT
703	AAGAGTTGGCCAAAATCTACTTTGGTCATTTTGTACAATTCGTCCATTCCTA ATGTTAT
704	ATAACATTAGGAATGGACGAATTGTACAAAATGACCAAAGTAGATTTTTGG CCAACCTCTT
705	ATCATAAGAAATTCGCTTATTTAGAAGTGTTTACCTTCTCTTGTTTCTTAAGA AGAACT
706	AGTTTCTTCTTAAGAAACAAGAGAAGGTAAACACTTCTAAATAAGCGAATTT CTTATGAT
707	ATCATAAGAAATTCGCTTATTTAGAAGTGTTTATGTTTCTTCTGGATCTTAT CCTCTACCAT
738	CGAATTCCTGCAGCCCGGGGGATCCACTAGCAGTTCAAATAACATGTGTCCA TTACCTGT
739	CTCACTAAAGGGAACAAAAGCTGGAGCTCCTGCCGGTAGAGGTGTGGTCAA TAAGAGCGA
708	ATGGTAGAGGATAAGATCCAGAAGGAAACATAAACTTCTAAATAAGCGA ATTCTTATGAT
749	AGTTGACATATCAGACCTACAGAAACATAGGAATCGGTAAAGATTGTA AGAGTGCAC
750	AGTATATAAATACAAAAGGGGTACTACATAAAAGATTTACTGTGCGGTAT TTCACACCG
762	CATGTTATCCTCCTCGCCCTTGCTCACCATTGTATATGAGATAGTTGATTGTA TGCTTGG

763	CCAAGCATACAATCAACTATCTCATATACAATGGTGAGCAAGGGCGAGGAG GATAACATG
764	TGTTTCCTTCTGGATCTTATCCTCTACCATCTTGTACAGCTCGTCCATGCCGC CGGTGGA
765	TCCACCGGCGGCATGGACGAGCTGTACAAGATGGTAGAGGATAAGATCCAG AAGGAAACA
773	TTTGAAGAGTATGGTAGAGGATAAGATCCAGAAGGAAACA
774	ATCATAAATCATAAGAAATTCGCTTATTTAGAAGTGTTTA
775	TAAACACTTCTAAATAAGCGAATTTCTTATGATTTATGAT
776	TGTTTCCTTCTGGATCTTATCCTCTACCATACTCTTCAA
899	ATCCTGTGGAGCGACGTTTATCCAGATAGTATGGTGAGCAAGGGCGAGGAG GATAACATG
900	CATGTTATCCTCCTCGCCCTTGCTCACCATACTATCTGGATAAACGTCGCTCC ACAGGAT
903	GTGGCCGTGGCTAGTTTCTTCTTATAAACACTTCTAAATAAGCGAATTTCTTA TG
906	GATAAGATCCAGAAGGAAACACTCAAGGGTGATGTCGTCGCTGGAGGCGTA C
907	GATAAGATCCAGAAGGAAACACTCAAGGGTGAGGTCGTCGCTGGAGGCGTA C
908	GATAAGATCCAGAAGGAAACACTCAAGGGTAAGGTCGTCGCTGGAGGCGTA C
909	GATAAGATCCAGAAGGAAACACTCAAGGGTCGTGTCGTCGCTGGAGGCGTA C
910	AAGGGTGTTGTCGTCGCTGGAGGCGTACTAGATGGCGCTGTGGCCGTG
911	AAGGGTGTTGTCGTCGCTGGAGGCGTACTAGAGGGCGCTGTGGCCGTG
912	AAGGGTGTTGTCGTCGCTGGAGGCGTACTAAAGGGCGCTGTGGCCGTG
913	AAGGGTGTTGTCGTCGCTGGAGGCGTACTACGTGGCGCTGTGGCCGTG
914	GTCGCTGGAGGCGTACTAGCCGGCGCTGTGGATGTGGCTAGTTTCTTCTTAA GAAACAAGAGAAG
915	GTCGCTGGAGGCGTACTAGCCGGCGCTGTGGAGGTGGCTAGTTTCTTCTTAA GAAACAAGAGAAG
916	GTCGCTGGAGGCGTACTAGCCGGCGCTGTGAAGGTGGCTAGTTTCTTCTTAA GAAACAAGAGAAG
917	GTCGCTGGAGGCGTACTAGCCGGCGCTGTGCGTGTGGCTAGTTTCTTCTTAA GAAACAAGAGAAG
918	GTA TAGCCGGCGCTGTGGCCGTGGCTAGTGATTTCTTAAGAAACAAGAGA AGGTAAACTTC
919	GTA TAGCCGGCGCTGTGGCCGTGGCTAGTGAGTTCTTAAGAAACAAGAGA AGGTAAACTTC
920	GTA TAGCCGGCGCTGTGGCCGTGGCTAGTAAGTTCTTAAGAAACAAGAGA AGGTAAACTTC
921	GTA TAGCCGGCGCTGTGGCCGTGGCTAGTCGTTTCTTAAGAAACAAGAGA AGGTAAACTTC
922	ATGGTAGAGGATAAGATCCAGAAGGAAACATGGCAGACAGTGACCATCTTT GTGGCTGGA

923	ATCATAAGAAATTCGCTTATTTAGAAGTGTTTCAGCCCATCTTCTTCCAGATG GTGAGCGA
924	ATGGTAGAGGATAAGATCCAGAAGGAAACAGGACTCGTGGGCATGGCCATC GTGGGAGGC
925	ATCATAAGAAATTCGCTTATTTAGAAGTGTTTCAGGATTTGGACTTGGACACA GCAAGTCC
951	ATGGTAGAGGATAAGATCCAGAAGGAAACACTGGGCATCATTAAAATTATT TTCTATATT
952	ATCATAAGAAATTCGCTTATTTAGAAGTGTTTCACCCGAACAGATGGAGTATT TTCCCTAT
953	ATGGTAGAGGATAAGATCCAGAAGGAAACACCCTGGCAAGGAATTGGTGTG GGCGCGGCC
954	ATCATAAGAAATTCGCTTATTTAGAAGTGTTTAACGGCGTGCCAGCAACAGT CCTAGTAC
955	ATGGTAGAGGATAAGATCCAGAAGGAAACACCCGCGCTGTGGATACTGTTA GTCGCGATT
956	ATCATAAGAAATTCGCTTATTTAGAAGTGTTTAACGAACCAGCCAGACCAGC ATCAGGAT
957	ATGGTAGAGGATAAGATCCAGAAGGAAACAGCATCTGGATTTGGCGCGGCA ACGATGGTG
958	ATCATAAGAAATTCGCTTATTTAGAAGTGTTTAACCCTGACGCGCCGCTTTC GCCATCAT
959	ATGGTAGAGGATAAGATCCAGAAGGAAACATTAGTGCAACATCATTATATC TCAGGAATT
960	ATCATAAGAAATTCGCTTATTTAGAAGTGTTTATTTACGGTAATATTTTCGGC AAAGATA
963	ATGGTAGAGGATAAGATCCAGAAGGAAACATGGTTTATGTATGGCGGTGGC GTGCTGGGG
964	ATCATAAGAAATTCGCTTATTTAGAAGTGTTTAGTTCATCCAGCGATCTTTGC GTTTGCG
965	ATGGTAGAGGATAAGATCCAGAAGGAAACAACGGCTGGGGCTATTGCCGGC GGGGCAGCT
966	ATCATAAGAAATTCGCTTATTTAGAAGTGTTTATTTTCGATAGAGCGATGATC CCCATCGT
967	ATGGTAGAGGATAAGATCCAGAAGGAAACATGGACGGGCGTGGGCATTGGC GCTGCAATC
968	ATCATAAGAAATTCGCTTATTTAGAAGTGTTTAACGACGCGACAGCAGAAC GCCGAGCAC
969	ATCCAGAAGGAAACACTCAAGGGTGTTGTCCCCGCTGGAGGCGTACTAGCC G
970	GAAACACTCAAGGGTGTTGTCGTCGCTGGACCCGTAAGCCGGCGCTGTGG
971	AAGGGTGTTGTCGTCGCTGGAGGCGTACTACCCGGCGCTGTGGCCGTG
972	GTCGCTGGAGGCGTACTAGCCGGCGCTGTGCCCGTGGCTAGTTTCTTCTTAA GAAACAAGAGAAG
973	CAGATCAGAGCACAGCCATACAACATAAGTATGACCAAAGTAGATTTTTGG CCAACCTCTT

974	AAGAGTTGGCCAAAAATCTACTTTGGTCATACTTATGTTGTATGGCTGTGCTCTGATCTG
984	TGTTTCCTTCTGGATCTTATCCTCTACCAT
1006	CTGTCTAGTTGATCCTCCGGAGTGTA AAAACTGATTTTCAAGATTGTACTGAGAGTGCAC
1007	TAGAGATTATATTATGTAAAGGTAAAAACGGGAGCGAGCACTGTGCGGTATTTCACACCG
1051	AAACGTACGACAAGAACAAGAAGATCATCACATTGTAATTAGATTGTACTGAGAGTGCAC
1052	TTATATGTCGTATGTATCTATTTATGGTATTCAGGGGCTTCTGTGCGGTATTTACACACCG
1057	GGAAACTCAAGGGTGTGTCGTCGTA CTAGCCGGCGCTGTGGCCGTGGCTAGTTTTCT
1058	GGAAACTCAAGGGTGTGTCGTCGGCGTACTAGCCGGCGCTGTGGCCGTGGCTAGTTT
1059	GGGTGTTGTCGTCGCTGGAGTACTAGCCGGCGCTGTGGCCGTGGCTAGTTTCTCTTAAG
1060	CTCAAGGGTGTGTCGTCGCTGCCGGAGGCGTACTAGCCGGCGCTGTGGCCGTGGCTAGT
1061	CTCAAGGGTGTGTCGTCGCTGCCGCAGGAGGCGTACTAGCCGGCGCTGTGGCCGTGGCT
1062	CTCAAGGGTGTGTCGTCGCTGCCGCAGCGGGAGGCGTACTAGCCGGCGCTGTGGCCGTG
fwdpos1	ATGGTAGAGGATAAGATCCAGAAGGAAACANNNAAGGGTGTGTCGTCGCTGG
rvspos1	TGTTTCCTTCTGGATCTTATCCTCTACCATA C
fwdpos2	GTAGAGGATAAGATCCAGAAGGAAACACTC NNNGGTGTGTCGTCGCTGGAG
rvspos2	GAGTGTTTCCTTCTGGATCTTATCCTCTACC
fwdpos3	GAGGATAAGATCCAGAAGGAAACACTCAAG NNNGTGTCGTCGCTGGAGGC
rvspos3	CTTGAGTGTTTCCTTCTGGATCTTATCCTC
fwdpos4	GATAAGATCCAGAAGGAAACACTCAAGGG TNNNGTCGTCGCTGGAGGCGTA
rvspos4	ACCCTTGAGTGTTTCCTTCTGGATCTTATC
fwdpos5	AAGATCCAGAAGGAAACACTCAAGGGTGT TNNNGTCGCTGGAGGCGTACTA
rvspos5	AACACCCTTGAGTGTTTCCTTCTGGATCT TATC
fwdpos6	ATCCAGAAGGAAACACTCAAGGGTGTGTC NNNGCTGGAGGCGTACTAGCC
rvspos6	GACAACACCCTTGAGTGTTTCCTTC
fwdpos7	CAGAAGGAAACACTCAAGGGTGTGTCGTC NNNGGAGGCGTACTAGCCGGC
rvspos7	GACGACAACACCCTTGAGTGTTTCC
fwdpos8	AAGGAAACTCAAGGGTGTGTCGTCGCTN NNGGCGTACTAGCCGGCGC
rvspos8	AGCGACGACAACACCCTTGAG
fwdpos9	GAAACTCAAGGGTGTGTCGTCGCTGGAN NNGTACTAGCCGGCGCTGTG

	G
rvspos9	TCCAGCGACGACAACACCC
fwdpos10	ACACTCAAGGGTGTGTCGTCGCTGGAGGCNNNCTAGCCGGCGCTGTGGC
rvspos10	GCCTCCAGCGACGACAACAC
fwdpos11	CTCAAGGGTGTGTCGTCGCTGGAGGCGTANNNGCCGGCGCTGTGGCCGT
rvspos11	TACGCCTCCAGCGACGACAACACCCTTGAG
fwdpos12	AAGGGTGTGTCGTCGCTGGAGGCGTACTANNNGGCGCTGTGGCCGTG
rvspos12	TAGTACGCCTCCAGCGACG
fwdpos13	GGTGTGTCGTCGCTGGAGGCGTACTAGCCNNNGCTGTGGCCGTGGCTAGTT TC
rvspos13	GGCTAGTACGCCTCCAGCG
fwdpos14	GTTGTCGTCGCTGGAGGCGTACTAGCCGGCNNNGTGGCCGTGGCTAGTTTCT TCTTAAG
rvspos14	GCCGGCTAGTACGCCTCC
fwdpos15	GTCGTCGCTGGAGGCGTACTAGCCGGCGCTNNNGCCGTGGCTAGTTTCTTCT TAAGAAAC
rvspos15	AGCGCCGGCTAGTACGC
fwdpos16	GTCGCTGGAGGCGTACTAGCCGGCGCTGTGNNNGTGGCTAGTTTCTTCTTAA GAAACAAGAGAAG
rvspos16	CACAGCGCCGGCTAGTACG
fwdpos17	GCTGGAGGCGTACTAGCCGGCGCTGTGGCCNNNGCTAGTTTCTTCTTAAAGAA ACAAGAGAAGG
rvspos17	GGCCACAGCGCCGGCTAGTACGCCTCCAGC
fwdpos18	GGAGGCGTACTAGCCGGCGCTGTGGCCGTGNNNAGTTTCTTCTTAAAGAAAC AAGAGAAGGTAAACACTTC
rvspos18	CACGGCCACAGCGCCG
fwdpos19	GGCGTACTAGCCGGCGCTGTGGCCGTGGCTNNNTTCTTCTTAAAGAAACAAGA GAAGGTAAACACTTC
rvspos19	AGCCACGGCCACAGCG
fwdpos20	GTA TAGCCGGCGCTGTGGCCGTGGCTAGTNNNTTCTTAAAGAAACAAGAGA AGGTAAACACTTC
rvspos20	ACTAGCCACGGCCACAGC
fwdpos21	CTAGCCGGCGCTGTGGCCGTGGCTAGTTTCNNNTTAAAGAAACAAGAGAAGG TAAACACTTCTAAATAAGC
rvspos21	GAAACTAGCCACGGCCACAGC
fwdpos22	GCCGGCGCTGTGGCCGTGGCTAGTTTCTTCNNNAGAAACAAGAGAAGGTAA ACACTTCTAAATAAGCG
rvspos22	GAAGAACTAGCCACGGCCACAG
fwdpos23	GGCGCTGTGGCCGTGGCTAGTTTCTTCTTANNNAACAAGAGAAGGTAAACA CTTCTAAATAAGCG
rvspos23	TAAGAAGAACTAGCCACGGCCAC
fwdpos24	GCTGTGGCCGTGGCTAGTTTCTTCTTAAAGANNNAAGAGAAGGTAAACACTTC TAAATAAGCGAATTC
rvspos24	TCTTAAAGAAGAACTAGCCACGGCC
fwdpos25	GTGGCCGTGGCTAGTTTCTTCTTAAAGAAACNNNAGAAGGTAAACACTTCTAA ATAAGCGAATTTCTTATG

rvspos25	GTTTCTTAAGAAGAAACTAGCCACGGCC
fwdpos26	GCCGTGGCTAGTTTCTTCTTAAGAAACAAGNNNAGGTAAACACTTCTAAATA AGCGAATTTCTTATG
rvspos26	CTTGTTTCTTAAGAAGAAACTAGCCACGG
fwdpos27	GTGGCTAGTTTCTTCTTAAGAAACAAGAGANNNTAAACACTTCTAAATAAGC GAATTTCTTATGATTTATG
rvspos27	TCTCTTGTTTCTTAAGAAGAAACTAGCCACG

